Aalto-yliopisto
Insinööritieteiden
korkeakoulu

Markku Andelin

Development of experimental methods for investigating sediment and nutrient transport in vegetated flows

Master's thesis for the degree of Master of Science in Technology submitted for inspection

Espoo 30.9.2019
Supervisor: Prof. Harri Koivusalo
Advisors: D.Sc. Kaisa Västilä, M.Sc. Walter Box,
D.Sc. Juha Järvelä, Asst. Prof. Tom Jilbert

Aalto-yliopisto
Insinööritieteiden
korkeakoulu

Aalto-yliopisto, PL 11000, 00076 AALTO
www.aalto.fi

Diplomityön tiivistelmä

Tekijä Markku Andelin

Työn nimi Sedimentti- ja ravinnekulkeuman mittausmenetelmien kehittäminen virtauksiin kasvillisuuden lomassa.

Maisteriohjelma Vesi- ja ympäristötekniikka **Koodi** WAT

Työn valvoja Professori Harri Koivusalo

Työn ohjaaja(t) Kaisa Västilä, Walter Box, Juha Järvelä, Tom Jilbert

Päivämäärä 30.9.2019 **Sivumäärä** 74+2 **Kieli** Englanti

Tiivistelmä

Empiiriset mittaukset ja aineisto parantavat monien kasvillisuuden ja virtauksen välisten fysikaalisten, kemiallisten ja biologisten ilmiöiden ymmärtämistä ja mallinnusta. Kasvillisuudella on merkittävä vaikutus esimerkiksi virtausoloihin ja virtausvastukseen, mikä osaltaan vaikuttaa myös kiintoaineen kulkeutumiseen ja ravinteiden pidättymiseen. Tämän työn päämääränä oli kehittää kokeellisia kouru-, kenttä- ja laboratoriomenetelmiä näiden prosessien määrittämiseen ajatellen virtauksia kasvillisuuden lomassa. Työn tavoitteina oli kehittää 1) pienoiskokoinen näytteenotin kiintoaineen pohjakulkeuman mittaamiseen laboratorio-oloissa, 2) voima-anturi kasvillisuuden virtausvastuksen määrittämiseen virtauskourussa, sekä 3) metodologia sedimenttiin pidättyvien ravinteiden kertymisen arviointiin kasvillisissa uomissa. Tiedossa ravinteiden kasautumisesta luonnonmukaisten uomien eri osiin on vielä puutteita, ja myös skaalattujen, Helley-Smith (HS) tyyppisten pohjakulkeuman näytteenottimien kohdalla on avoimia kysymyksiä.

Kouru-olosuhteissa tutkittiin pohjakulkeuman näytteenottimen ja voima-anturin toimintaa eri virtausoloissa. Kokeet kasvillisissa oloissa osoittivat, että pienemmäksi skaalattu HS näytteenotin soveltuu käytettäväksi pohjakulkeuman mittaamiseen laboratoriokourussa. Näytteenotin antoi optiseen takaisinsironta-anturiin verrattavia tuloksia, ja näytteiden välinen vaihtelu oli suhteellisen pientä. Näytteenotin toi myös hyvin näkyviin erot pohjakulkeuman suuruudessa kasvillisen ja kasvittoman uoman osien välillä. Testit voima-anturilla tuottivat hyvin samansuuntaisia tuloksia kuin muissakin tutkimuksissa, ja mitatut voimat vaihtelivat vähäisesti ajan suhteen jopa hyvin lyhyillä mittausjaksoilla.

Sedimentti- ja maanäytteet kerättiin maatalousuomasta, jonne on vuonna 2010 rakennettu luonnonmukainen, kasvillinen tulvatasanne. Näytteet analysoitiin ravinteiden ja alkuaineiden määrittämiseksi, ja erilaisten esikäsittelyvaiheiden vaikutuksia tutkittiin. Tulosten perusteella useimmissa tapauksissa näytteet voidaan jauhaa koneellisesti ja ilman märkäseulontaa ilman merkittäviä vaikutuksia ravinteiden ja alkuaineiden pitoisuuksiin. Näytteiden ominaisuuksista erityisesti kuivatiheys, sekä magnesiumin ja alumiinin suhde vaikuttivat soveliailta uoman kunnostuksen jälkeisen kiintoaineen ja ravinteiden pidättymisen arvioimiseen.

Jatkotutkimuksia suositellaan skaalatun HS näytteenottimen kalibroimiseksi eri virtausnopeuksille, jos tavoitteena on saada luotettavia tuloksia pohjakulkeuman määrästä. Mainittujen maa- ja sedimenttinäytteiden ominaisuuksien soveltuvuutta pidättymisen määrittämiseen suositellaan tutkittavaksi myös muissa uomakohteissa. Kehitetyillä metodeilla on myös ilman jatkokehitystä hyödyllisiä käyttökohteita, ja ne mahdollistavat suoraviivaiset ja nopeat mittaukset esimerkiksi prosessien alueellisen vaihtelun ymmärtämiseksi kasvillisissa virtauksissa.

Avainsanat Kiintoaineen kulkeuma ja pidättyminen, Kasvillisuuden virtausvastus.

Aalto University
School of Engineering

Aalto-University, P.O. BOX 11000, 00076
AALTO
www.aalto.fi

Abstract of master's thesis

Author Markku Andelin

Title of thesis Development of experimental methods for investigating sediment and nutrient transport in vegetated flows

Master programme Water and Environmental Engineering **Code** WAT

Thesis supervisor Professor Harri Koivusalo

Thesis advisor(s) Kaisa Västilä, Walter Box, Juha Järvelä, Tom Jilbert

Date 30.9.2019 **Number of pages** 74+2 **Language** English

Abstract

Empirical measurements are needed for improving understanding and modelling of various physical, chemical and biological phenomena present in vegetated flows. Vegetation has a substantial effect for example on flow resistance, velocities and patterns, which in turn affects sediment transport and nutrient deposition. The goal of this work was to develop experimental flume, field and laboratory methods for investigating these processes. The objectives were to develop 1) a downscaled sampler for measuring bed load sediment transport in flume conditions, 2) a drag force sensor for determining vegetative flow resistance in laboratory flows, and 3) a methodology for estimating sedimentary nutrient deposition in vegetated channels. There are knowledge gaps in understanding nutrient deposition in environmentally preferable channel designs, and in using miniature Helley-Smith (HS) bed load samplers.

The performance of the bed load sampler and drag force sensor was investigated in different flow conditions. The experiments in vegetated conditions indicated that the downscaled bed load sampler is suitable for determination of bed load fluxes in flume conditions, giving results comparable to an optical backscatter instrument. The measurement variability was found to be relatively low. The sampler was capable of capturing the large differences in bed load transport between unvegetated and vegetated parts of the flume. Experiments with the drag force sensor provided results comparable to other studies, and the variability in results was minor. The soil and sediment cores were collected from an agricultural drainage channel, adjacent to which a vegetated floodplain had been constructed in 2010. The collected samples were subjected to elemental analysis, and the effect of several pre-processing steps was studied. According to the results, in most cases the samples can be analyzed after mechanical grinding without sieving, without significant effect on the measured nutrient and element concentrations. Analysis of soil properties indicated that the bulk density and the ratio of magnesium and aluminum have potential for estimating the amount of post-construction sediment and nutrient deposition in engineered channels.

Further experiments are recommended for calibration of the miniature bed load sampler in different flow velocities, if reliable measurements of bed load transport are needed. The extendibility of the proposed soil and sediment properties for determining the rate of net retention is recommended to be investigated in other channels. The developed methodologies have useful applications and provide straightforward and time efficient measurements for example to understand the spatial variations of different processes in vegetated flows.

Keywords Sediment transport and deposition, Vegetated flow resistance.

Acknowledgements

The present study complemented ongoing scientific research activities in the Environmental Hydraulics Lab of the Aalto University, and contributed to the development of experimental methods required in using the Environmental Hydraulics Flow Channel as well as associated field and laboratory analyses on sediment and nutrient processes. This work was funded by Maa- ja vesitekniikan tuki ry.

I'm grateful to my advisor Kaisa Västilä, who provided excellent guidance, detailed comments and encouragement from the very beginning, making sure that at no point was I left struggling on my own. I want to thank my second advisor Walter Box for the constructive feedback and discussion he provided for my work, and for the effort he put in organizing the flume experiments while teaching me the principles of working at the flume. My advisor Juha Järvelä gave me valuable comments and taught me of good writing, helping me to find the proper structure and focus in the key parts of the thesis. I'm thankful for Tom Jilbert from University of Helsinki for organizing the elemental analysis, and for the important comments he provided for improving the chemistry-related parts of the thesis. I want to thank my supervisor Professor Harri Koivusalo for helping me make the work more concise and overall structure more logical with his throughout feedback.

My work at the Aalto University Water Laboratory was a great experience thanks to the staff and co-workers. I want to thank Antti Louhio for his efforts on the practical implementations throughout my stay. I'm thankful for Aino Peltola and Marina Sushko at the laboratory, who were always ready to assist when I had questions, and for Heikki Särkkä, who helped with the work practicalities and with arranging some of the equipment used in this work. I also want to thank the helpful staff at Aalto Fablab, especially Krisjanis Rijnieks and Jason Selvarajan, whose help was vital in getting the 3-D printing process started quickly.

Espoo, September 2019

Markku Andelin

Contents

Tiivistelmä
Abstract
Acknowledgements
Contents
Symbols
Abbreviations
Introduction 1
1.1 Research context 1
1.2 Objectives, rationale and organization of the thesis 3
2 Literature review 5
2.1 Sediment transport and its determination 6
2.1.1 Measuring suspended load 6
2.1.2 Bed load: samplers and their calibration 7
2.2 Vegetative flow resistance 13
2.2.1 Parametrization of vegetative flow resistance 14
2.2.2 Determination of drag forces 14
2.3 Sedimentary nutrients 17
2.3.1 Physical and chemical properties of soil and sediment 18
2.3.2 Pre-processing of soil and sediment samples 21
2.3.3 Elemental analyses with ICP-OES and CHN -analyzers 21
3 Materials and methods 23
3.1 Flume experiments on sediment transport and vegetative flow resistance 24
3.1.1 Flume setting for sediment transport measurements 24
3.1.2 Methodology for measuring suspended sediment transport 25
3.1.3 Bed load measurements 27
3.1.4 Vegetative drag force measurements 31
3.2 Field experiments on fluvial sedimentary nutrients 34
3.2.1 Field setting 34
3.2.2 Soil and sediment sampling 34
3.2.3 Pre-processing and elemental analysis of soil and sediment samples 37
4 Results and discussion 39
4.1 Down-scaled HS bed load sampler 39
4.1.1 Sample collection and validation of the used DHS in vegetated flows 39
4.1.2 Recommendation on the sampling duration of the DHS in vegetated flows 45
4.1.3 Discussion on measurement uncertainties and errors 49
4.2 Drag force measurements: influence of flow velocity, plant alignment and height 50
4.3 Laboratory nutrient analysis of soil and sediment samples 54
4.3.1 Soil and sediment profiles, medium-term nutrient accumulation 54
4.3.2 Effect of pre-processing steps on measured nutrient and element content 61
5 Conclusions 66
References 68
Appendix

Symbols

A_C	characteristic reference area
b	zero position of calibration curve
C_1	element concentration in <63 µm fraction
C_2	element concentration in >63 µm fraction
C_3	element concentration in non-sieved sample
C_D	drag coefficient
$C_{D\chi,F}$	drag coefficient of foliage
$C_{D\chi,S}$	drag coefficient of stem
C_{OBSa}	suspended sediment concentration at sensor A
C_{OBSc}	suspended sediment concentration at sensors C
F	force
k	slope of calibration curve
L	length of lever arm
l	distance between strain gauges
l_u	length of unscaled sample
l_s	length of scaled sample
M	bending moment at gauge
m_1	mass of <63 µm fraction
m_2	mass of >63 µm fraction
n	number of samples
p_n	scaling parameter of interval n
q_b	time averaged bed load transport rate
q_t	time averaged total sediment transport rate
q_s	time averaged suspended sediment transport rate
S	time-averaged load cell signal
t	time from beginning of experiment
u_C	characteristic approach velocity
$u_{\chi,F}$	reference velocity for foliage
$u_{\chi,S}$	reference velocity for stem
$\bar{V}$	moving mean of voltage
V_a	sensor A voltage
V_M	voltage measurement
x	longitudinal position in the flume
y	horizontal position in the flume
z	vertical position in the flume
α	calibration gain
β	calibration offset
ρ	density
χ	reconfiguration parameter
χ_F	reconfiguration parameter for foliage
χ_S	reconfiguration parameter for stem

Abbreviations

Al	aluminum
AS	acid sulfate
Ba	barium
C	carbon
Ca	calcium
CH/CHN	carbon, hydrogen and nitrogen (analyzer)
CV	coefficient of variation
DHS	downscaled Helley-Smith type bed load sampler
Fe	Iron
HS	Helley-Smith type bed load sampler
ICP-OES	inductively coupled plasma optical emission spectrometry
K	potassium
LISST	laser in situ scattering and transmissiometry
Mg	magnesium
Mn	manganese
N	nitrogen
OBS	optical backscatter sensor
P	phosphorus
S	sulfur
SSC	suspended-sediment concentration
Zn	zinc

Introduction

1.1 Research context

The presence of vegetation in aquatic environments can be both beneficial and undesired from the human perspective. Vegetation can hinder potable water conveyance or aggravate flooding, while it is important part of aquatic ecosystems (Luhar and Nepf 2013). Vegetation is the foundation of food webs, and provides several ecosystem services such as improvement of water quality through nutrient uptake and oxygen production, reduction of erosion and stabilization of riverbanks (Nepf 2012). Reduction of flow velocity by vegetation leads to changes in sediment transport and deposition, modifying river morphology (Vargas-Luna et al. 2015), and affecting sediment-bound nutrient and pollutant transport (Vanoni 2006). Whether deposition or transport of sediment is wanted in engineered channels depends on the boundary conditions, as both of them can cause negative impacts. For example, sediment deposition may lower the flood-carrying capacity of rivers, and sediment transport may decrease usability of water for human consumption and other forms of use (Vanoni 2006). Near agricultural fields, sediment transport in surface runoff is typically not desired as it can transport pollutants into surface waters (Lee et al. 2003). To decrease sediment transport from agricultural areas, riparian vegetation can be used to reduce the amount of suspended sediment from the runoff (Lee et al. 2003). Term riparian refers to transitional areas between terrestrial and aquatic ecosystems, such as river banks and floodplains (National Research Council et al. 2002).

Because of the effects of sediment on water systems from both environmental and human aspects, sediment sources are important in controlling the loads transported in rivers. Excessive amounts of sediment can enter river systems for example through erosion, or human activities such as mining and forestry operations (Owens et al. 2005). Urban drainage can also increase sediment loads in surface waters, and because sediments can transport contaminants and nutrients, efforts in improving water quality should recognize the importance of sediments as source of contaminants (Simpson et al. 2016). The sediment-bound nutrients can be used to assess health status of aquatic ecosystems, or to study seasonal and spatial variations of contaminant concentrations (Skordas et al. 2015). Environmentally preferable engineering solutions such as vegetated two-stage channels and bank vegetation can stabilize the channel by reducing erosion (Västilä and Järvelä 2011), and improve water quality by retention of sediments, sediment-bound nutrients and other substances (Västilä and Järvelä 2018).

The positive effects of vegetation on water quality were commonly neglected in the past in engineering and management of streams and rivers. For instance, the negative effects on flow conveyance led to management or removal of vegetation (Curran and Hession 2013). Current understanding of the importance of vegetation in riverine environment has initiated preservation of riverbank and floodplain vegetation, as well as river restoration and rehabilitation (Järvelä 2002). Improvement and protection of water quality has become a worldwide policy goal, and management of riparian vegetation has been commonly applied to pursue these goals (Dosskey et al. 2010). As an example, EU Water Framework Directive seeks to improve and preserve quality of aquatic ecosystems and riparian zones (Västilä and Järvelä 2018). Naturally, effects of riparian vegetation on chemical water quality has to be well understood as the results vary with different pollutants and site-specific conditions (Dosskey et al. 2010). Despite the recent focus on surface water quality, there are still knowledge gaps

in understanding role and parametrization of riparian vegetation e.g. for erosion and sediment transport and retention (Västilä and Järvelä 2018). In addition, the flood aggravation due to vegetative flow resistance remains (Wunder et al. 2009), estimation of which is needed for management and restoration purposes (Västilä et al. 2013).

To estimate effect of vegetative resistance on open channel flows in models, typically the flow resistance coefficients are modified to account for vegetation (Muste et al. 2017). Approaches consider vegetation at different scales (Västilä 2015), and the models used often require measurements for parametrization of the flow resistance (Muste et al. 2017) and performance evaluation (Västilä and Järvelä 2018). Similarly, understanding sediment transport in rivers requires measurement of bed load (Vericat et al. 2006), i.e. the sediments transported near the channel bed by rolling and sliding (Muste et al. 2017). As rivers change form by bed load transport, measurement of transport rates is necessary when assessing river restoration, channel stability and reservoir longevity (Marr et al. 2010). Direct measurement of bed load is needed because computational models cannot be reliably applied to all sediment sizes or flow conditions, and because the measurement can reveal the sediment size distribution (Helley and Smith 1971). Modelling in the presence of vegetation has progressed over the years, but still important aspects affecting sediment transport require further research. For example, vegetative drag reduces bed-shear stresses, which in turn directly affect sediment entrainment (Vargas-Luna et al. 2015). According to Vargas-Luna et al. (2015), research focusing on both the drag forces and bed-shear stresses are rare. Because of these challenges in sediment transport modelling, direct, preferably relatively straightforward measurements are beneficial.

Because of the important context and phenomena related to vegetated flows, reliable data is required to improve the understanding of the processes and to develop modelling, as well as for practical application of nature-based solutions. Specific attention is required for quantifying sediment transport, nutrient retention and vegetative flow resistance in both downscaled laboratory experiments and in complex natural conditions. For example, use of miniature bed load samplers, as well as use of samplers in sand beds have not been studied thoroughly (Gaudet et al. 1994). Differences in sampler properties and deployment reflect to measured sediment transport rate (Bunte et al. 2008), stressing the importance of calibration in case of modified sampler and measurement design. For vegetative flow resistance, parametrization of vegetation for modelling still needs improvement (Västilä and Järvelä 2018), and thus measurements directly determining the vegetation induced flow resistance are needed. In addition, nutrient deposition in new environmentally preferable channel designs including regions with variable inundation, vegetative and sediment conditions is not well understood (Rowiński and Kubrak 2002). Methods to estimate deposition in e.g. nature-based two-stage channels consisting of the main channel and a vegetated floodplain would improve knowledge of the phenomena and inform the design and management of such channels.

Flumes are commonly used for calibration of devices intended for field use, and can also be used to study flow and related phenomena in a controlled environment. Initiation of measurement devices used in flume or in field has to be thoroughly documented, and errors and uncertainties need to be analyzed to make the measurement process as transparent as possible and to ensure the device is accurate in later use. It is beyond the scope of this thesis to determine to what extent flume measurements represent field conditions. The framework described above is the context of this thesis, leading to the objectives presented in Section 1.2.

1.2 Objectives, rationale and organization of the thesis

The main goal of this work is to develop experimental methods for investigating flow resistance, sediment and nutrient transport in vegetated flows. Within the context of vegetated flows, there are knowledge gabs and need for improvement both in the theory and in practical methods as discussed in Section 1.1. The objectives aim to directly support the ongoing research by improving the methodology needed to measure bed load sediment transport, vegetative flow resistance, and long-term nutrient accumulation in vegetated channels, which are the three specific focus areas of this work. A literature review is conducted in the beginning of this work (Section 2) with the objective to identify different methodological approaches and their limitations, to support the main objectives discussed next.

The first objective of this work is to develop measurement methodology suitable for determining bed load transport in laboratory flume environment based on a down-scaled Helley-Smith type bed load sampler (DHS). Reliability of the downscaled sampler in measuring the same amounts of bed load in repetitive measurements in unchanged conditions, along with its accuracy regarding measurement uncertainties, are investigated. In the target laboratory, suspended sediment load is measured using optical turbidity sensors, but these instruments are not suited for monitoring sediment load in the close proximity of the flume bed, thus the need for separate bed load measurements. The DHS would potentially allow inexpensive and simple way to obtain indicative results e.g. on the influence of vegetation on bed load transport in flume investigations. Following research questions are related to the first objective: Does the original 7 x 7 cm HS sampler design work as downscaled version without disturbing the flow, with the limitations for wall thickness and roughness imposed by the 3-D printing? How is the DHS validated and compared to other existing methodologies used to measure sediment fluxes, and what are the errors and uncertainties related to the measurement process?

The second objective is to develop drag force measurement system for flume conditions to allow advanced parameterization of the vegetative flow resistance, such as the effect of plant alignment. At the target laboratory, previous drag force measurements have been conducted in a towing tank, but the system to be developed allows them in flume conditions. In the towing tank, the length of the tank and towing velocity limits the measurement duration. In comparison, the duration of drag force measurement in flume is not limited. More importantly, the measurement system in flume is intended to allow for example quick and simple changing of alignment of the studied plant. Research questions for the second objective are: How different practices in using the drag force sensor, such as re-attachment and alignment of the plant affect the vegetative flow resistance measurements? How plant leaf configuration affects the measurements?

The third objective is to develop methodology for investigating decadal-scale nutrient accumulation in environmentally preferable channels with complex soil and sediment conditions. Accurate data of ground level change in a constructed two-stage channel will be used to assess whether straightforward, cost-effective analyses of the physical and chemical soil and sediment characteristics can be used to determine long-term nutrient accumulation at sites where ground levels and depositional history have not been recorded. In addition, the conventional sample analysis process includes few heavily time-consuming steps such as wet sieving and manual grinding with pestle and mortar. In this work, possibility of leaving samples non-sieved, and instead electro-mechanically grinding even the large non-organic sand and gravel particles contained in the dried sample is investigated, to allow for more rapid

sample pre-processing prior to nutrient and elemental analysis. The experiments conducted in this work are necessary to determine if the sand and gravel particles release nutrients and elements in a way that affects the total concentrations measured from the samples, when subject to different levels of grinding. Research questions related to the third objective are following: What soil and sediment characteristics could distinguish the matter deposited after the channel was constructed? How do total elemental concentrations of soil and sediment samples depend on applied pre-processing?

The thesis is organized to support the development of the measurement methodologies related to the three objectives. The scope of the work is on the measurement processes, their development and related uncertainties. The data acquired in the experiments is used mainly to investigate the measurement process, and not the phenomena. That being said, some of the data from soil and sediment samples has implications and potential application for studying nutrient deposition.

2 Literature review

In the literature review, the concepts, methodology and procedures related to sediment transport, vegetative flow resistance and sedimentary nutrients are introduced (Sections 2.1, 2.2 and 2.3) to the extent required to support the development and practical implementation of related measurements in the experimental part of this work. The intent of the review is to study how measurements similar to this work have been conducted in past, to identify best approaches and potential uncertainties to be taken in account. At the end of Sections 2.1.1, 2.1.2, 2.2.2 and 2.3.1, it is explained how the considerations from the literature were used in measurements and data analysis in the experimental part of this work. Figure 1 illustrates the relationship between the main concepts, and the focus points of the addressed literature. Each of the three themes have a few focus areas, and methodologies used to measure these phenomena are discussed through examples (see bottom row of Figure 1).

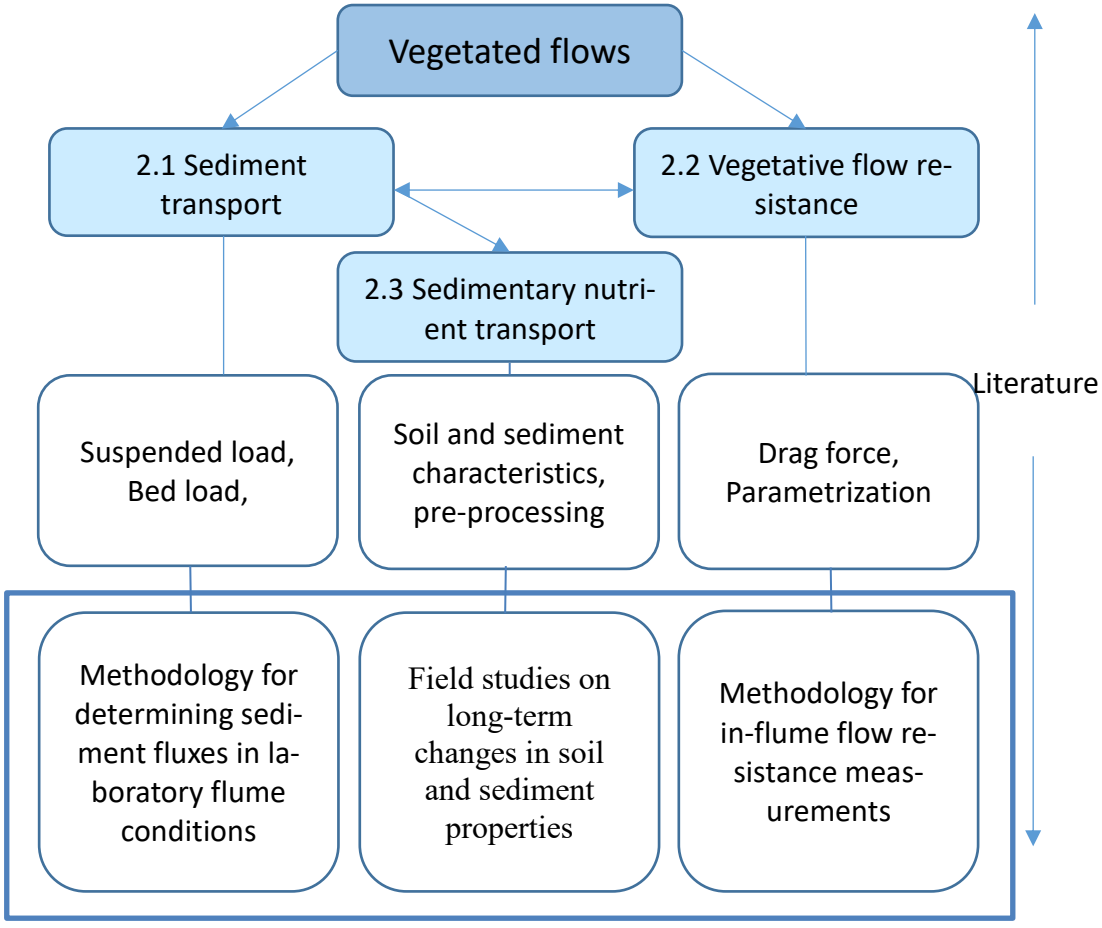

Figure 1: Scope of the literature review. Vegetated flow is the major theme under which sub-themes of sediment transport, vegetative flow resistance and sedimentary nutrient transport reside. Each sub-theme is addressed from points of view shown in the white cells. Number in front of sub-themes correspond to the corresponding section of the thesis. The cells surrounded with blue rectangle on the bottom row correspond to example studies beneficial for the practical application conducted in this work.

2.1 Sediment transport and its determination

Soil and sediment can enter water systems through erosion (Owens and Collins 2006), in which energy from water or wind dislodges soil particles from the surface (Pimentel 2006). Soil erosion can cause both on-site and off-site impacts. On-site impacts can be for example loss of agricultural productivity through erosion of fertilized top soil, and off-site impacts for example reduction of reservoir storage capacity through sediment deposition (Owens and Collins 2006). Measurement and modelling tools are required to manage erosion and sediment redistribution in river basins, as they provide necessary information for decision-making (Owens and Collins 2006). Sediment-bound nutrients and contaminants can also cause impacts in rivers. Sediment is commonly transported in rivers as suspended load and bed load (Sections 2.1.1, 2.1.2) (Muste et al. 2017). Transport of the sediment particles is not tied to one mode and depending on the flow conditions, particles can alternate between bed load and suspended load (Emmett 1980).

2.1.1 Measuring suspended load

Sediment is considered to be in suspension when it has no frequent contact with the bed (Julien 2010), and the weight of the particles is supported by the fluid (Einstein 1950). Suspended sediments are typically finer than sediments being transported as bed load, and are usually measured as concentration in the fluid in unit [mg/l] (Julien 2010).

Merten et al. (2014) explained that monitoring of suspended sediment transport is useful for estimating reservoir lifespan, considering land use management and estimating flux of pollutants absorbed by the sediments. In addition to measuring suspended sediment concentration, sometimes the sediment properties are of interest. For example, Smith and Owens (2014) explained how particle size distribution, nutrient and pollutant content, and organic matter of sediment are important factors when assessing impact of sediment in river systems. In these cases, a sufficient mass of sediment has to be collected for analysis (Smith and Owens 2014). Muste et al. (2017) discussed representative sampling of suspended sediment, which imposes several requirements for both the sampling methodology and the sampler. For example, if suspended sediment concentration is heterogeneous in vertical profile, not sampling near the bed leads to sampling being not representative of the whole cross-section (Muste et al. 2017).

Suspended-sediment concentration (SSC) is generally measured by either manual sampling, optical backscatter (OBS) or with acoustic backscatter (Admiraal and Garcia 2000). Admiraal and Garcia (2000) listed characteristics of the methods, and generally only manual sampling can measure sediment size distribution. Laser in situ scattering and transmissiometry (LISST) is exception to this, for LISST is capable of determining both SSC and sediment size distribution (Schillereff 2015). Other differences between manual sampling, OBS and acoustic backscatter relate to sampling rate and measuring volume (Admiraal and Garcia 2000). The different methods are discussed in higher detail next.

Optical turbidity sensors are an appealing choice for measuring SSC because of their capability of providing automated continuous data of SSC with high temporal resolution, and their relatively low cost (Schoellhamer and Wright 2003, Muste et al. 2017). The sensor operates by detecting infrared light scattered from suspended matter (Guillén et al. 2000). This suspended matter can consist of organic matter, clay, silt, microbes or dyes (Muste et

al. 2017). In principle, light scattered from suspended matter is received by the sensor and is converted into electrical impulse (Merten et al. 2014). The magnitude of the sensor impulse depends on the area of the illuminated particles, their shape and reflectivity (Downing 2006). SSC is proportional to the area of the particles scattering the light, which allows indirect estimation of SSC in conditions with concentrations typical for natural river flows (less than 50 000 mg/l for sand) (Downing 2006). Factors complicating the use of optical sensors include the low spatial resolution of the measurement, visibility through the lens due to residue accumulation, and various characteristics of sediments that cause differences in scattering of light (Merten et al. 2014).

Acoustic backscattering instruments can be used to measure flow velocity as well as suspended material concentration (Muste et al. 2017). The operating principle is similar to optical backscattering, but acoustic signal is more sensitive to grain size, which may limit the method applicability depending on grain size and SSC (Vousdoukas et al. 2011). Similar to optical backscatter, the intensity of return echo is proportional to amount of backscattering particles in the water (Kim and Voulgaris 2003). Estimation of SSC based on acoustic intensity becomes possible when most of the backscattering particles are sediment (Kim and Voulgaris 2003).

SSC can also be analyzed using standard water analysis methods from physical water samples. Muste et al. (2017) stressed how physical sampling of water- sediment mixture is necessary in many situations and is the only accepted reference technique to which new methods have to be compared. One type of physical suspended sediment sampler is isokinetic sampler. Isokinetic samplers are designed to collect representative samples of sediment load at their point of operation (Davis 2005). The sample is representative because the sampler is designed to have matching flow velocity through its nozzle compared to incident stream velocity (Davis 2005). Isokinetic samplers also try not to alter the direction of flow approaching the nozzle (Edwards et al. 1999). Two types of isokinetic samplers exist depending on the measurement method: depth-integrating and point-integrating (Davis 2005). In principle, depth-integrating samplers are moved vertically through the flow at uniform rate, collecting velocity- or discharge weighted sample along the way (Edwards et al. 1999). Point-integrating samplers are similar to depth-integrating samplers, but remotely controlled valve allows initiation and ceasing of sampling at desired point (Edwards et al. 1999).

OBS sensors appeared most suitable for measuring SSC in this work because of their high temporal resolution. The mentioned complications regarding their use are not an issue, as the sensors have lens wipers and are also manually cleaned, and sediment used is relatively uniform in particle size, meaning that changes in scattering of light depending on sediment characteristics are low. As a reference for OBS calibration, physical water samples were used in calibration of the OBS sensors and for scaling of the data between runs. This procedure is described in Section 3.1.2.

2.1.2 Bed load: samplers and their calibration

Bed load which consists of particles moving near the bed, can be separated into contact load and saltation load, but for convenience, they are joint under term bed load (Vanoni 2006). Contact load represents movement of particles by rolling and sliding, whereas saltation de-

scribes short jumps of the grains (Vanoni 2006). Contact load is initiated at lower flow velocities than saltation, higher flow speeds increase the frequency of saltation and may cause the particles to become part of suspended load (Vanoni 2006).

Bed load is measured by mass, volume or weight, which can be converted between each other using density or gravitational acceleration (Julien 2010). Bed load discharge corresponds to flux of sediment moving on the bed, measured as mass, volume or weight per unit time (Julien 2010). Finally, bed load unit discharge is bed load discharge averaged for unit width (Julien 2010).

Hubbell (1964) categorized bed load determination into three different approaches: direct measurement, estimation based on physical relations, and quantitative measurement of sedimentation processes such as erosion or deposition. In the case of deposition, the method would measure amount of sediment not transported further downstream. According to Hubbell (1964), each approach has its limitations: physical instruments are useful in limited hydraulic conditions and range of sediment, incompleteness of physical relations has not allowed precise bed load estimation, and quantitative measurements only describe the studied site. That being said, some recent models have greatly improved the estimation of bed load compared to earlier. For example, ratio of Recking's (2010) model estimation to measured bed load was within one order of magnitude in 83% cases, and the model required only few parameters of the site. To be exact, the load was calculated in three steps using discharge Q, slope S, grain diameters D_{50} and $D_{84,}$ and width W of the flow (Recking 2010). Accuracy of one order of magnitude can be considered satisfactory for a bed load transport model, as bed load measurements can typically differ with such magnitude (Ryan and Porth 1999, Recking 2010). Hubbell et al. (1985) explained how analytical bed load estimations often require large datasets and indirect-measurements are expensive. For these reasons, direct bed load measurements are an appealing choice, even though apart from pit-type samplers, they need calibration (Hubbell et al. 1985).

Commonly used field instrument for bed load sampling is the Helley-Smith (HS) pressure-difference sampler (Ryan and Porth 1999) (Figure 2), which was originally designed for use in natural rivers with coarse sediments, meaning that its accuracy in measuring finer sediment is not ideal (Helley and Smith 1971). Helley and Smith (1971) listed following design criteria for the instrument: it should be hydraulically stable, cause minimal flow disturbance, be operable by one person, and allow swift and efficient sampling. The shape with expanding rear section is designed to cause pressure-difference to trap the sediment, but also to match surrounding flow speeds at the orifice (Helley and Smith 1971). The original design has a 7.62 by 7.62 cm nozzle, but larger versions were designed to trap more and larger sediments in higher flowrates (Emmett 1980). The original sampler is constructed of 6.35 mm thick brass (Helley and Smith 1971).

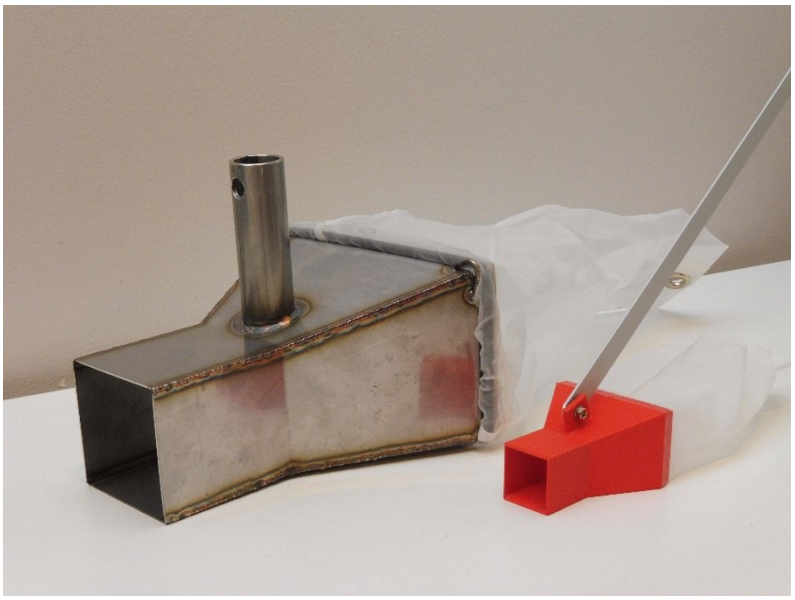

Figure 2: Original HS sampler and 3D-printed miniature sampler. Miniature sampler is discussed in section 3.1.3.

HS samplers do not solely capture bed load, but also some suspended sediment is caught (Emmett 1980). However, similar samplers have been designed to mitigate this effect. For example, Gaweesh and van Rijn (1994) used sediment collection bag with a patch of larger mesh size to allow flow-through of suspended sediments above estimated bed load layer. The patch and estimated streamline above which no bed load is transported is shown in Figure 3. The dimensions of their sampler are also different compared to HS sampler, and unlike HS sampler, it was designed for sand-bed rivers (Gaweesh and van Rijn 1994).

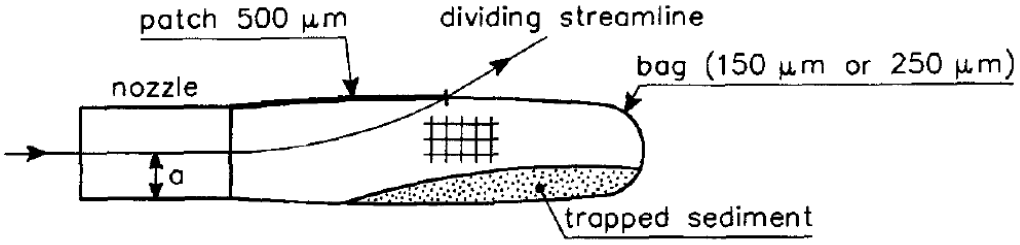

Figure 3: Details of Delft-Nile bed load sampler (Gaweesh and van Rijn 1994).

Changes in sampler design or scale (i.e. wall thickness, size, intake size and shape) are reflected in the measured bed load (Gaudet et al. 1994, Ryan and Porth 1999, Childers 1999, Vericat et al. 2006). Differences in measured bed load are obvious with large design changes, but in some cases, merely changing sampler wall thickness may lead to two-fold disparity in collected samples (Ryan and Porth 1999). Different sizes of HS samplers have been compared with each other and generally, larger samplers have caught larger amounts of sediment (Gaudet et al. 1994, Vericat et al. 2006). For example, in the experiments of Gaudet et al. (1994), 7.62 by 7.62 cm HS sampler captured approximately two times the amount of 3.0 by 3.0 cm HS sampler. Vericat et al. (2006) also described how sampler intake should be much larger than the collected sediments to better capture the real grain-size distribution.

Hydraulic characteristics of bed load samplers have also been researched. Helley and Smith (1971) used pitot pipe to measure flow velocities inside and outside of standard HS sampler. They measured ambient velocities as well as velocities within the sampler at vertical level matching nozzle centerline. Overall, velocities within the sampler were higher than ambient velocities. With ambient velocity of around 0.85 m/s, velocity within the sampler reached as high as 1.05 m/s. In addition, flow began to accelerate approximately 10 cm before the nozzle. Helley and Smith estimated that this acceleration would not greatly affect the sampler performance when used for coarse sediment. Druffel et al. (1976) state that Helley and Smith measured the velocities by towing the sampler in a tank, which allowed water to flow also under the sampler. For this reason, the results may be different should the sampler be placed on river or flume bed.

Druffel et al. (1976) conducted several experiments on HS samplers to determine its hydraulic efficiency, compare expansion ratios, study effect of sediment in the bag and to visualize flow in front of the sampler. Both original and larger 15.24 by 15.24 cm HS samplers were studied in varying flow conditions, placed on the flume bottom. With ambient velocity of 1.12 m/s, vertical velocity profile inside the nozzle of original HS sampler resembled that of an undisturbed flow, but was of higher magnitude. In this flow condition, acceleration of flow began approximately 7.6-20 cm upstream of the sampler. Results from sediment bag tests indicated that for coarse sediment, filling the bag even to 40% full did not affect the hydraulic efficiency of the sampler. However, finer sediment whose size matched that of the 0.2 mm mesh lowered the hydraulic efficiency. Druffel et al. (1976) also noticed that the sediment would plug the mesh and cause some sediment to start leaving the bag.

To determine the sampling efficiency, bed load samplers are usually calibrated in flumes (Hubbell 1964). Hubbell (1964) described the procedure as comparing weight of collected bed load to weight of bed load that would have passed the sampler width if the sampler was not there. Some general difficulties exist in determining bed load transport. Sampling efficiency is not necessarily constant, but varies in regard to transport rate and particle size (Hubbell et al. 1985). Another difficulty rises from the cyclic variation of bed load transport; when dunes are present, transport rate is near zero in the troughs (‘valleys’ between the dunes) (Hubbell et al. 1985). Examples of calibration procedures are given next.

Summary of the reviewed bed load sampler calibrations are given in Table 1, and the first three are described in detail in following paragraphs. More calibration instances exist, but flume studies were prioritized for the table. While the sampling efficiencies seem relatively similar between the different instances, it must be noted that most of the studies had several sampling efficiencies for different conditions, and only one value is shown here for each source. Calibrations of Helley and Smith (1971) and Emmet (1980) for sampling efficiency are not described here, yet they were included in Table 1 as additional examples of sampling efficiencies.

*Table 1: Reviewed instances of bed load sampler calibrations. Sampling efficiency is highly variable even within one source, meaning that the values are only indicative. *Approximate value from calibration curve, Fig. 8 of source. **Efficiency was given for 0.25-0.5 mm sediment, and was converted from (Measured bed load / 'Real' bed load).*

Sampler type	Nozzle (cm)	Flume Dimensions (Width, Depth, Length) (m)	Water depth (m)	Flow speed (m/s)	Sediment median size (mm)	True bed load / Sampled bed load	Source
Delft Nile	9,6 x 5,5	1,0 x 1,0 x 26,00	0.50	0.45	0.28	0.66	(Gaweesh and van Rijn 1994)
Helley-Smith	7,62 x 7,62	2,70 x 1,80 x 83,00	Q= 2.0-3.6 m^3/s		0.6-1.8	-	(Marr et al.(2010)
Helley-Smith	7,62 x 7,62 & 15.2 x 15.2	2,70 x 1,80 x 83,00	1.21	0.98	6.50	~0.44*	(Hubbell et al. 1985)
Helley-Smith	7,62 x 7,62	2,44 x 1,22 x 60,96	0.30	0.51	1.15	0.70	(Helley and Smith 1971)
Helley-Smith	7,62 x 7,62	River, width of ~14 m	~ 1	~1	1.25	0,57**	(Emmett 1980)

Gaweesh and van Rijn (1994) calibrated their Delft-Nile bed load sampler in a flume with 0.2 m thick sand bed. The bed material had a mean diameter (D_{50}) between 0.3 – 1 mm. Sampling periods were either 1, 3, 5, 10 or 15 minutes, and sampling was initiated when equilibrium conditions in terms of flow and sediment were reached within 80-100 hours. The sediment feed consisted of a container with three tubes releasing sediment approximately 0.2 meters above the bed. A sediment trap located at the end of the flume was used with sediment feed to determine total sediment transport rate. Suspended sediment was sampled with seven intake nozzles connected to hoses and pumps. Suspended sediment transport rate was calculated by integrating product of sediment concentration and flow velocity over the depth of flow. As for the calibration, Gaweesh and van Rijn (1994) estimated time averaged sediment transport rate from sediment feed and trap systems, and then subtracted time averaged suspended load transport rate to obtain actual bed load transport rate. This calculation is shown in Equation 1. It is important to acknowledge that the notations are not always universal between sources. For example, Hubbel et al. (1985) denote bed load measured by sampler with q_s, which does not match notation shown in Equation 1.

$$q_b = q_t - q_s \quad (1)$$

Where q_b is the actual time averaged bed load transport rate
q_t is the time averaged total sediment transport rate
q_s is the time averaged suspended sediment transport rate

Gaweesh and van Rijn (1994) then calibrated the sampler by comparing actual bed load transport rate computed with Equation 1 with transport rate measured by the sampler ($q_{b,m}$). Transport rate measured by sampler was averaged for width and time, and initial scooping of bed material was determined and subtracted from the measurements. The ratio of measured and actual bed load is called Sampling efficiency, and is denoted with α in their study. However, the ratio is sometimes calculated the other way around (Helley and Smith 1971). Gaweesh and van Rijn (1994) conducted several tests, each having different combination of

flow and bed conditions. From 30 to 100 bed load samples were taken during each run, and statistical moving average was used to calculate mean of the samples.

Marr et al. (2010) conducted similar experiments as Gaweesh and Van Rijn (1994) to calibrate several bed load samplers. Samplers were tested with sand and gravel beds, and among the tested samplers was a standard HS sampler. While the sediment trap used by Gaweesh and van Rijn (1994) was not elaborately described in their study, Marr et al. (2010) gave a very detailed description of their system. The bed load monitoring system consisted of five adjacent aluminum drums, which measured the submerged weights of trapped sediments. The drums were emptied automatically, but data was processed to record cumulative weight. Post-processing of the weight data was necessary to remove oscillating noise resulting from turbulence. For calibration, rate of change of the trapped sediment weight was of interest, to which bed load sampler measurements were compared. Sediment collected by the drums was recirculated back to the flume 10 m upstream of the test section. The tested samplers were operated manually by inserting them 8.5 m upstream of the weight-drums, in positions matching the five drum centers. Longitudinal position was kept consistent between runs by a tether line connected from upstream above the flume to bottom of the sampler rod. Sampling duration of either 15, 30, 45, 60, 75 or 90 seconds long were used. Finally, the samples were wet-weighted and automatically converted to dry weights. Actual calibration results were not included in this study (Marr et al. 2010), but presumably sampling efficiency would be calculated similarly to Gaweesh and Van Rijn (1994) using the rate of change of the weight measured by the weight-drums.

Hubbell et al. (1985) calibrated several bed load samplers, including standard 7.62 by 7.62 cm HS and larger 15.2 by 15.2 cm HS samplers. Their experimental setting was quite similar to that of Marr et al. (2010), as both tests were conducted at St. Anthony Falls Laboratory. It is important to know that while the settings are not identical, bed load monitoring done by weight-drums in Marr et al. (2010) were called weight-pans in Hubbell et al. (1985). Hubbell et al. (1985) discussed traditional calibration via sampling efficiencies, but acknowledged that if relationship between true and measured bed load transport rates is not linear, using group averages in estimating the sampling efficiency will cause errors. They used probability-matching method instead, which was valid under three conditions. Requirement was that amount of bed load samples was large enough to represent probability distribution of their population. Then, true rates at longitudinal positions and rates measured by weigh-pans should be identically distributed. Finally, for every sampled rate, there should exist a true rate at same relative position in the distribution. Hubbell et al. (1985) described it better: "That is, for every sampled rate, q_1, there is a corresponding true rate, q_2, that would have occurred at the time and place of sampling had the sampler not been there". First two conditions were easy to deem true, as over 120 samples were taken and hydraulic stationarity was observed along the channel. For the calibration, they used two different methods to determine relation between measured and true transport rate. First, a relation between bed elevation and true transport rate was conducted, and cumulative frequency distributions for both were formed. Then, bed elevation and weigh-pan rates were plotted on the same figure at selected probability levels. A high correlation coefficient of 0.990 was observed. Now, bed elevation measured at time and location of sampling could be used to estimate real transport rate of that given sample. The second method for the calibration was the probability matching method, where bed load values were picked from probability distribution functions of sampler and weigh-pan rates at 0.01 intervals, to plot the calibration relation. Both curves, derived from bed elevation and probability matching method, were plotted in same figure to

confirm viability of probability matching method. Hubbell et al. (1985) estimated that probability matching provides better calibration results for it utilizes more rate data and is more direct. However, Thomas and Lewis (1993) disagreed with the probability matching method of Hubbel et al. (1985). Their main issue with the method relate to the made assumptions, which according to them are invalid if any measurement or sampling errors exist.

The above-described procedures form a good basis for the calibration of bed load samplers. Main insight from the descriptions is that there has to be a way to estimate real bed load transport. Good solution for it appears to be a sediment trap, which in theory captures all sediments moving on the bed. Also, due to the sampling efficiency being affected by flow velocity, it is advised to determine the efficiency to different velocities instead of using average for a velocity range. Aside from not directly determining sampling efficiency of the DHS, the previous studies were used to design suitable sampling procedure and durations for the experimental part of this work. Since the DHS is used to estimate (total) near-bed sediment transport, the fact that HS type samplers collect also suspended sediment is not an issue. Also, plugging of the sediment bag was expected to be absent, because sampling bag of 35 μm mesh was used with sediment diameter ranging between 90-250 μm.

2.2 Vegetative flow resistance

Vegetation can cause several changes in fluvial conditions: it increases flow resistance, modifies sediment transport and deposition, and changes backwater profiles (Yen 2002). Increased flow resistance reduces flow velocities, which in return may decrease water turbidity, as the sediments are not kept in suspension as easily (Muste et al. 2017). Furthermore, vegetation maintains balance in fluvial ecosystems by nutrient uptake and oxygen production (Muste et al. 2017). Predicting these types of effects can be of use in flood management, stream restoration, agricultural drainage and also allow management of environmentally friendly sediment transport (Västilä and Järvelä 2018).

In principle, vegetation can be included in open channel flow calculations by modifying the flow resistance coefficient (Muste et al. 2017). Different approaches consider the vegetative resistance at different contexts, from small scale of leaves to reach scale (Västilä 2015). However, choosing the drag coefficient is difficult due to different conditions in which they were determined, due to coefficients being rarely studied on real plants, and because the parametrization presentation is not fully comparable between sources (Vargas-Luna et al. 2015). Also, bending and streamlining of plants reduce the drag and flow resistance, which is something that the numerical models should take into account (Västilä and Järvelä 2018). To assess performance of such models, experimental measurements can be conducted to provide values for comparison. For example, Västilä and Järvelä (2018) used towing tank data of measured drag forces of real plants and then compared them to resistance model outputs. In addition to model validation, in more complex cases data from experimental measurements is needed to parametrize drag coefficient for the vegetation (Muste et al. 2017). For example, Järvelä (2002, 2004) conducted experiments to determine friction factors and also computed drag coefficients for different plant species. Section 2.2.1 presents some approaches on how vegetative drag forces are parametrized, and Section 2.2.2 discusses how flow resistance can be measured in practice for either model validation or parameter determination.

2.2.1 Parametrization of vegetative flow resistance

Drag equation is often used when expressing drag forces exerted by a plant (Västilä 2015). The equation is as follows:

$$F = \frac{1}{2}\rho C_D A_C {u_C}^2 \quad (2)$$

Where
F is the drag force (N)
ρ is the density of the fluid (kg/m^3)
C_D is a drag coefficient of the object (dimensionless)
A_C is the characteristic area of the object (m^2)
u_C is the characteristic approach velocity (m/s)

Equation 2 is commonly used in conjunction with drag force measurements to determine C_D. In Section 2.2.2, some examples are given on how parameters such as A_C are determined or used with the equation.

To account for reconfiguration of plants, Västilä and Järvelä (2018) described following modified drag equation for drag forces caused by plants:

$$F = \frac{1}{2}\rho C_D A_C {u_C}^{2+\chi} \quad (3)$$

Where
χ is a parameter for plant reconfiguration

To better take into account the individual effects of foliage and stem on drag force, Västilä and Järvelä (2018) presented following equation with separate drag coefficients and reconfiguration terms for foliage and stem, denoted with subscripts f and s:

$$F = \frac{1}{2}\rho \left[C_{D\chi,F} \left(\frac{u_C}{u_{\chi,F}} \right)^{\chi_F} A_L + C_{D\chi,S} \left(\frac{u_C}{u_{\chi,S}} \right)^{\chi_S} A_S \right] {u_C}^2 \quad (4)$$

Where
$C_{D\chi,F}$, $C_{D\chi,S}$ are drag coefficients for foliage and stem, respectively
$u_{\chi,F}$, $u_{\chi,S}$ are the reference velocities for foliage and stem
χ_F , χ_S are reconfiguration parameters for foliage and stem

Reference velocities $u_{\chi,F}$, $u_{\chi,S}$ used in Equation 4 are the velocities in which reconfiguration parameters χ_F and χ_S were determined (Västilä and Järvelä 2018).

2.2.2 Determination of drag forces

Examples in this section are presented to demonstrate how vegetative flow resistance can be measured and what the general procedure required for the calibration is. Depending on the used methodology, additional steps in data processing may be required. For example, mounting structures used for the plants may exert forces in addition to the plant itself, and these additional forces have to be taken into account.

Direct measurements of plant drag forces are often conducted using load cells, which experience change in resistance in response to displacement caused by force exerted by the flow on the attached object (Wilson et al. 2008). This displacement or strain is converted to electrical signal, and in some cases the force and torque can be determined in all directions (Muste et al. 2017). Wilson et al. (2008) describe how main differences between load cell uses are often related to how the plant is attached to the cell, which is challenging when attempting to minimize forces coming from sources other than the plant itself. Generally, sensor is either submerged or above the water surface (Muste et al. 2017). Muste et al. (2017) explain how in some applications separate mounting installation is used for the plant, in which case the mounting structure also has its share in the measured drag. The load cells require accurate calibration, but the measurements after calibration may still be subject to errors e.g through improper alignment, temperature changes and vibrations from the setting (Muste et al. 2017). Some studies on drag force measurements are reviewed next, to explore different ways the measurements can be conducted and for which purpose.

Experiments by Statzner et al. (2006) were initiated to compare three different vegetation drag force parametrizations for macrophytes. They measured drag forces to calculate drag coefficients for vegetation, with a compression load cell integrated into the flume bed. Reynold's number was also calculated based on other measurements, to plot relations between drag coefficient and Reynold's number in different conditions. Aim of their study was to show that different ways of determining drag coefficient and Reynold's number leads to results not directly comparable.

Callaghan et al. (2007) had developed the drag force measurement setup used by Statzner et al. (2006). In principle, their setup consisted of trolley in which the plant is attached, and a horizontally mounted compression load cell, which measures the forces affecting the plant via the trolley. They had two different setups for low- and high flow conditions, mainly differing in weight to stop the trolley from being lifted. The actual setup could be either mounted beneath the flume or inside the flume under false floor. Callaghan et al. (2007) calibrated the measurement device by applying known forces with cable in tension, forces ranging from 0 and 4 N for both light and heavy setups described earlier. The tension was held for three seconds, during which load cell measured and sent signals at 10 Hz. These signals were averaged for time. The load cells were calibrated using Equation 5.

$$F_j = \beta_i + \alpha_i S_{j,i} \tag{5}$$

Where F_j is the force for time series j
β_i is the calibration offset for test i
α_i is the calibration gain for test i
$S_{j,i}$ is the time-averaged load cell signal

Callaghan et al. (2007) used least squares to linearly fit Equation 5 between load time-series and load-cell signals. This allowed the determination of calibration parameters β and α. Finally, Callaghan et al. (2007) also compared drag coefficients of different objects measured by their setup to those from literature. The drag coefficient was calculated from measured drag force using Equation 2, and the coefficient agreed well with literature values.

Similar to Statzner et al. (2006), Wilson et al. (2008) also used a drag force measurement system that allowed embedding of the device under the flume. Their study focused on effect

of foliage on vegetative drag forces. They attached single branch at a time to the measurement device. In their setup, two strain gauges measured bending momentums to determine drag force caused by the attached plant, and the distance of this moment from the gauges. Their setup and related notations are illustrated in Figure 4. Wilson et al. (2008) used Equation 6 to calculate distance of the drag force from strain gauges, and Equation 7 to calculate the actual drag force.

$$L = l\left(\frac{M_1}{M_2 M_1}\right) \tag{6}$$

$$F_D = \frac{M_1 - M_2}{l} \tag{7}$$

Where L is the length of lever arm
l is the distance between two strain gauges
M_1, M_2 are the bending moments at gauges 1 and 2
F_D is the drag force

When using Equation 2 to determine drag coefficient from drag force measurements, the frontal area of the object often causes difficulties as vegetation streamlines (Wilson et al. 2008). Wilson et al. (2008) avoided this by keeping drag coefficient C_D and projected area A_p (A_c in eq. 2) together as a product $C_D A_p$. For their purposes this was sufficient, as the ratio of $C_D A_p$ and drag force is directly proportional, meaning that foliated and leafless drag forces can be compared without determining frontal area of the plant.

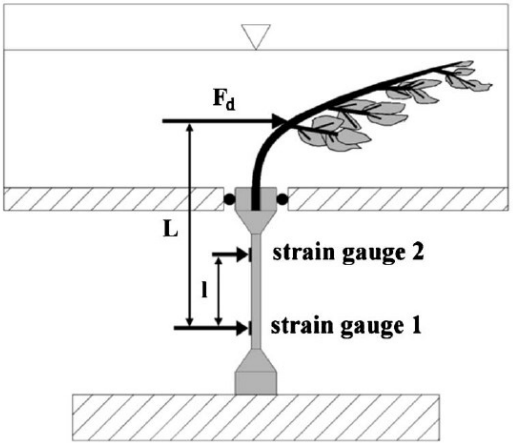

Figure 4: Drag force measurement using strain gauges (Wilson et al. 2008).

Wunder et al. (2009) developed a mounting device for measuring vegetative drag forces. Previous examples have utilized mounting of the device under or within the flume, but Wunder et al. (2009) attached it to flume walls. They conducted experiments in flow velocities in range of 0.3 – 0.6 m/s. The rectangular mounting framework was attached to flume walls and sat on toe bearings. Force sensor touched the framework with a spike, and would measure force as the flow tries to tilt the framework. The measurement device is illustrated

in Figure 5. Due to lever arm of the framework, corrections were needed for the measurements. A vertical balance point was chosen for these corrections, and is shown in Figure 5.

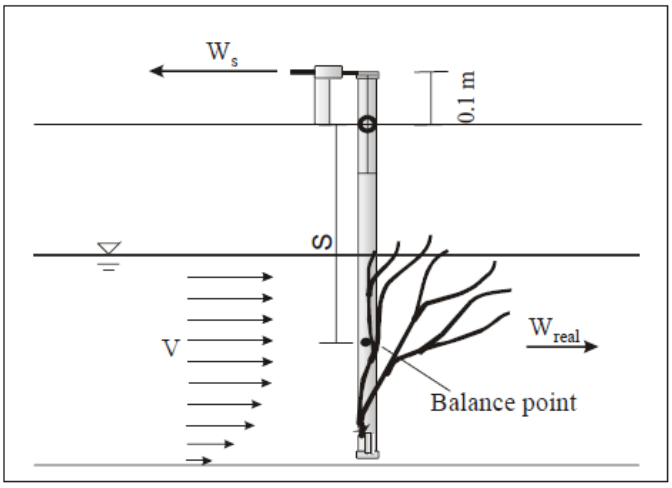

Figure 5: Side view of the mounting structure for drag force measurement, and related forces (Wunder et al. 2009)

Wunder et al. (2009) started their calibration by quantifying drag forces caused by the device itself. Empty framework was exposed to varying flow velocities to later subtract this force from vegetation measurements. Also, effect of toe bearings was considered by applying known forces to the system, allowing its removal from real measurements. Like has been mentioned before, Equation 2 requires projected area of the vegetation. Wunder et al. (2009) used underwater camera and image processing to calculate it. Finally, cylindrical elements were attached to the framework and their drag forces were measured. They calculated corresponding drag coefficients at different Reynold's numbers and compared the relation to literature sources. Their results agreed with literature verifying the applicability of their setup.

Based on these studies, a setup where sensor is submerged under the flume, appears the most suitable for plant parametrization. The fact that no mounting structures are subject to the flow means that only the vegetation exerts the forces on the sensor, making the use of Equations 2-4 more straightforward.

2.3 Sedimentary nutrients

This section describes how some sediment and soil properties change in time and what implications they may have regarding the soil and surrounding water systems. In the context of this work, soil and sediment properties are of interest as tools for assessing the amount of deposition, but also because the properties impose some requirements for the pre-treatment.

Of the fine-grained sediments transported in rivers, especially <63 µm fraction is chemically active and thus transports many contaminants and nutrients (Owens et al. 2005). The nutrient levels in rivers strongly correlate with quantity of agriculture in the area, and increased use of nitrogen in agriculture has been observed also in river concentrations (Stålnacke et al. 2003). Long term monitoring suggests that amounts of sediment transported in and into rivers are increasing in areas subject to human activity, and can cause problems from both

quantity and quality perspectives (Owens et al. 2005). According to Owens et al. (2005), these quality concerns can be for example eutrophication or human health related.

Nutrient and pollutant content of sediment can be of interest for different purposes. For example in lakes, the sediments can be used to analyze pollution history of the given lake (Bing et al. 2013). In rivers, runoff from agricultural areas can be analyzed to estimate influx of sediments and associated bound nutrients to the river (Lee et al. 2003). Lee et al. (2003) focused on determining effect of vegetation buffer zones on trapping sediment runoff from agricultural fields.

2.3.1 Physical and chemical properties of soil and sediment

In lakes, chemical characteristics of bottom sediment layers can be used as sequential record of post-glacial matter deposited in the lake (Mackereth 1965). It is hypothesized that composition of deposited material is affected by the rate of erosion in the basin, because the erosion rate affects how much time the sensitive components have to directly leach into water (Mackereth 1965). With high erosion rates, the sedimented material resembles the origin more closely, as the eroding particles have been subject to leaching for shorter amount of time and are generally larger in size (Mackereth 1965). According to Mackereth (1965), Sodium (Na) and Potassium (K) could be considered these kind of sensitive components that are easily removed in solution, meaning that variation of their concentration in lake sediments could be linked with the rate of erosion. In principle, high Na and K concentrations in lake sediments indicate period of high erosion rates of mineral particles, and low concentrations period of soil stability (Mackereth 1965). Patterns of Magnesium (Mg) in sediment are also result of the same phenomena as with Sodium and Potassium (Mackereth 1965).

Sediment removal from aquacultural ponds strongly disturbs the bottom soil characteristics. Yuvanatemiya and Boyd (2006) compared some physical and chemical attributes of the pond bottom soil between renovated and un-renovated ponds, and they also used data of original pond bottom soil from other studies. Differences were observed in bulk density, which was much higher for bottom soils of renovated ponds and original beds than un-renovated ponds, indicating that the deposited sediment had lower density than the original bed. Also, un-renovated ponds had less compact bottom soil, which led to higher pore space and moisture content compared to renovated and original pond beds. Concentrations of elements such as phosphorus, calcium, magnesium, potassium and sodium were higher in sediments of un-renovated ponds. However, elevated concentrations of many of these elements was said to be due to fertilizers, feeds and liming materials used for the aquacultural activity. Therefore, differences between renovated and un-renovated bottom soils of locations where aquaculture is not practiced may differ from results presented in this study. The fact that bulk density of renovated ponds differs from deposited material needs to be considered in analyzing sediment data. The level in soil cores where deposition starts likely shows visible difference in bulk density.

Passoni et al. (2009) studied changes in soil properties in wetland between years 1996-2007. The wetland was constructed for removing contaminants from surface flows coming from farmlands, and vegetation of cattail and common reed was planted on the wetland. The wetland was excavated for depth of 0.4 m from the original soil surface, and soil properties were monitored at different depths in years 1996, 2003, and 2007. In the results of Passoni et al.

(2009), organic carbon concentration remained fairly constant for the first 7 years, but increased significantly during the timeframe 2003-2007. This change was observed in the top 5 cm soil layer, and is believed to result from large amount of biomass present in year 2003. Difference in nitrogen concentrations between top 5 cm layer and 20-25 cm layer increased significantly by year 2007. Carbon to nitrogen ratio increased between years 2003-2007, especially in the 20-25 cm layer. Total phosphorus concentration remained fairly constant during the monitoring period, which they suspect to relate to low phosphorus inputs. Soil bulk density after the initial excavation was fairly homogeneous in the depth profile in year 1996. In year 2003, bulk density had decreased in the first 15 cm of soil and slightly increased deeper than 20 cm. It is difficult to assess absolute change at one point in the profile as the study does not state which parts are possibly newly deposited soil on top of the original soil.

Ballantine and Schneider (2009) also studied soil development in wetlands. Their data extended over period of 55 years and focused on soil bulk density, organic matter, standing biomass and litter, and different nutrients. Regarding soil bulk density, results of Ballantine and Schneider (2009) agreed with those of Passoni et al. (2009); soil bulk density decreases over time. The change in soil bulk density seemed to be fastest in the top 0-5 cm layer (Ballantine and Schneider 2009). Concentrations of some nutrients such as Potassium, Magnesium, Phosphorus and Calcium increased over time, while concentrations of iron, manganese and aluminum did not show relation to time. Finally, soil organic matter increased over time, and the change was largest in the first 0-15 cm from the soil top.

Some soils are classified as acid sulfate (AS) soils, and they are found in different locations around the world (Boman et al. 2008). In Finland, they locate mostly in the western coast, and originate from sediments deposited in the Baltic sea containing iron sulfide (Boman et al. 2008). Lands containing these sediments are formed as a result of land uplift (Nyberg et al. 2012). Agricultural drainage removes water from the soil which exposes the iron sulfides to air, leading to oxidization (Boman et al. 2010). In principle, the oxidization leads to formation of acidic soil as well as acidic runoff containing different metals (Boman et al. 2010). The runoff contains also large amounts of sulfate, which reflect to the soil profile in which sulfur is present at notably lower concentrations above depth of artificial drainage compared to the non-oxidized layers (Boman et al. 2008). The soil profiles are illustrated in Figure 6, showing how sulfur concentrations are much lower in the region where the soil is occasionally dry due to water level variations. Therefore, it is hypothetically possible to locate the lowest depth that water surface has been at from the sulfur profile, at depth where sulfur levels rise significantly. Also, in cases where part of the soil has been excavated in past, the deposited sediment has lower sulfur concentration as most of the sediment has likely eroded from the oxidized topsoil (from soil where sulfur has already leached). Large increase in sulfur concentrations therefore indicates the lower limit for past ground level created by excavation, as either oxygen has reached further into the soil than before excavation, or because new deposited sediment is lower in sulfur concentration.

Burton et al. (2011) studied how re-flooding of once dried coastal lowland acidic-sulfate soil affects mineralization of Fe-S in Australia. The site was originally tidal marsh, and it was drained for agricultural purposes. The water level was drained around 0.6-0.8 meters below sea level, but median water level after remediation was slightly above sea level. Daily fluctuations would occasionally dip below sea level. Lime was also used in the remediation. Burton et al. (2011) studied pore water and soil samples taken from the site 7 years after the

re-flooding was initiated. Their results indicated that acidity of the soil was neutralized and sulfate was reduced. The sulfate reduction products included elemental sulfur, greigite and pyrite. It could be also observed from their data that sulfur concentrations were substantially larger below the depth of original drainage, similar to Boman et al. (2010). This may indicate that even after re-flooding, clear increase in sulfur amounts below the drained layer remain.

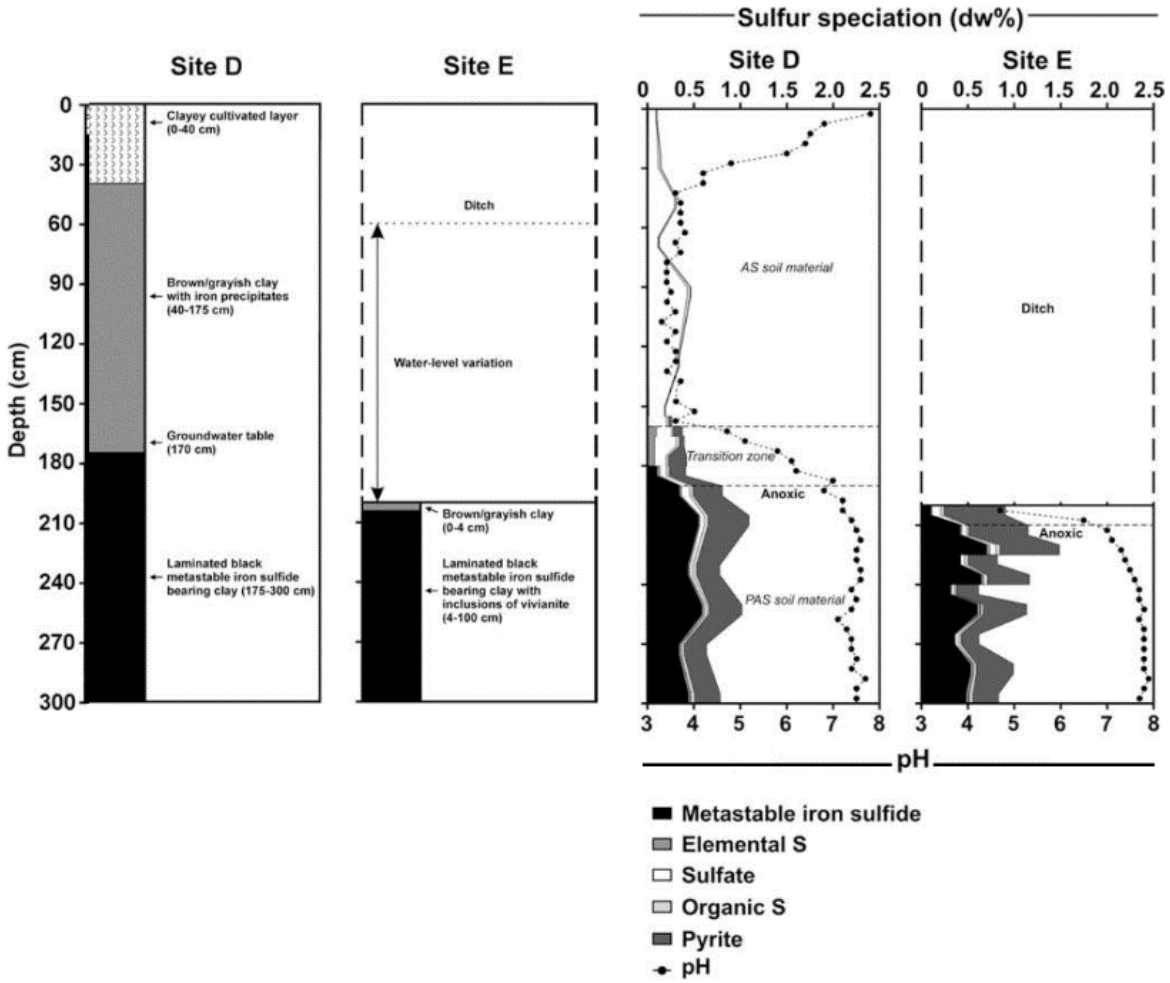

Figure 6: Soil conditions, water levels, sulfur concentrations and pH of sites studied by Boman et al. (2010) (modified). Site D represents drained acid sulfate soil, and site E is a drain adjacent to site D.

Based on these studies, it appears that soil properties are not commonly used in estimating amount of deposition the way that is attempted in this thesis. Changes in the properties were often linked with time, but it is still different from linking them with deposition. Generally, the deposited soil was not explicitly separated from the original soil (study by Yuvanametiya and Boyd (2006) was an exception). While the previous examples can form a basis for interpreting soil and sediment data in this work, they should not be considered strictly true for all cases. Conklin (2014) explains how soil properties are formed differently depending on the climate, source material, biota, topography, climate and temperature. Different components of soil can affect its chemistry for example by controlling how air and water move within (Conklin 2014). For these reasons, soil properties and their chemistry differs from case to case, meaning that extending observations between sites should be done with caution. Also, with the reviewed studies it was difficult to assess if the changes in soil properties were

at the same point in the profile or did the later profiles perhaps start higher because of deposited sediment. Therefore, to interpret data acquired in this work, there is a need to retrieve a benchmark sample from position where depth profile can be associated with real deposition. This could be used to link soil and sediment properties with deposition on other sites.

2.3.2 Pre-processing of soil and sediment samples

Before chemical or toxicity tests of sediment samples, manipulation such as sieving and removal of indigenous biota need to be considered depending on the research question. If information is needed on how contaminants are distributed in different sediment size fractions, coarse material needs to be removed to not interfere with subsequent analysis (Simpson et al. 2016). However, the sediment manipulations likely alter the sediment properties, and therefore the possible effects need to be considered (Simpson et al. 2016). Effect of pretreatment on soil properties is also acknowledged in ISO standard 11464 (ISO 2006). In case of acid sulfate soils, pre-processing can affect metal fractionation (Claff et al. 2010). Drying and grinding of samples reduced amount of metals in pyrite-fraction and increased metals in labile fraction (Claff et al. 2010).

To analyze physico-chemically stable and non-volatile parameters of soil samples, some pretreatment is required according to ISO standard 11464 (ISO 2006). In summary, samples are dried, weighted, sieved, mixed and subdivided. After sieving, particles larger than 2 mm are often crushed. The crushed particles can be mixed with the smaller fraction. If a small portion (<2 g) is taken for the final analysis, larger mass is ground to smaller particle size to ensure homogeneity before subsampling. The standard does not describe the purpose of the pre-treatment, but it is likely suggested to ensure homogeneity and representativeness of the sample. According to Claff et al. (2010), process of drying, sieving and grinding of soil prior to laboratory analysis creates a more homogeneous and stable sample. There may be other motivations in addition to homogenization. For example, Leong and Tanner (1999) wet sieved their samples prior to organic carbon analysis to remove inorganic carbon contained in coarse particles, as well as to avoid effect of grain size in further analysis.

2.3.3 Elemental analyses with ICP-OES and CHN -analyzers

Heavy metal content in sediments can be of interest for example to assess contamination level or origin of the soil or sediment (Bettinelli et al. 2000). Human activity can elevate heavy metal levels in ecosystems, which in turn can cause harmful effects for environment and human health (Alomary and Belhadj 2007). When assessing the contamination of sediment, typically the total element content of the sediment is compared to national guidelines to determine if the metal content is in the range of background levels (Chand and Prasad 2013). In addition to heavy metals, the micro and macro nutrients (for example sulfur (S), phosphorus (P), magnesium (Mg), potassium (K) and nitrogen (N)) of soil and sediment can be of interest, for example to assess nutrient deposition in different parts of natural channels. Element contents of samples can be determined with inductively coupled plasma optical emission spectrometry (ICP-OES) (Naozuka et al. 2011), and carbon, nitrogen and hydrogen contents with CHN-analyzers (Yamamuro and Kayanne 1995).

In ICP analyzer, sample is introduced into plasma, where light emitted from elements contained in the sample is focused to a mono- or polychromator (Olesik 1991), which separate

light according to wavelength (Charles and Fredeen 1997). Elements have characteristic wavelengths at which they emit light, and observation of such spectral lines can be used to determine which elements are in the sample (Charles and Fredeen 1997). To assess quantities of certain element in the sample, intensity of emitted light can be compared to calibration curves (Charles and Fredeen 1997). The sample exposed to the plasma needs to be in solution, and is mainly digested in acid (Chand and Prasad 2013).

CHN-analyzers operate by introducing sample along with oxygen and carrier gas into a combustion column, from which combustion products move on to a reduction column (Yamamuro and Kayanne 1995). Combustion products include NO_X, CO_2 and H_2O, of which NO_X is reduced to N_2 after removal of excess oxygen from the column (Yamamuro and Kayanne 1995). Finally, the Nitrogen and carbon contents are detected by measuring thermal conductivity. The analysis process may include calibration and control using samples of known carbon content. For example, Leong and Tanner (1999) used Cystine for calibration and as control samples in their tests to monitor if the instrument conditions remained constant.

3 Materials and methods

The experiments conducted in this work are divided to flume experiments for the DHS and drag force sensor, and into field and laboratory experiments conducted for the soil and sediment samples (Figure 7). Section 3.1 describes the used flume conditions, instruments, data processing and other steps related to the flume experiments of both bed load sampler and drag force sensor. In Section 3.2, the study area, and the sampling and pre-processing steps conducted for the soil and sediment samples prior to nutrient and elemental analyses are described.

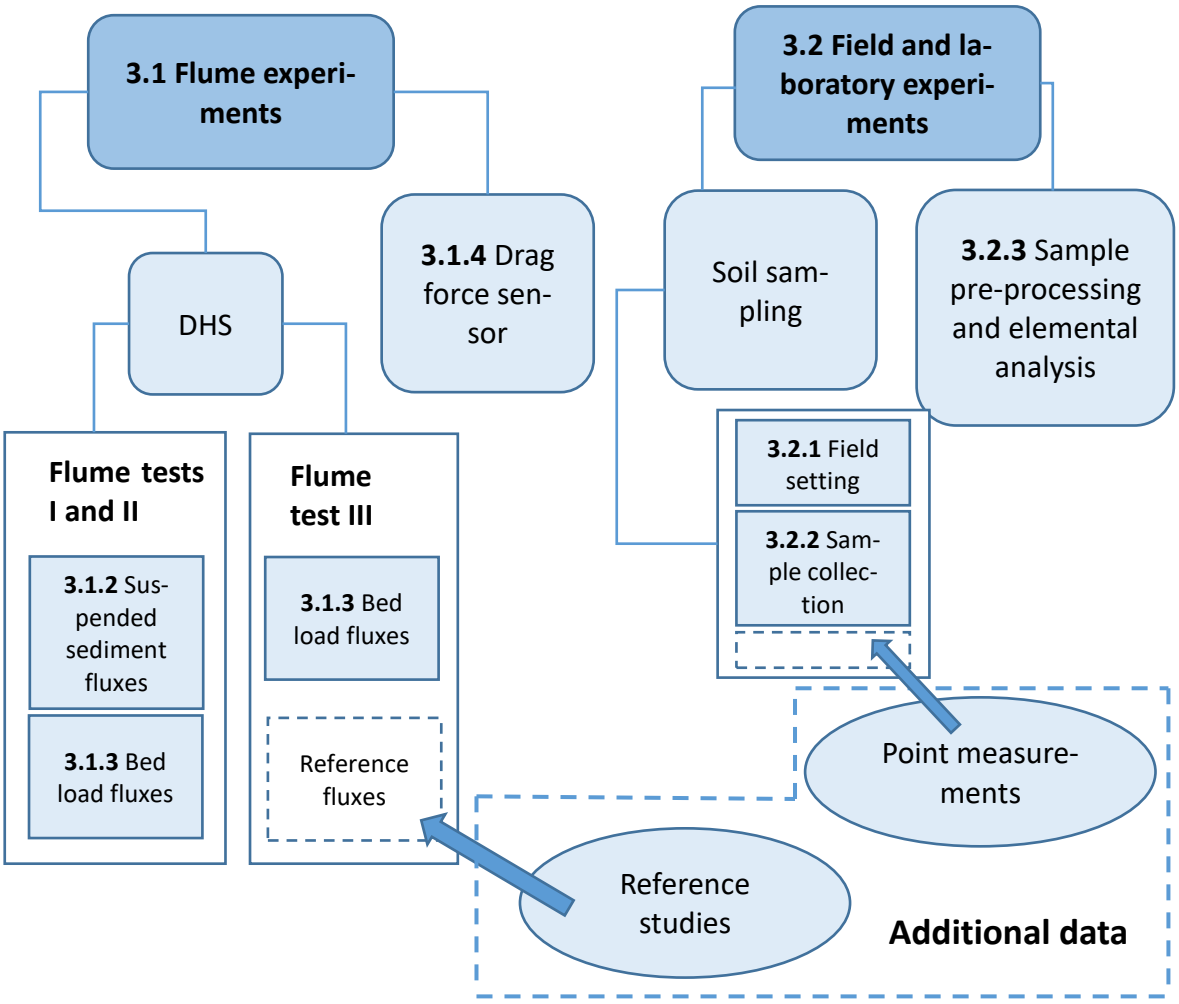

Figure 7: Structure of materials and methods (Section 3). Numbers in the figure indicate the Section in which the settings are described. Additional data not collected in this work was also used in the analysis, and is indicated with the dashed borders.

3.1 Flume experiments on sediment transport and vegetative flow resistance

The flume experiments for bed load sampler and drag-force sensor were conducted at Aalto Environmental hydraulics laboratory. The flume is 20.3 m long, 0.6 m wide and 0.8 m deep. The working section is glass paneled and 16 meters long, and is illustrated in Figure 8. The flume is capable of producing flow rate of 0.120 m^3/s in self-contained mode, and can be tilted between -0.75-2.1% (Järvelä 2018). Water depth was monitored along the length of the flume by electronic manometers measuring the water pressure.

3.1.1 Flume setting for sediment transport measurements

In the bed load experiments, a sediment feed system was located upstream of the working section, capable of feeding rate of 1.3 – 2.4 g/s. Suspended sediment loads were continuously monitored using optical turbidity sensors. The suspended load can be monitored at chosen longitudinal, horizontal and vertical positions, which can be changed during the run. More details on the conducted suspended sediment measurements are given in Section 3.1.2. The sediments were re-circulated back into the inlet of the flume, which increased the sediment load gradually over the duration of experiments.

The OBS sensors and bed load sampler were mounted on rails located on top of flume walls. Longitudinal position (x) of the instruments could be changed with the rails, and the mounting devices allowed for horizontal (y) and vertical (z) adjustment.

Overall, 3 different flume tests were conducted using the DHS, and one experiment for the vegetative drag force measurements. The flume setting was different in the drag force measurements compared to DHS sampler experiments, and is described in its own section 3.1.4. The purpose of the DHS measurements was to investigate the reliability and accuracy of the samplers, to evaluate their suitability for in flume bed load measurements. In tests I-II, the samplers were used to collect bed load fluxes of various magnitudes in the channel-cross section under different vegetative conditions. Test III was intended for comparing bed load fluxes measured by the DHS with literature values. Vegetative conditions and used sampler of each DHS experiment are described in Table 2, grass and vegetation pattern used is visualized in Figures 8-9. The experiments are described in higher detail in Section 3.1.3.

Table 2: Summary of bed load measurement settings.

Test	Grass	Plants	Sampler	Sediment source
I	X	Foliated	2 by 2 cm	Feed
II	X	Leafless	2 by 2 cm	Feed
III	-	-	2 by 2 cm	Bed

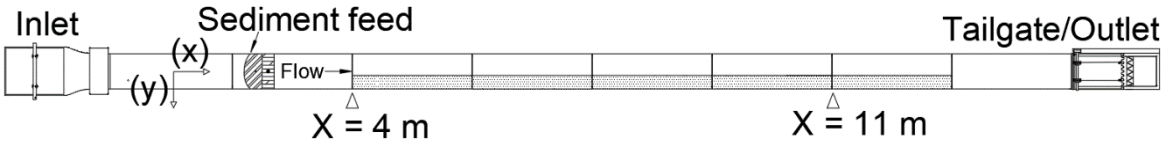

Figure 8: Top view of the 16 m working section, inlet and outlet of the flume. The area with bottom grasses in tests I, and II is indicated by the dotted pattern. Sampling location in tests I and II was at X=11.595 m. Figure is drawn to scale.

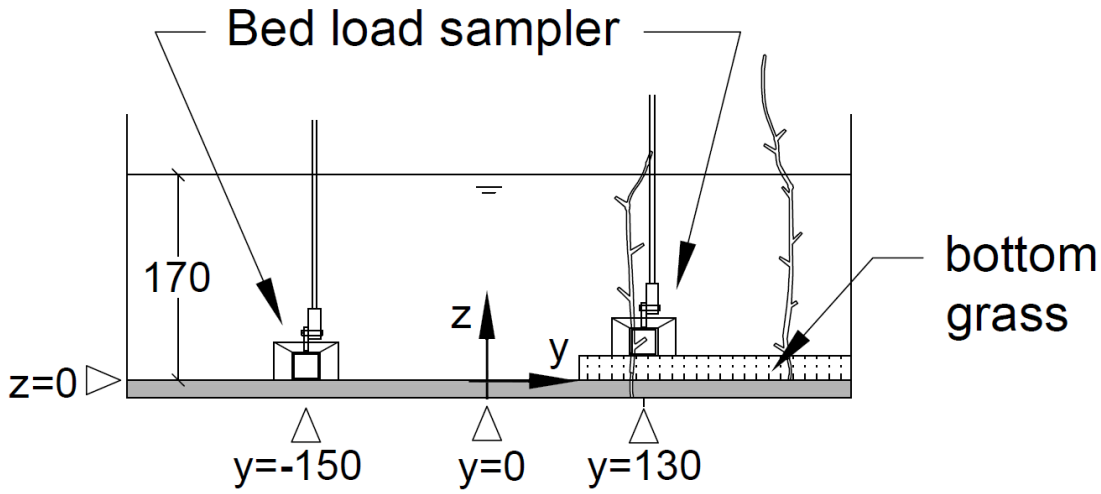

Figure 9: Schematic cross-section of the vegetated flume setting without reconfiguration of the vegetation. The leafless plants correspond to setting II. The 2 by 2 cm samplers are drawn to scale, but the mounting device is not. The positions of the samplers match to the sampling locations used in tests I and II. All units are in millimeters.

3.1.2 Methodology for measuring suspended sediment transport

The sediments used consisted of natural silica quartz, with dry bulk density of 1.4 g/cm^3 and median diameter of 150 µm, similar as in Box et al. (2018). Part of the sediment has been used in other experiments prior to this work, and it is possible that some of the finer particles have been lost in the process. Therefore, the mean particle size is likely larger than documented, but this is not believed to affect the measurements.

Suspended sediment concentrations were measured in tests I and II (introduced in detail in Section 3.1.3) with three OBS sensors: A, B and C. Sensors A and B were used as reference sensors placed at a fixed position, both mounted at water depth of 95 mm. Longitudinal positions were x=3 m and x=8 m for sensors A and B, respectively. Sensor C was used to measure suspended sediment concentrations at different vertical positions. In experiments I and II, OBSc measured between bed load measurements at the same longitudinal position as bed load sampler, x = 11.595 m. Vertical position z was altered between 10 and 85 mm in unvegetated part of the channel, and between 30 and 85 mm in vegetated part of the channel.

Due to interference to the sensor from the vegetation, minimum height of suspended sediment measurements had to be higher in vegetated part of the channel than in unvegetated part.

The sensors were installed to record voltage with 20 Hz. Voltage was converted to suspended sediment concentrations in mg/l, using a sensor specific voltage-concentration –calibration, following equation 8. Calibration curve indicates how sensor voltage output responds to water sediment concentrations. In the calibration, water was extracted at same x- and z-positions as the OBS sensors, and y-positions were -100, 100 and 200 mm for OBS sensors and 0 mm for the water extraction. Extraction was done with a tube, from which approximately one liter of water was bottled through a filter. By weighing the filter and bottled water, estimation of real concentration could be calculated. A set of five measurements of increasing concentration between 20-250 mg/l were taken.

$$C_{OBSa} = V_a k + b \tag{8}$$

Where C_{OBSa} is SSC at sensor A
V_a is Voltage measured with sensor A
k is slope of calibration curve
b is zero position of calibration curve

Sediment concentrations increased over time due to recirculation of sediments back into the inlet of the flume. Therefore, direct comparison of concentration measurements taken at different times during the experiment required scaling in relation to first measurement. Sensor A was used for the scaling, and scaled concentrations at time t=n was calculated with Equation 9.

$$C_{OBSc}(t = n)_{Scaled} = \frac{C_{OBSa}(t=0)}{C_{OBSa}(t=n)} C_{OBSc}(t = n) \tag{9}$$

Where C_{OBSa}, C_{OBSc} is SSC at sensors A and C, respectively
t is time from beginning of experiment

To account for the sensitivity of the calibration used, the OBS measurements were scaled for individual runs using physical samples, taken few times throughout the run, similarly as with the calibration. The scaling was done to take into account differences in conditions compared to calibration setup. The differences were result from inconsistency in removing sediments from previous runs and also from fine sediments suspended in the water.

Temporal variations in suspended sediment concentrations were estimated using moving mean of the OBSc voltage data, shown in Equation 10. In the analysis of the results, 1-second and 10 second (n = 20 or 200 Hz) moving averages were used to reveal short- and long-term temporal variations in SSC.

$$\bar{V} = \frac{1}{n}\sum_{i=0}^{n-1} V_{M-i} \quad (10)$$

Where $\bar{V}$ is the moving mean of voltage
V_M is the voltage measurement
n is the number of samples

3.1.3 Bed load measurements

Sampler design and 3-D printing

Two miniature HS samplers were 3D-printed at Aalto FabLab. The samplers were printed from polylactic acid (PLA) using LulzBot Mini 3D printer. The 3D models for the samplers were based on 2D drawings of Helley and Smith (1971), and were drawn in Solid Edge. The design of 3 by 3 cm HS sampler is shown in Figure 10 (the actual printed product is in Figure 2). The miniature 3D model was exported as stl. filetype, and was sliced and converted to gcode in Cura to be used by the printer. The dimensions of the original sampler were scaled down with ratios 7.62:3 and 7.62:2 after converting to SI units, to produce miniature samplers with 3 by 3 and 2 by 2 cm nozzles. To ensure the samplers are sturdy enough, walls of 2 mm and 1.5 mm thick were chosen for the larger and smaller one, respectively. The printer operates by printing the object in layers. Despite the layering, the walls were hydraulically smooth minimizing flow disturbance by the samplers. Number of layers used for the miniature samplers was in the range of 500-800, and the layers were perpendicular to the longest dimension shown in Figure 10.

A small extent with a 4 mm diameter hole was included on top of the sampler, which was used to attach the sampler to a holder. The holder was used to move and fix the sampler on the desired in flume locations. A sediment collection bag with 35-µm mesh was glued to indent on the rear of the sampler. The bag was relatively large and long to avoid blockage of flow caused by collected sediment. The indent was designed to keep the profile of the sampler smooth even with the bag attached. Finally, part of the nozzle touching the flume bed was sharpened to allow entrance of sediments without them getting stuck against the sampler bottom wall.

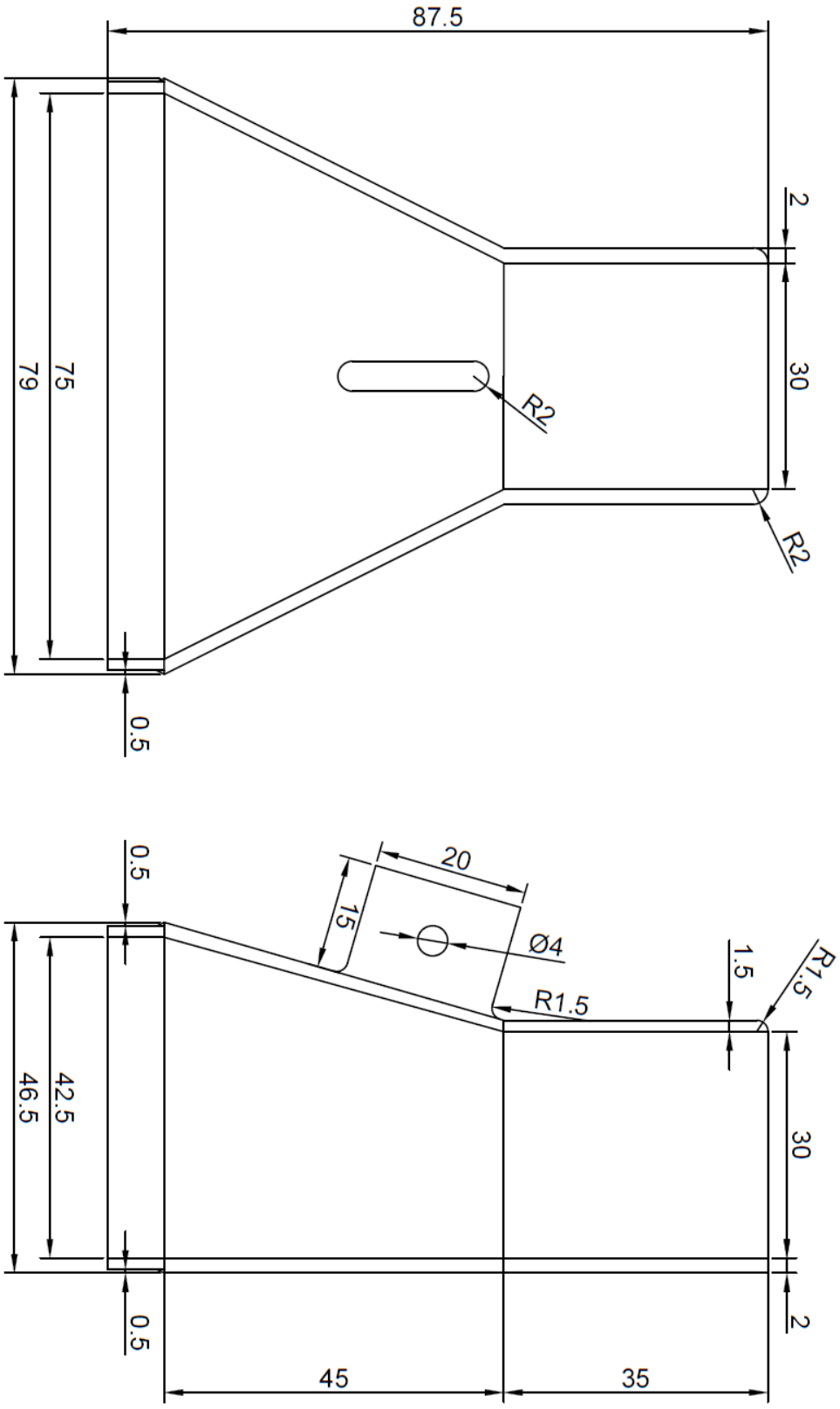

Figure 10: Schematic top view (top figure) and side view (bottom figure) of 3 by 3 cm HS sampler. Design is based on drawings of Helley and Smith (1971). All dimensions are in millimeters.

Flume tests I and II

Two flume tests (I: high flowrate (HQ), II: medium flowrate (MQ)) were conducted to estimate bed load sampling variability in vegetated conditions, and to validate HS sampler measurements with suspended sediment measured with OBS. The OBS data was also used to assess if bed load sampling durations were sufficient, by seeing if temporal patterns of sediment transport were captured. Metadata of the two experimental runs is shown in Table 3. In these tests, HS sampler with 2 by 2 cm nozzle was used, mounted into a trolley from which it could be lowered into the flume bed 11.595 m in the downstream. Sampler was lowered into the water bag-first, nozzle facing upwards to allow all air to escape the sampler bag. When the sampler was fully submerged, it was tilted parallel to flume bed and lowered to correct depth. During test I (HQ), measurement timing was initiated right when the sampler was submerged, but during test II (MQ), both time when sampler entered water and time when sampler was properly aligned at correct depth were recorded. This was done because of uncertainty if notable amount of sediment is being collected even if sampler is not properly placed yet. To further study this, one sample was taken without lowering it to the flume bed. This could be used as estimate on how much sediment will enter the sampler before it is properly placed one the flume bed, and to compare the sampler measurement to OBS measurement taken from same distance above the bed. Bed load measurement positions given in Table 3 are shown in Figures 8-9, where placement of vegetation and grass is also shown.

Table 3: Details of bed load measurement runs conducted in vegetated conditions. Positions (x, y, z) and duration of the bed load measurements in the unvegetated and the vegetated part of the channel.

Experimental run	**Vegetation**	**Discharge (m^3/h)**	**Slope (%)**	**Water depth (mm)**	**Sediment feeding rate (g/s)**
I	Foliated	300 (HQ)	0.7	170	2.4
II	Leafless	180 (MQ)	0.11	170	2.4
Measurement	**z-Position (m)**	**y-Position (mm)**	**z-Position (mm)**	**Duration (s)**	**Number of measurements /run**
Bed load in unvegetated part	11.595	-150	0	60	6
Bed load within vegetation	11.595	130	20	180	6

After each sample, the sampler was detached from the mounting structure. The samples were flushed into glass beakers, and were put into oven to dry at 105º C. After relatively low amount of water was left, samples were flushed into smaller, pre-weighted beakers to allow use of more accurate weighing scale. The smaller beakers were weighted after samples were completely dried at 105º, to record sample masses. Error caused by sample collection was estimated in a separate test, by measuring the sediment that remained in the sampler after sediment removal. These results were used to estimate errors related to the measurement process. Sediment batches were weighted and inserted into the sampler separately. Before removal of the sediment, it was watered to mimic real sampling situation where collected

sediment and sampler are completely wet. Sampler was then held nozzle down towards weighted glass beaker, into which sediment was flushed. Flushing was started by pouring approximately 100 ml water above the sampler bag, after which a wash squeeze bottle was used to go through the corners and crevices of the bag. Flushing was finished by pouring approximately 100 ml water similarly as in the beginning. Flushing procedure was kept constant, and sampler was washed properly between each test. Vessels containing water and sediment were dried at 45º C, after which they were weighted.

Because of the continuous sediment feed and sediment recirculation, sediment quantities gradually increased throughout the run. To be able to compare the bed load measurements taken at different times during the run, the obtained bed load fluxes were scaled to conditions at the time of the first sample taken in the same experimental run. This was done by assuming a linear increase of the bed load fluxes over time due to feeding and re-circulation, and subtracting the estimated increase of the bed load flux from the measurements taken at later time instances depending on time difference to first measurement. This is similar to scaling of suspended sediment concentrations with Equation 9.

Flume test III

The third flume test (III) was conducted to validate the 2 by 2 cm HS sampler by reproducing three flume conditions from literature (listed in Table 4). The effect of the sampler on near-bed flow and sand bed was also recorded using a video camera. The three flume settings were chosen from literature based on how close they could be recreated in the flume used in this work. Emphasis was on sediment D50 and flume dimensions as these were not possible to change, but also on the sediment flux given in the source. Too low total sediment flux would not have been measurable with DHS, and too high flux would have caused the sand bed to deplete. For the validation, sediment discharges given in literature were compared with bed load measurements conducted in test III. Assumptions made in the comparisons are discussed later in Section 4.1.1. The reference flume conditions and conditions used in test III are shown in Table 4. The sediment used as sand bed in settings A, B, C1, C2 and C3 is the same that was described in Section 3.1.2. Due to limited amount of sediment, only a 4 m section of 1.5 cm thick sand bed was created for the tests. This section started 6 meters (x = 6) from the beginning of the flume, and bed load measurements were taken close to the end of the sand bed (x = 9.4). In the reference studies (Table 4), the bed was generally thicker and covered more or less the whole flume. Exact details on the dune heights was often available, but thickness of the whole sand bed was explicitly stated only by Barton and Lin (1955) (7.6-10.2 cm). Three 3-minute bed load measurements were taken from settings A, B, C1, and two 3-minute measurements from settings C2 and C3. Sampler was held by hand with a rod attached to the top of the sampler. Rest of the steps in collecting the sediment from the sampler and weighing the samples are identical to earlier descriptions. Mean flow velocity in setting B was supposed to match that of Barton and Lin (1955), but due to error in calculations, incorrect discharge and thus velocity was used in the test.

Table 4: Flume conditions used in test III (settings A, B, C1, C2, C3). Highlighted rows indicate the settings used in other studies that were recreated in this work.

Setting	Q (m3/h)	V (m/s)	L (m)	W (m)	Depth (m)	S (%)	D50 (mm)
Guy et al. (1966)	908	0.34	45.7	2.4	0.3	0.028	0.19
A	223.5	0.34	20.3	0.6	0.3	0.028	0.15
Barton and Lin (1955)	453.6	0.43	21.3	1.219	0.24	0.088	0.18
B	117.8	0.35	20.3	0.6	0.24	0.088	0.15
Kennedy and Brooks (1965)	145.7	0.28	18.3	0.85	0.17	0.056	0.142
C1	100.3	0.28	20.3	0.6	0.17	0.056	0.15
C2	108.6	0	20.3	0.6	0.17	0.056	0.15
C3	126.7	0.35	20.3	0.6	0.17	0.056	0.15

Presentation of sediment discharge differed slightly between the sources (Table 4). Guy et al. (1966) gave the total bed material concentration and suspended concentrations in ppm. The suspended sediment concentrations were measured with a depth integrating sampler located approximately 30 meters downstream, and total bed material concentrations with a depth-width integrating sampler from the water flowing out of the flume (Guy et al. 1966). Bed load concentration could be approximated by subtracting SSC from total bed material concentration, but in the setting chosen for this work, the SSC measurement happened to be larger than the total concentration. Both the SSC and total bed material concentration in this reference setting were very low, 7 and 3.7 ppm for SSC and total concentration, respectively.

Kennedy and Brooks (1965) presented their total sediment concentration as grams per liter, and it was measured by taking water samples of one liter from vertical pipe near pump in the water circuit. Similar to Guy et al. (1966), Barton and Lin (1955) measured both total sediment load and SSC. In their documentation total sediment load was presented as pounds per second, and SSC as weight percentage. Documentation by Brownlie (1981) was used in selecting the reference studies and collecting the data in uniform units.

3.1.4 Vegetative drag force measurements

The drag force sensor used in the flume experiments is a single point load cell, submerged and mounted under a false floor in the flume similarly as in Wilson et al. (2008), but the sensor is not susceptible to momentum. After calibration, direct conversion from voltage data to force was possible. The cell was connected to a HBM AE101 bridge amplifier, and as a data acquisition module, Advantech USB-4716 was used. Data was recorded with Dasylab on PC. The load cell was calibrated using known weights, by establishing a relationship between recorded voltage and weight. The zero point and slope of the calibration curve was used within the program to directly convert the voltage to force in units of Newton (N). The calibration curve is shown in Figure 11.

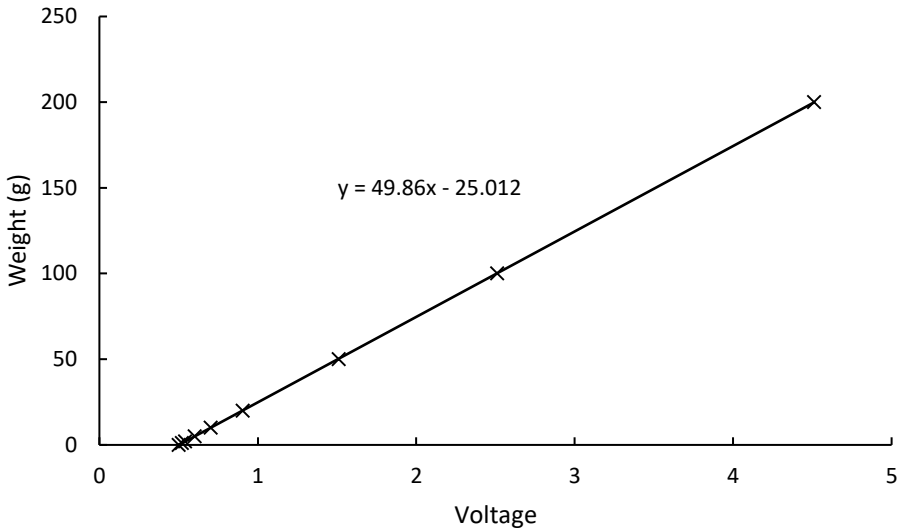

Figure 11: Calibration curve of the load cell used in the experiments.

An artificial plant was attached to the drag force sensor through a hole in the false floor. Since the mounting structure was not exposed to the flow, only the vegetation exerted forces on the sensor. The base of the plants was of rectangular shape, which allowed mounting the plant in 4 different positions. Tall (~24.5 cm excluding base) and short (~16 cm excluding base) artificial plants were used in the experiments, and both were used in 3 and 4-leafed configurations. The 3-leafed configuration and overall picture of the plants is shown in Figure 12. Two positions were used in this work (Figure 13). In position 1, the plant is facing the main flow direction with the largest projected leaf area, and in position 2, the plant was rotated 90 degrees counterclockwise from position 1, resulting in the smallest projected leaf area relative to the main flow direction.

Figure 12: Artificial plants used in drag force measurements. Tall (left) and short (right) plants in their 3-leaf configurations. Both plants have their largest projected leaf area facing towards the camera.

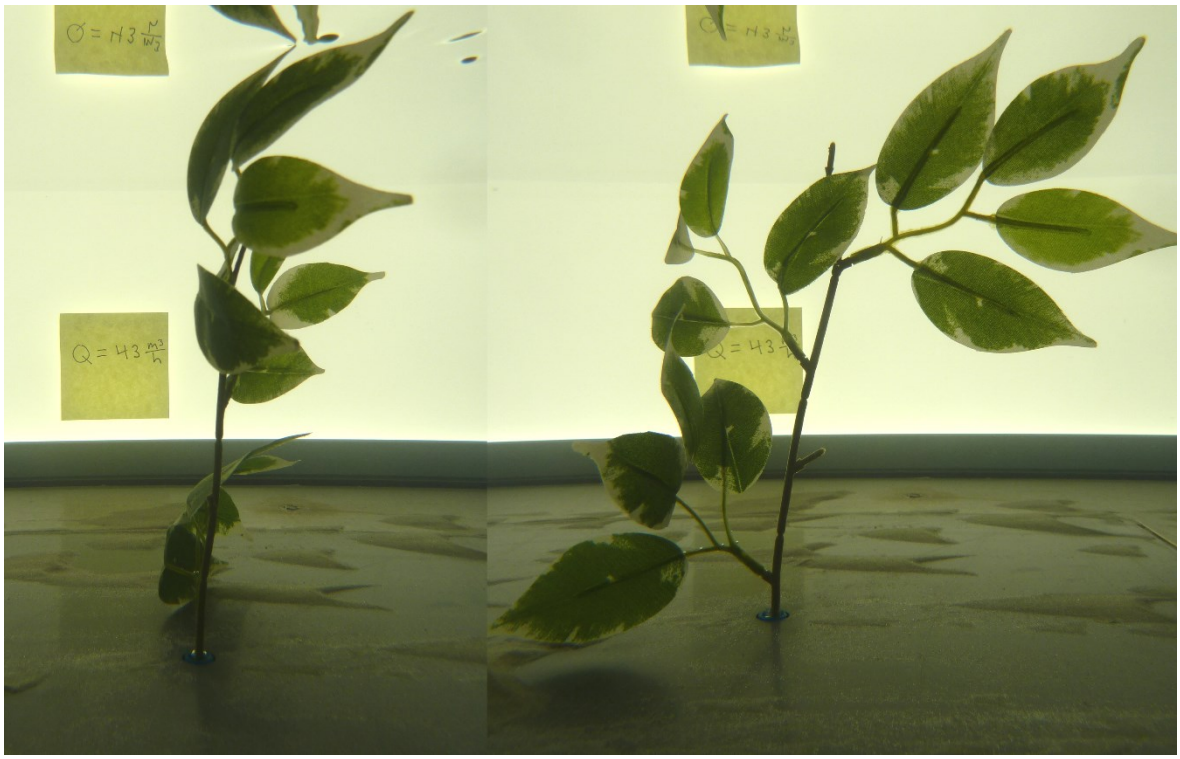

Figure 13: Short plant in 3-leaf configuration, attached to the drag force sensor in 0.1 m/s flow condition in positions 1 (left) and position 2 (right). The flow direction is from left to right.

The drag forces of the plants were measured at four different flow velocities: 0.1, 0.2, 0.3 and 0.4 (m/s), each with constant 20 cm of water depth. At each velocity, both the tall and short plant were measured in 4 and 3-leaf configurations, in both positions 1 and 2. Also, 3 repetitive measurements were taken with flow speed of 0.3 m/s by removing and reattaching the short 4-leafed plant between the measurements. The measurements were coded in the following way: S4L_1 (Short plant, 4-leaf configuration, position 1) (Table 5). The drag force was measured at 5 Hz, and one-minute measurements were taken with each position/leaf configuration. During the measurements, the zero point of the measured force (Figure 11) shifted by -0.02 N. This amount (positive) was added to the results from velocities 0.3 m/s and above for each plant except S4L_1, as this configuration was measured successfully without changes in the zero point.

Table 5: Plant configuration naming scheme.

Code	Explanation
S/T	Short/tall plant
4L/3L	Four/three leaf clusters
1/2	Positions 1 and 2 (largest and smallest projected leaf area facing the flow, respectively)

3.2 Field experiments on fluvial sedimentary nutrients

3.2.1 Field setting

Soil and sediment samples were collected from Ritobäcken Brook, a two-stage channel located in Sipoo, Southern Finland. The channel is used for agricultural drainage of the nearby fields, and it was originally channelized several decades ago with conventional methods (Västilä and Järvelä 2011). In time, natural recovery of the channel led to decrease in the water conveyance capabilities, and the channel was constructed into a more environmentally preferable two-stage channel in 2010 (Västilä and Järvelä 2011). The channel consists of an 850 m long flood-plain designed to improve water conveyance during high flows, excavated bank, main channel and unexcavated bank on the opposite side of flood plain (Västilä 2015).

Changes in ground elevation at selected cross-sections have been monitored with point measurements in years 2010, 2012 and 2019 (Västilä et al. 2015). These cross sections are visible in Figure 14. This elevation data was not collected in this work, but was available for use, and was used to determine amount of deposition since 2010 at different points in the cross sections.

3.2.2 Soil and sediment sampling

In total, 12 sediment and soil cores were collected from Ritobäcken. Cores C, J and N from main channel, cores E, M and R from channel bank, and cores D, F, G, K, O and T from floodplain (Figures 14-15). The core C was taken with a plastic sediment tube, D and E were collected with the Eijkelkamp piston sampler while the rest were taken with AMS split soil core sampler. The sampler consists of a hollow shell that can be split in half, coring tip, core cap and slide hammer. Transparent plastic liners were used inside the sampler to collect and contain the soil. The liners were taped together from 0.5, 0.667, 1 and 2-inch long sections designed to aid in slicing the core. The smaller sections were used to get more samples from shorter distance, to better monitor how the soil characteristics change over the profile. Most of the changes were hypothesized to occur in the top soil and thus the small sections were often placed on the top part of the liners.

The soil cores were sliced either directly in the field or later in laboratory, by sawing directly between the plastic liners with a small fretsaw, producing soil slices of 0.5, 0.667, 1 and 2 inches. The sediment cores were sliced using Pylonex HTH sediment corer equipment. The sediment corer was rotated to extrude sediment from the top, and the length of sample was controlled by the amount of rotations. The sample was then be scraped for either storing or further processing. In case of in field slicing, the slices were stored in a cool box until placed in either refrigerator or freezer depending on when the samples were planned to be processed. When sliced in the laboratory, the samples were usually put directly into an oven. Processing of the samples is described in Section 3.2.3.

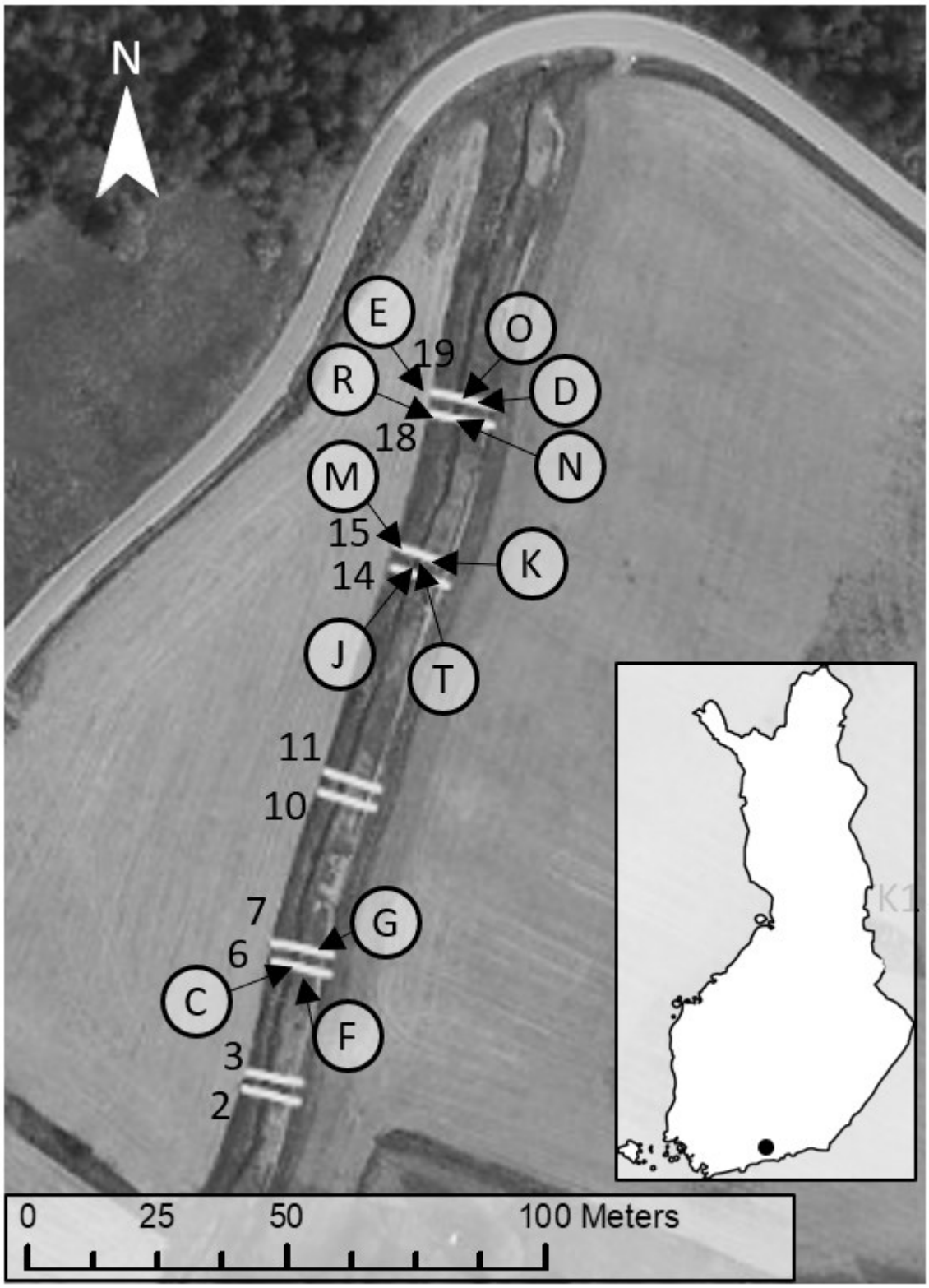

Figure 14: Cross-sections (numbered) and approximate sediment coring locations (Letters) at Ritobäcken two-stage channel. Location of Ritobäcken in Southern Finland is indicated on the map.

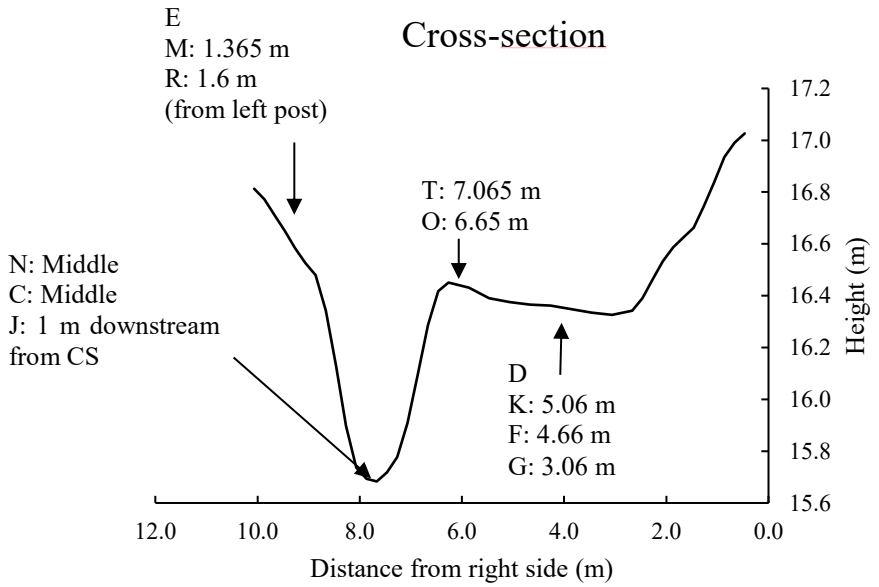

Figure 15: Cross-sectional view of soil- and sediment coring locations. The cross section is drawn based on point measurements taken from CS 18 (Figure 14), using three point moving average. The general form is similar between all cross-sections, but large differences exist in the elevations.

Soil cores were notably compacted during the sampling, and therefore sample depths had to be scaled up for the sample lengths to be correct. This was done by comparing sample and ground levels during the coring, and then calculating how much the sample compacted as the corer was lowered deeper into the soil. Compaction was measured for progressively larger intervals, for example 0-5 cm, 0-10 cm and 0-15 cm for the same core. As an example, if corer was lowered 5 cm into the ground and sample inside was compacted by 1 cm, the samples within this 4 cm interval were scaled to match the correct 5 cm length. Approximately 3 length measurements were taken from each core, and the correction method took into account the assumption that compaction was expected to occur both during the penetration of the soil into the cutting head and while the soil was moving upwards in the sampler. In particular, the topsoil was less dense than the deeper layers, expected to lead to larger compaction for the upmost layers. The scaling calculation is shown in Equation 11. The scaling parameters were calculated by solving which factor (p_1, p_2 *or* p_3) sum of samples (matching the length of measurement interval) had to be multiplied by to equal the amount of compaction within that interval.

$$l_{s1} = l_u(1 + p_1 + p_2 + p_3) \quad (11)$$
$$l_{s2} = l_u(1 + p_2 + p_3)$$
$$l_{s3} = l_u(1 + p_3)$$

Where l_u is the length of unscaled sample
l_{sn} is the length of scaled sample belonging to interval n
p_1, p_2, p_3 are the scaling parameters for intervals 1, 2 and 3, respectively

The compaction of soil cores ranged at 20-40%, and generally longer samples were more compacted. From this point forward, thickness of each soil sample has been scaled up, unless

told otherwise. Sediment samples were not scaled, as they did not seem to suffer from compaction during the sampling.

3.2.3 Pre-processing and elemental analysis of soil and sediment samples

The following experiments were conducted to study if the rate or amount of sediment deposition after the establishment of the two-stage channel (year 2010, see Section 3.2.1) can be identified based on the elementary data of soil and sediment cores. Effect of pre-processing of the samples was also studied to determine if the mechanical grinding of included mineral particles leads to higher measured concentrations of analyzed elements by breaking larger grains, which could increase the amount extracted into solution compared to sample ground manually in mortar. Some of the samples were wet sieved before grinding to remove larger particles and organic matter from the sample, and to provide basis for comparing the effect of wet sieving on elemental analysis.

The effect of pre-processing was studied as described in Table 6. CN-analysis was analyzed with >63 µm fractions of samples 26, 28 and 32 (Core C) from main channel, and with non-sieved samples 68, 74 (Core D), 92 and 100 (Core E) from floodplain and bank. The sample numbers were used to identify the order of the samples within each core (coring locations shown in Figures 14-15). ICP-OES analysis included >63 µm fractions of samples 22, 25, 26, 28, 30 and 32 from main channel (Core C), and both fractions of samples 250, 252 and 255 taken from other field site. From samples 26, 28 and 32, several replicate (5 for CN, 2 for ICP-OES) sub samples ground both manually and mechanically were subject to CN and ICP-OES analysis for the MEK-MAN comparison. To study variability in analysis, 3 replicate mechanically ground sub samples were taken from samples 68, 74, 92 and 100 for CN-analysis, and 2 replicate manually ground sub samples from >63 µm fractions of samples 250, 252 and 255 for ICP-OES. Effect of wet sieving was considered by calculating how much the element concentration differed between non-sieved sample and sample containing only < 63 µm fraction (Appendix A).

Table 6: Conducted tests to study effect of sample pre-processing on sample element concentrations. ******* *The concentrations were mainly compared directly, but the differences between grinding types were tested on three samples using standard Student's T-test.*

Test	Method
Repeatability	Coefficient of variation (CV)
MEK-MAN difference	Differences (relative and arithmetic) in average concentrations, T-test*
Effect of wet-sieving	Calculation of element concentration in case if >63 fraction is removed from the sample (Appendix A)

Summary of the main steps regarding the pre-processing prior to ICP-OES and CN-analysis is given in Table 7. Frozen samples were un-freezed in fridge overnight or in room temperature when frequent monitoring of the sample melting was possible. Two sample vessels were prepared for each sample by drying and weighing, one for <63 µm fraction and other for >63 µm fraction. Samples were homogenized before flushing them into a 63-µm sieve, mounted to a sieve shaker. The sample was wet sieved until discharging water was clear,

which indicated that most of the <63 µm fraction had passed the sieve. The sieve containing >63 µm fraction was flushed into the other vessel. Sieved samples were dried in oven at 45º C not to volatilize compounds, the same conditions in which the vessels were prepared. Drying of the sample was monitored by weighing. After the weight no longer changed between measurements, samples were removed from the vessels and stored in plastic bags. Weights of fractions was used to determine ratio of the two fractions in the sample, and total weight of the fractions was used along with the sample volume to calculate bulk density.

Table 7: Pre-processing steps for soil and sediment sample preparation for ICP-OES and CN-analysis. Step 1 was not always necessary depending on where the sample was stored. Step 2 was also not used on all samples to allow studying the effect of sieving.

Step	Description
1	Un-freezing of sample
2	Wet-sieving (separation of particles > and < than 63 µm)
3	Drying of samples at 45° C
4	Weighing
5	Grinding (either electro-mechanical or manual)

Dried, sieved fractions > 63 µm and < 63 µm, and non-sieved samples were either manually ground in mortar or electro-mechanically using an IKA analytical mill. Some samples were subject to both types of grinding for comparison. Approximately 5 grams of ground sample was taken randomly for further analysis, but some small samples were taken as whole. Prior to ICP-OES, the dried, ground samples were subject to a HNO_3 extraction procedure based on method 3050B from U.S Environmental Protection Agency (EPA 1996). In this procedure, small amount from each sample was digested with HNO_3 on a hotplate, to extract oxides, organic matter and reactive minerals. After the digestion, small sub-samples of each sample were diluted and taken for the ICP-OES analysis, in which Al, Ba, Ca, Fe, K, Mg, Mn, P, S and Zn concentrations were analyzed. CN-analyzer was used to measure N, and C concentrations. In case of some samples, the ICP-OES and CN-analyses were conducted for several sub-samples of the same sample.

After the elemental analysis, the concentrations (excluding N and C and S) were scaled with aluminum concentrations, which is commonly used for normalization because it is abundant, and in most cases comes from a natural source (Alomary and Belhadj 2007). This allows inspecting the changes in mineral matter of the soil without dilution caused for example by organic matter.

4 Results and discussion

4.1 Down-scaled HS bed load sampler

4.1.1 Sample collection and validation of the used DHS in vegetated flows

Focus in this section is in validation of the 2 by 2 cm DHS in flume conditions (details in Sections 3.1.2, 3.1.3). The results from tests I and II are discussed in terms of measurement variability, and the fluxes determined with DHS and OBS sensor are compared for validation. Measured sediment fluxes from test III are compared to literature, and sampler video documentation is shortly reviewed to assess sampler performance in terms of how the flow and sediment is affected in the close proximity of the sampler.

Results from flume tests I and II

Measured bed load tests I (HQ) and II (MQ) are shown in Table 8. Clearly higher bed load fluxes were measured on unvegetated (y=-150) part of the flume compared to vegetated (y=130) part. Measurement variability between the repetitive measurements was relatively low. The highest coefficient of variation (~27%) occurred in unvegetated part of the flume during high flowrate run, suggesting that the sampler can be used in measuring bed load fluxes reliably in vegetated conditions. High flowrate caused higher variability in both vegetated and unvegetated parts of the flume compared to medium flowrate. Bed load fluxes in vegetated part of the channel in MQ run had quite high variation compared to unvegetated part of the channel. This is likely result from measurement accuracy instead of natural bed load variation, as the captured amounts of sediments were very low. Similarly, higher amounts of captured sediment during HQ run in vegetated part reduced the effect of measurement errors, which explains why CV in vegetated part increased only from 18 to 24% while in unvegetated part the increase was considerably larger (from 7% to 27%) when flow increases from MQ to HQ.

Table 8: Results from repetitive bed load experiments II and I. Sediment amounts and fluxes are scaled to take into account increase in concentrations during the experiments. y=-150 and y=130 correspond to positions in middle of the unvegetated and vegetated parts of the channel, respectively.

II: MQ. leafless							
Unvegetated, y=-150. z=0				Vegetated, y=130. z=0			
N.	Duration (s)	Sediment (g)	Flux (g/s/m2)	N.	Duration (s)	Sediment (g)	Flux (g/s/m2)
1	62	11.33	456.69	2	180	0.135	1.872
3	67	14.61	534.42	4	180	0.073	1.027
5	62	11.39	444.26	6	181	0.101	1.413
7	64	14.02	520.46	8	185	0.131	1.791
10	60	11.86	467.27	9	185	0.107	1.476
11	60	12.66	498.22	12	180	0.107	1.551
	AVG	12.64	486.89			0.11	1.52
	STDEV	1.27	33.24			0.02	0.28
	CV (%)	10.05	6.83			18.75	18.11
I: HQ. Foliated							
Unvegetated, y=-150. z=0				Vegetated, y=130. z=0			
N.	Duration (s)	Sediment (g)	Flux (g/s/m2)	N.	Duration (s)	Sediment (g)	Flux (g/s/m2)
1	61	14.79	606.28	2	184	0.64	8.7
3	65	14.49	536.74	4	180	0.4	5.4
5	70	12.22	377.61	6	180	0.4	5.2
7	65	9.71	317.59	8	183	0.36	4.5
9	60	11.05	431.74	10	180	0.64	8.3
11	60	17.69	701.9	12	180	0.51	6.4
	AVG	13.32	495.31			0.49	6.4
	STDEV	2.65	133.03			0.11	1.58
	CV (%)	19.86	26.86			23.19	24.63

Bed load flux over unvegetated part of the channel in both MQ (test II) and HQ (test I) conditions was 2-3 orders of magnitude higher than within vegetation (Table 8). While the fluxes within vegetation increased with increasing flowrate, bed load flux over unvegetated part of the channel was almost equal in both HQ and MQ tests, aside from higher CV in HQ test. This is different from suspended sediment measurements near the bed (Table 9), where the sediment flux at 10- and 20-mm height was around twice as high in HQ test than in MQ test 5 and 15 minutes after initiation of the experiment. It would make sense that this increase in sediment load near the bed should be visible also in the bed load measurements (Table 8). Scaling of the bed load measurements (see Section 3.1.3) cannot explain this similarity, since first bed load measurements of the test (t = 5 min) were not scaled at all. Also, measurements not scaled for overall increase of sediment in the flume show that the sampler was capable of capturing even double the amount of sediment in the same period of time, so the sediment bag was not likely clogged. Possible explanation for the similar bed load measurements in HQ and MQ tests (Table 8) is that with the increase of flow velocity and increase of turbu-

lence caused by the leaves present in HQ test, increasingly more sediment is being transported in suspension. Since the HS sampler collects sediment both from the bed and suspended sediment up to 20 mm above the bed, increase in suspended sediment flux in 10-20 mm region is compensated with decrease in bed load in the HQ test, resulting in similar total flux measured by HS sampler in both MQ and HQ tests (Table 8).

Table 9: Suspended sediment fluxes in unvegetated (Y=-150) and vegetated (Y=130) parts of the flume at elevations ranging in 10-85 mm. Data is scaled as described in section 3.1.2. Time (min) indicates how long time has passed since the beginning of the test. Flux (mg/s) is calculated from the measured SSC, for the area of the 2 by 2 cm sampler nozzle.

II: MQ, Leafless							
Unvegetated, y=-150				Vegetated, y=130			
z (mm)	Time (min)	Flux (mg/s)	g/s/m2	z (mm)	Time (min)	Flux (mg/s)	g/s/m2
10	5	35.34	88.36	30	10	11.68	29.2
20	15	26.72	66.8	35	20	10.13	25.33
25	25	24.93	62.32	40	30	7.56	18.9
35	35	18.66	46.64	85	35	6.09	15.21
85	45	11.91	29.77	30	40	16.68	30.94
10	50	186.99	283.79	35	55	16.82	28.35
40	80	30.58	51.69				
I: HQ, Foliated							
Unvegetated, y=-150				Vegetated, y=130			
z (mm)	Time (min)	Flux (mg/s)	g/s/m2	z (mm)	Time (min)	Flux (mg/s)	g/s/m2
10	5	73.74	184.34	30	10	13.75	34.37
20	15	48.69	121.72	35	20	9.86	24.66
25	25	41.01	102.53	40	30	8.1	20.24
35	35	35.49	88.72	85	40	10.59	26.48
85	45	27.77	69.41	30	85	12.02	16.78
10	80	58.97	147.43	35	90	15.62	19.66

Test in MQ run indicated that the 2 by 2 cm HS sampler measures about 34% higher suspended sediment flux than the OBSc sensor. Both HS sampler and OBSc measured at y = -150 mm, z = 40 mm in MQ run for 1 minute. Flux of 69.3 g/s/m^2 was measured with the HS sampler, and 51.7 g/s/m^2 with OBSc. With only one measurement with each device, a proper relation is not achieved but the result still indicates that the two methods provide results in the same order of magnitude. Sampler performance in flume bed is more difficult to assess, as the lowest position for OBS measurements was 10 mm, while the HS sampler captures in the range 0-20 mm. The SSC indicated highly increasing concentrations towards the flume bed (Table 9), which lead to higher fluxes measured by HS sampler than OBS near the bed. That being said, suspended sediment flux measurement from MQ run, z = 10 mm & T=50 min, was of similar magnitude as the average bed load measurement from MQ run (283.79 vs 486.89 g/s/m^2 for suspended sediment (Table 9) and bed load (Table 8), respectively).

Results from flume test III

Results from flume test III are shown in Table 10. Overall, the measured concentrations were partly very far from the reference values (~500 vs ~4 ppm in test III and reference setting, respectively), but this does not necessarily mean that the HS sampler measures incorrectly. Setting B was closest to the reference, but as was mentioned in Section 3.1.3, the mean flow velocity was lower than in the reference (0.35 instead of 0.43 m/s), meaning that the conditions are not directly comparable. Also, the reference concentrations are total sediment concentrations (see table caption for exception), whereas concentrations in test III were calculated from bed load as measured by the sampler. The sediment concentrations near the bed are higher, meaning that concentration measured by the sampler is likely higher than reference concentration even in cases where the reference condition would be perfectly replicated. To convert bed load fluxes ($g/s/m^2$) into ppm for comparison to the reference value, velocity within the sampler had to be estimated. In setting A, the reference data from Guy et al. (1966) included velocity distributions as close as 2.1 cm above the bed. This velocity was used in setting A for flux to concentration conversion (0.152 m/s compared to mean velocity of 0.34). In setting B, velocity profile data from Barton and Lin (1955) did not extend close enough to the bed to be used for velocity estimation. However, to estimate velocity at depth of 2 cm, exponential line was fitted on the depth-velocity profile of Barton and Lin (1955). Even though the profile was for higher mean velocity than what was used in setting B, the computed velocity at depth of 2 cm was considered to better describe the near bed velocity than simply using mean velocity. For setting C1, mean flow velocity was used in flux to concentration conversion because the reference data included no velocity profiles. This results in underestimation of sediment concentration, due to using higher flow velocities.

There are several factors explaining why concentrations from settings A and C1 differed noticeably from the reference (Table 10). The differences in how the sediment concentrations were presented (total sediment concentrations in reference settings, compared to concentrations calculated based on bed load measurements in test III) were already discussed in previous paragraph. It is also likely that the reference conditions were not correctly reproduced in the present tests. While the flow depth, velocity, sediment median diameter and slope were close to the reference values, flume width, bed thickness and length were different. The different length of the sand bed possibly explained why the results differ from the literature with such a large margin. The flow would interact with the bed over longer distance, affecting bed formations and possibly sediment entrainment. Also, in the reference studies the measurements were initiated only after equilibrium conditions were reached. In the case of Guy et al. (1966), equilibrium was defined as having consistent bed configuration, and parallel slopes between the water surface and the bed. This took approximately 2-3 hours for steep slopes and 3-4 days for lower slopes (Guy et al. 1966). In the flume test III conducted in this work, each setting was run approximately only 5 minutes before initiation of the measurements. That being said, the bed configuration was observed to stay uniform after the initial effects caused by changing of the flow velocity.

The standard deviations of bed load measurements in flume tests I and II (Table 8) were very low compared to for example standard deviations from measurements of Helley and Smith (1979). In their studies, the standard deviations were often as large as the mean bed load discharge, whereas in experiments I and II of this work, the standard deviation was between 6-30% of mean bed load discharge. This difference is very likely caused by the flume conditions, as Helley and Smith (1971) conducted their tests on sand bed whereas no sand bed was used in tests I and II. However, a sand bed was used in test III, and as can be seen for

example in setting A (Table 10), the third measurement was around 3-4 times lower than the first measurement. This indicates that larger variability in the bed load measurements is present on sand bed, and that similar variability in bed load measurements occurs with both the original 7.62 by 7.62 cm sampler and DHS sampler.

*Table 10: Measured fluxes and sediment concentrations from calibration tests (III), and sediment concentrations from literature. * 550 ppm is the average total sediment concentration, and 1240 is the suspended sediment concentration measured approximately 7 cm above the bed.*

Setting	Measurement N.	Sediment (g)	Flux (g/s/m^2)	Concentration (ppm)	ppm (reference)
A	1	8.66	120.23	788.91	
	2	5.61	77.96	511.56	
	3	2.59	35.93	235.76	
	avg.	**5.62**	**78.04**	**512.08**	**3.7**
B	4	5.31	73.72	612.47	
	5	6.67	92.68	770.01	
	6	8.35	116.04	964.08	
	avg.	**6.78**	**94.14**	**782.19**	**550/1240***
C1	7	1.79	24.84	89.62	
	8	1.88	26.11	94.23	
	9	1.7	23.62	85.22	
	avg.	**1.79**	**24.86**	**89.69**	**14**
C2	10	1.4	19.39	64.63	
	11	4.95	68.74	229.15	
	avg.	**3.17**	**44.07**	**146.89**	**-**
C3	12	17.99	249.89	713.97	
	13	24.09	334.52	955.76	
	avg.	**21.04**	**292.2**	**834.86**	**-**

In settings C1-C3 velocity was gradually increased (in range 0.28-0.35 m/s) while keeping other parameter values constant (see Table 4). Based on the visual observations made during the run and from the recorded videos, the sampler could be used in this velocity range without too large flow disturbance caused by the sampler. Also, filling of the bag in high bed load flux conditions did not appear to disturb the measurement nor block the flow through the sampler. In Figure 16, some scouring near the sides of the sampler is visible, but the bed in front of the sampler did not seem to be affected (Figure 17). Due to irregularities and dunes on the sand bed, the nozzle of the sampler was in some measurements slightly off the bed (Figure 16), which will likely lead to lower measured bed load flux than when placed on even surface. Instead of sand bed, the DHS was planned to be used in flume conditions where sediment is being fed from the beginning of the flume (like in tests I and II), meaning that placement of the sampler is not an issue.

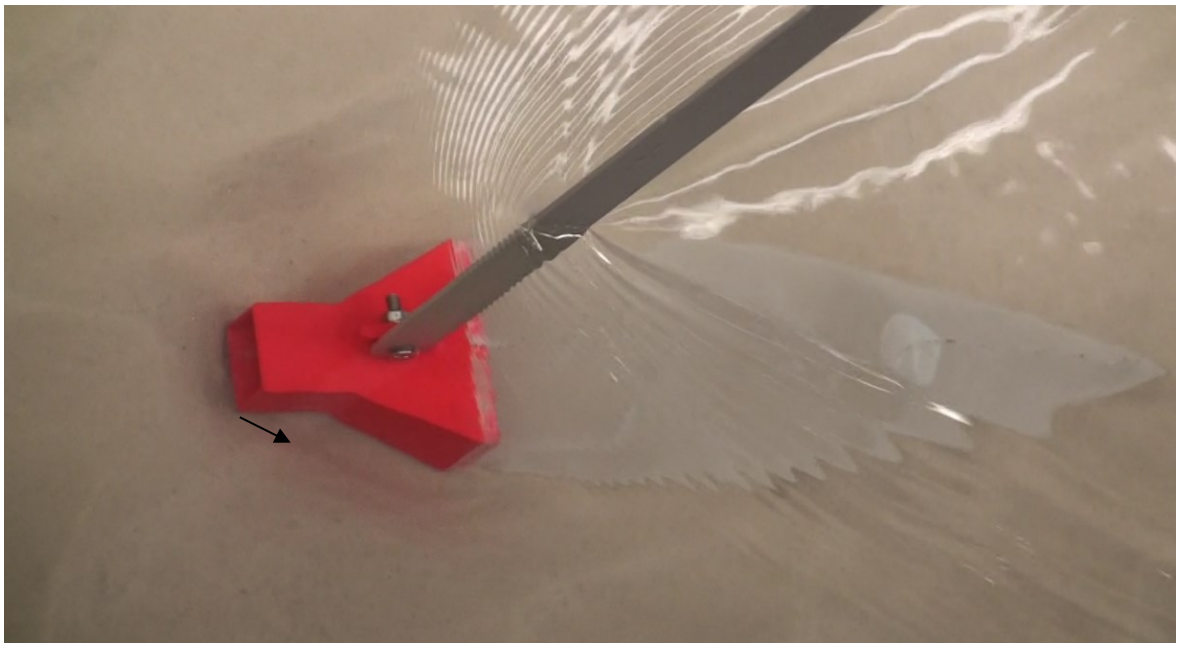

Figure 16: 2 by 2 cm DHS sampler placed on sand bed in flume experiment III. Some scouring is visible on the sides of the sampler, indicated by arrow. Due to dunes and bed roughness, the nozzle of the sampler is slightly off the bed.

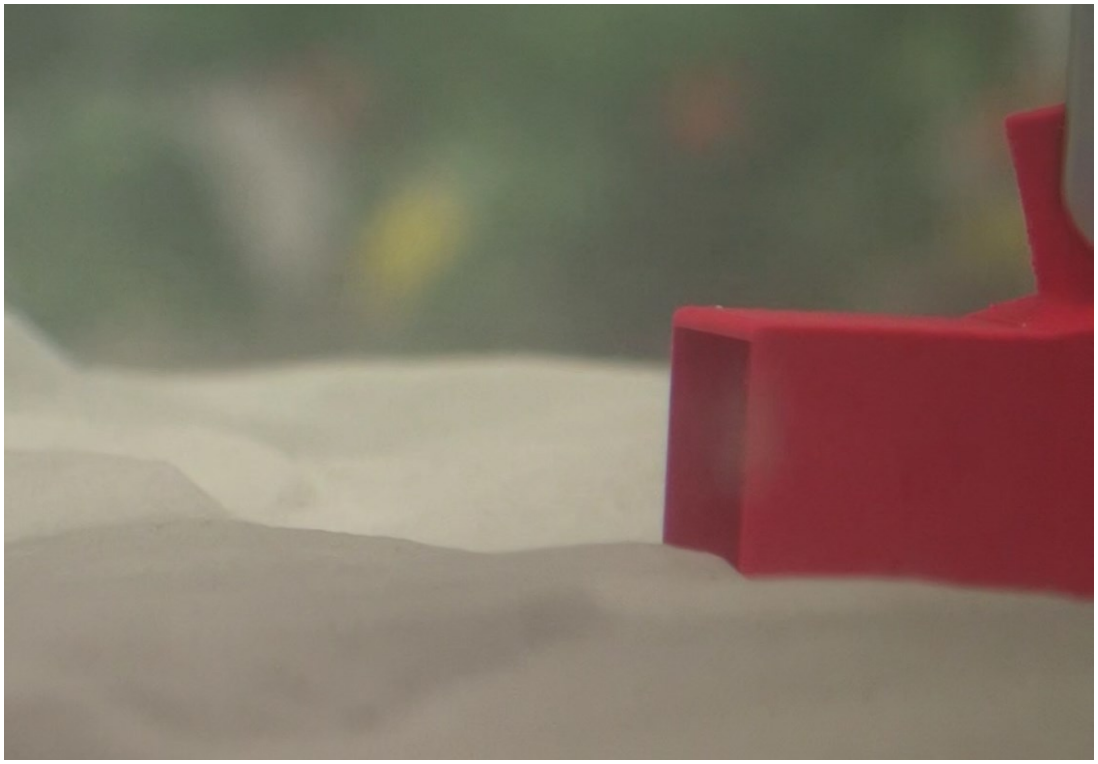

Figure 17: Sand bed near the nozzle of the DHS sampler in flume experiment III.

4.1.2 Recommendation on the sampling duration of the DHS in vegetated flows

Bed load sampling duration of 60 seconds was used with the DHS in unvegetated part of the flume, and 180 seconds in the vegetated part (see Section 3.1.3). The accuracy of these sampling durations in capturing mean bed load fluxes was estimated with the coefficients of variation shown in Figure 18. When CV was calculated for progressively longer duration of OBSc data (currently in volts), point where it no longer changed was considered the time when most of temporal variations were captured. It is this duration that should be measured with also the bed load sampler if average bed load transport is of interest. For these considerations it was assumed that variations in suspended sediment concentration near the bed reflected how bed load varied at this location, and that the variations visible in OBS data were result from natural SSC variations of the flume setting, and not for example from uneven sediment feeding.

The coefficients of variation were overall relatively low in Figure 18, and appeared to stabilize within the used sampling duration. This indicates that the durations are suitable for measuring the mean bed load. The CVs were especially low within vegetation (1-2% in MQ and 2-6% in HQ), meaning that the variation in SSC (and hypothetically bed load) does not require long measurement duration. However, due to low bed load fluxes, measurement duration has to be quite long to capture sediment of measurable quantity. Variability in OBSc data was larger in unvegetated part of the channel (CV in the range of 15-30% for HQ and ~10-25% for MQ, Figure 18). CVs of OBSc measurements Z=20 mm and Z=25 mm seemed to increase until the end of the measurement period, making it difficult to assess if the CVs stabilize.

Similar to CVs in Figure 18, OBSc voltage plots (Figures 19-21) can be used to estimate if bed load measurement duration is sufficient. At first glance, the sampling duration in HQ conditions (Figure 20) appears sufficient, because no long-term variations were visible. In the case of one-second moving average plot of MQ conditions, there appeared to be quite large short-term fluctuations in the OBS voltage measurement, especially near the bed in the end of the run (Figure 19a). With 10-second moving average, long term fluctuations are visible. Especially in the points near the bed (Figure 20a-b), it appears that there were some temporal patterns extending beyond the measurement window. For example, in Figure 20b, there were quite large long-term fluctuations within the measurement duration of around 70 seconds. Assuming that similar pattern is present in bed load, this might indicate that the measurement duration should not be less than the 60 seconds. This in combination with inspected CVs could suggest that measurement duration for unvegetated part of the channel should be even more than the used 60 seconds. In HQ run, unvegetated part of the channel (Figure 20) did not seem to have this issue, as there were only short-term fluctuations. However, these short-term fluctuations were larger than in MQ conditions (figure not shown here, but larger CVs in HQ conditions are visible in Figure 18). These results suggest that short-term variations are more important in HQ conditions, and long-term variations in MQ conditions. With these considerations, HQ conditions may not require as long measurements as MQ conditions.

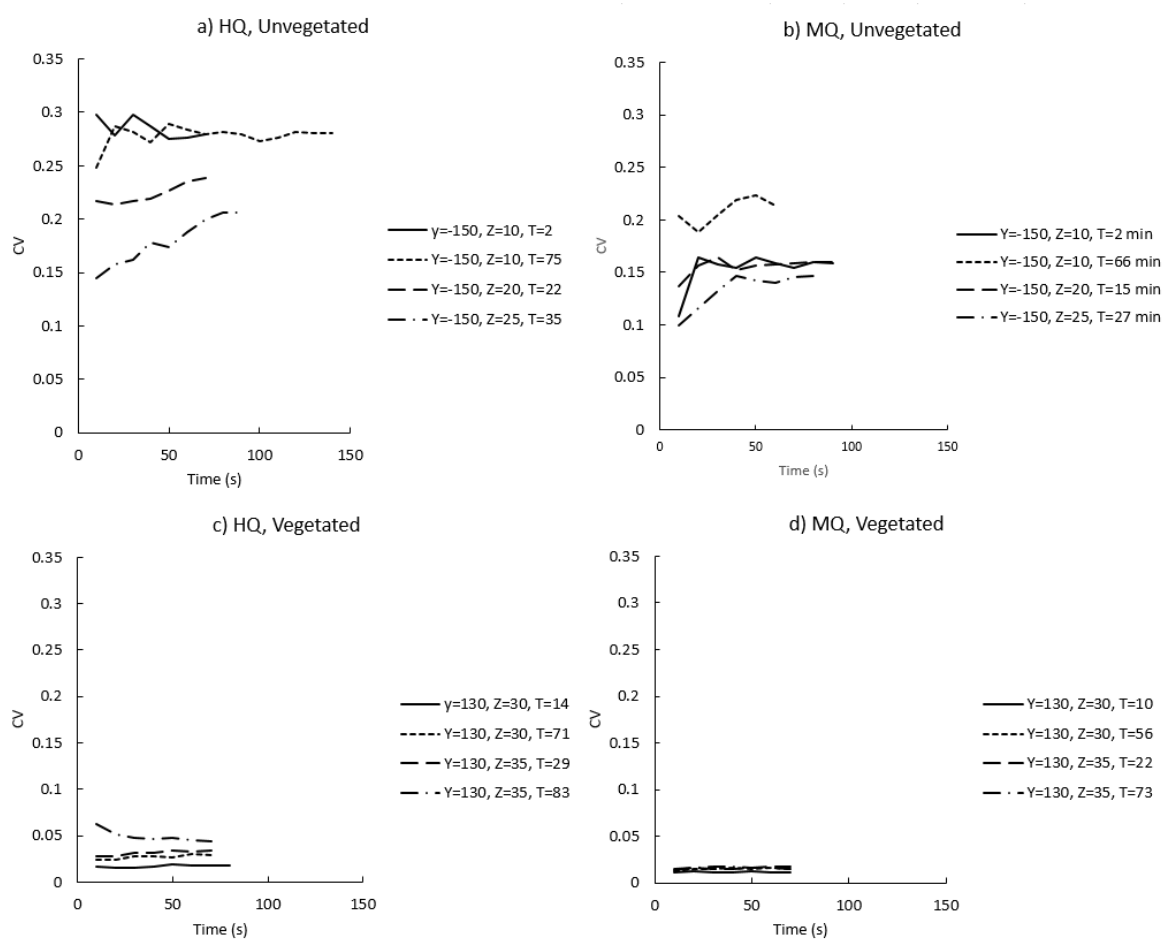

Figure 18: OBSc voltage coefficients of variation (CV) for increasing measurement lengths. The CVs were calculated under high (HQ) flowrate conditions for a) unvegetated and c) vegetated parts of the channel, and under medium (MQ) flowrate conditions for b) unvegetated and d) vegetated parts of the channel. The full/dotted lines represents the lower position (z = 10 or 30 mm) and the dashed lines the higher (z = 20-35 mm). T in legend indicates how long (in minutes) after initiation of the run the measurement was taken.

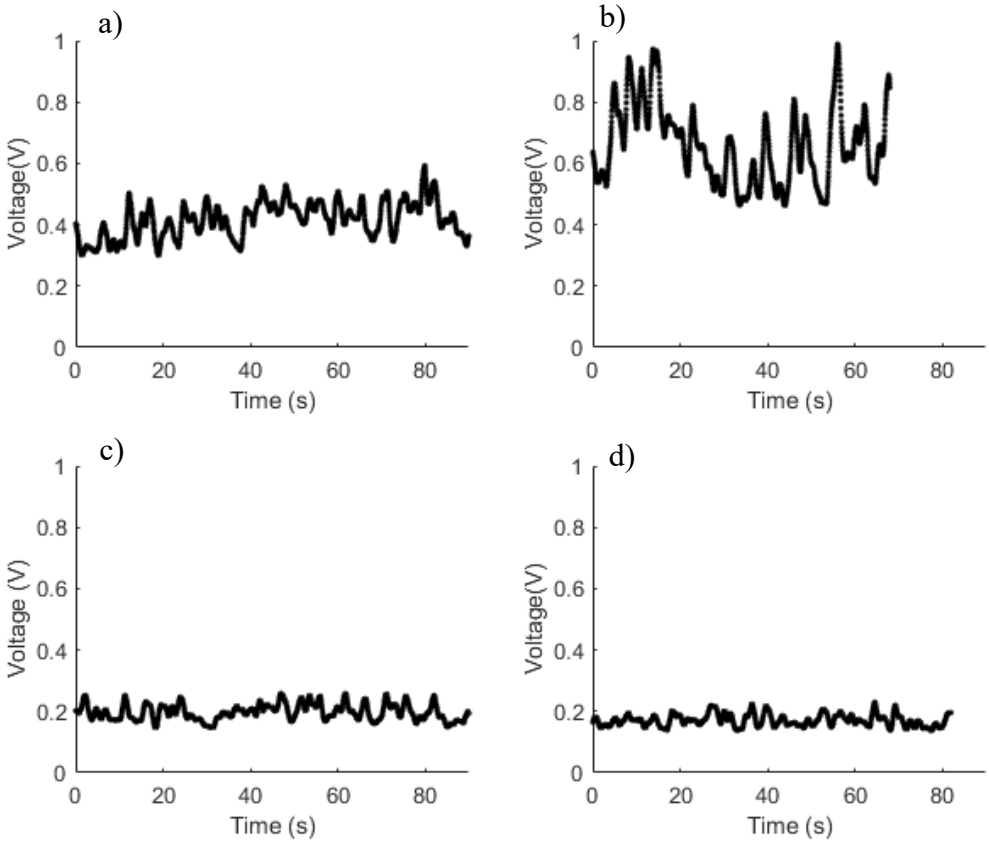

Figure 19: The time-series of the one-second moving average unscaled OBSc measurements (Volts) in the MQ conditions, unvegetated part of the flume for three locations over the vertical a, b) z = 10 mm (in duplicate), c) z = 20 mm and d) z= 25 mm. The measurements were taken 2, 60, 15 and 27 minutes after initiation of the experiment for plots a), b), c) and d), respectively.

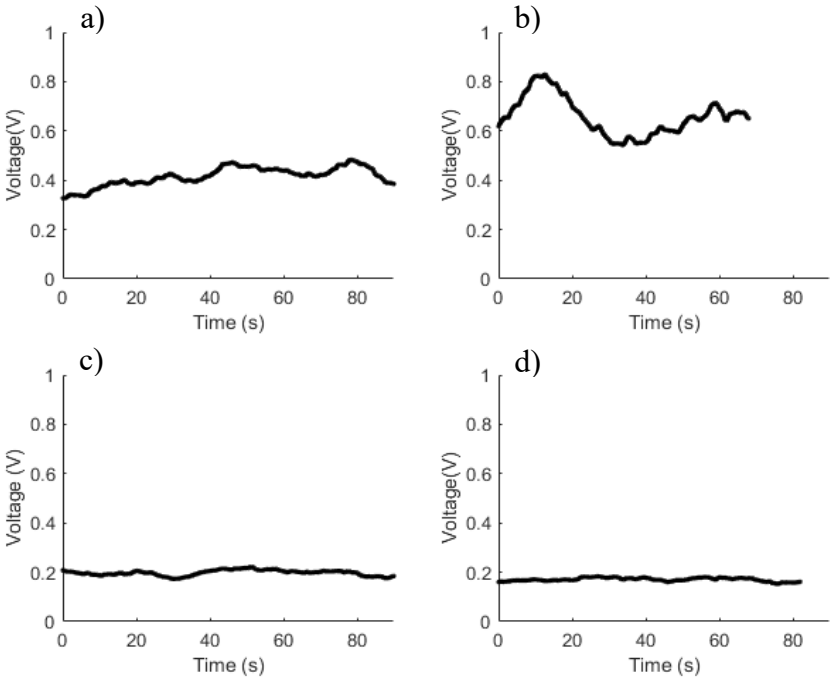

Figure 21: The time-series of the ten-second moving average unscaled OBSc measurements (Volts) in the MQ conditions, unvegetated part of the flume for three locations over the vertical a, b) z = 10 mm (in duplicate), c) z = 20 mm and d) z= 25 mm.

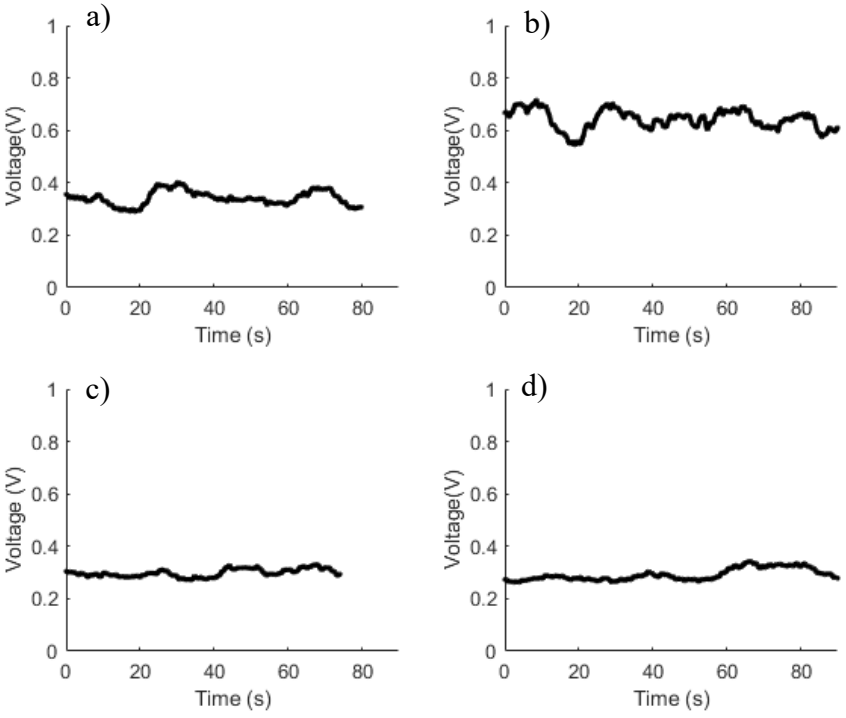

Figure 20: The time-series of the ten-second moving average unscaled OBSc measurements (Volts) in the HQ conditions, unvegetated part of the flume for three locations over the vertical a, b) z = 10 mm (in duplicate), c) z = 20 mm and d) z= 25 mm. The measurements were taken 2, 75, 22 and 35 minutes after initiation of the experiment for plots a), b), c) and d), respectively.

As a summary of the sampling duration results, the following recommendations for different conditions are given. Because of low amount of captured sediment within vegetation, sampling time shorter than 3 minutes is not recommended. Some repetitive measurements should be taken when determining mean bed load transport within vegetation, as the CVs were in the range of 20% for both in MQ and HQ runs. In unvegetated part of the channel, measurement time can be as low as 1 minute, because by this time CV of SSC measurements seems to stabilize and sufficient amount of sediment is captured. Amount of repetitive measurements can be lower in MQ than HQ runs for unvegetated part of the flume as the coefficient of variation was considerably lower with the lower discharge. However, sampling duration should be longer in MQ, as more long-term fluctuations were visible. If merely comparing the difference in magnitude of bed load between unvegetated and vegetated part of the channel, few repetitions are sufficient. The variability in repetitive measurements is not concern as the sediment flux in unvegetated part is around 100-300 times larger than within vegetation.

Sampling times used in tests of Gaweesh and van Rijn (1994) were 1, 3, 5, 10, or 15 minutes, and 15, 30, 45, 60, 75 or 90 seconds in experiments of Marr et al. (2010) (see Section 2.1.2). Both of these studies were made with full-sized samplers, which partly explains the long sampling times of Gaweesh and van Rijn (1994). They also allowed the bag to fill up to 50% of the capacity, which is much more than the amounts captured in tests I and II of this work. Regardless, the sampling times used in tests I and II are similar to what has been used in other studies. Amount of samples and sampling interval has been generally much larger in other studies (see Helley and Smith (1971) or Gaweesh and van Rijn (1994)), possibly because of high variability in bed load due to use of sand bed.

4.1.3 Discussion on measurement uncertainties and errors

The results from sediment removal test, regarding accuracy of the sampling process are shown in Table 11. A large amount of sediment was used in samples number 1-3, and small amounts in numbers 4-7. The absolute amount of sediment lost (or in some cases sediment added, due to some sediment being left from previous sample), was on average ~0.1 g. The amount was generally larger with large amount of sediment, and vice versa. The relative error was around 1% for large sample, and around 15% for small sample. This larger error with small amounts of sediment may explain some of the measurement variability observed in Section 4.1.1. For example, the OBSc CVs (Figure 18) compared to bed load CVs (Table 8) in vegetated part of the channel were much lower (1-5% vs 18-25%), and can possibly be caused by sediment being left in the sampler.

Table 11: Removal of sediment from 2 by 2 cm DHS.

N.	Sediment in sampler (g)	Sediment removed from sampler (g)	Difference (g)	Relative difference (%) (absolute)
1	9.69	9.59	0.097	1.00
2	11.83	11.74	0.091	0.77
3	10.57	10.45	0.115	1.09
4	0.302	0.248	0.054	17.96
5	0.071	0.082	-0.011	16.06
6	2.365	2.07	0.295	12.46
7	0.097	0.101	-0.004	4.12
		avg.	0.091	7.64

Errors related to sediment entry while sampler was being placed were low. In unvegetated part of the channel, starting the timing when sampler was placed on the flume bed underestimated the flux by up to 4.3% compared to starting timing when sampler entered the water. Test with HS sampler at z = 40 mm, y = -150 mm in MQ (II) conditions indicated that around 3.2 g of sediment (unscaled 11.73 g, t = 88 min) was captured per minute when sampler was not placed on the flume bed. In the MQ (II) test, it took at maximum ten seconds to place the sampler to the flume bed. If the sampler was aligned towards the flow for this 10 second duration, up to 0.51 g of sediment was collected before the sampler was placed on the flume bed. This sediment amount is highly overestimated, since most of this time the sampler was not properly aligned and likely collected no sediment. The sampler collects even less sediment in the vegetated part of the channel because of the overall lower sediment fluxes. In any case, the sediment amounts captured while sampler is not placed on flume bed are not negligible, and the sampler should be quickly lowered on the bed. When the placing is done quickly, there is no issue in starting the timing after placement.

Errors from sediment removal and sediment entry during sampler placement were low. With large samples, the errors were considerably lower than the CVs of measured bed load fluxes. In test III and other studies (discussed in Section 4.1.1), use of sand bed leads to the sampler operation having larger impact on the results. Nevertheless, in settings without sand bed (test I and II), the sampler can be operated reliably without large errors.

4.2 Drag force measurements: influence of flow velocity, plant alignment and height

The drag force measurements were conducted to assess how different plant and leaf configurations, alignment and re-attachment of the plant affected the measured values. Also, the relation of forces exerted by the plants and velocity were compared to literature sources to see if the sensor responded properly to increasing force under flow.

Higher forces were measured with the shorter plant compared to tall plant, with 4 leaves compared to 3 leaves, and in position 1 compared to position 2 (Table 12). The latter two are as expected, as both the 4-leafed plant and position 1 cause higher leaf area to be perpendicular to the flow compared to 3-leafed plant and position 2. Characteristic area of the plant is directly proportional to the drag force (Equation 2), explaining the higher forces measured from 4-leafed plant and position 1. Reason for shorter plant causing higher forces

than the tall plant is likely related to the stem length. The leaves of tall plant were higher in the stem, which likely allowed the stem to bend more than with the short plant, reducing the projected leaf area facing the flow. Visualization of the average forces for S4_L1, S4_L2, T4_L1 and T4_L2 are shown in Figure 22. The force increased almost linearly with increasing flow velocity with all of the visualized plants. Similar observations have been made in other studies. According to Jalonen et al. (2012), several studies on isolated flexible trees suggested that almost a liner relationship existed between the mean flow velocity and drag force. This in addition to initial calibration under dry conditions suggests that the sensor is correctly measuring the studied phenomena under flow conditions.

Table 12: Resulting forces and statistics from drag force measurements at each measured velocity. The plant codes (as described in Section 3.1.4) represent the plant height (short or tall, S or T), number of leaves (4 or 3 clusters), and positions (1 or 2).

Plant	Flow velocity (m/s)	0.1	0.2	0.3	0.4
S4L_1	**avg. Force (N)**	0.151	0.268	0.4	0.493
	st.dev.	0.005	0.006	0.01	0.012
	CV (%)	**2.99**	**2.27**	**2.62**	**2.53**
S4L_2	**avg. Force (N)**	0.057	0.199	0.257	0.383
	st.dev.	0.005	0.004	0.004	0.015
	CV (%)	**8.04**	**1.79**	**1.71**	**3.95**
T4L_1	**avg. Force (N)**	0.119	0.218	0.264	0.371
	st.dev.	0.005	0.006	0.008	0.014
	CV (%)	**3.95**	**2.57**	**3.17**	**3.66**
T4L_2	**avg. Force (N)**	0.04	0.149	0.219	0.304
	st.dev.	0.004	0.006	0.006	0.01
	CV (%)	**9.29**	**4**	**2.71**	**3.17**
S3L_1	**avg. Force (N)**	0.099	0.209	0.315	0.343
	st.dev.	0.003	0.006	0.009	0.01
	CV (%)	**3.41**	**2.81**	**2.7**	**2.79**
S3L_2	**avg. Force (N)**	0.056	0.167	0.252	0.299
	st.dev.	0.005	0.008	0.006	0.01
	CV (%)	**8.86**	**4.7**	**2.33**	**3.25**
T3L_1	**avg. Force (N)**	0.104	0.18	0.257	0.314
	st.dev.	0.005	0.004	0.006	0.01
	CV (%)	**4.68**	**2.15**	**2.46**	**3.12**
T3L_2	**avg. Force (N)**	0.031	0.117	0.204	0.282
	st.dev.	0.004	0.006	0.007	0.01
	CV (%)	**12.19**	**4.93**	**3.41**	**3.42**

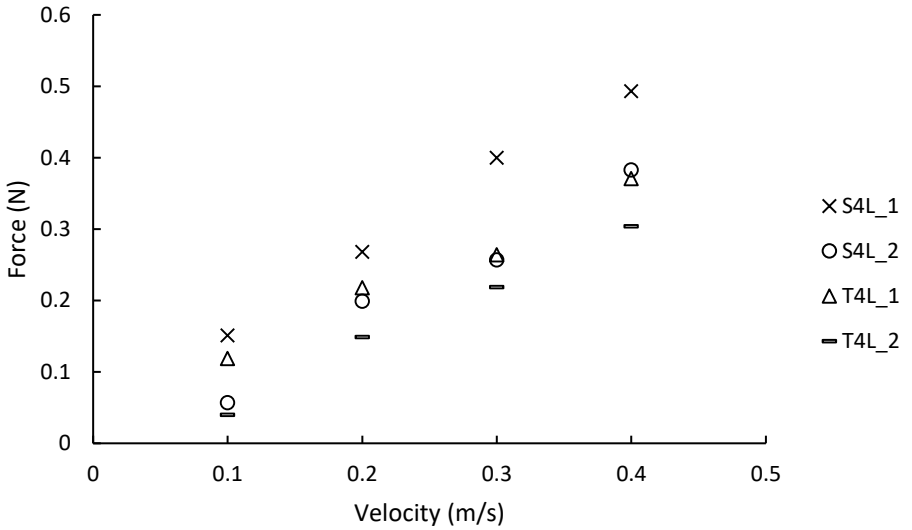

Figure 22: Relation of velocity and average measured force for 4-leaved short and tall plants in positions 1 and 2.

Variability in the measured forces can be assessed with the CVs shown in Table 12. With all of the plant leaf configurations and positions, the relative variability was largest with the lowest velocity. Similar observations were made by Västilä et al. (2013): CV of measured force decreased with increasing velocity in their study with single poplars. According to their study, this indicated that drag force varied the most at low velocities (Västilä et al. 2013). Constant background noise from the sensor would be relatively larger with low velocities, but the variability caused by the plant and flow themselves is more probable cause. In the low velocities, the plants have not yet reconfigured, but might be on the verge of starting to bend and align leaves with the flow. These minor oscillations may possibly have relatively large impact on the measured force, seen as high CVs in the low velocity measurements. What explains the even larger CVs when plant is in position 2 is more difficult to answer. One possibility is that while in position 2, the plant is more susceptible to turbulence in the direction perpendicular to the mean flow.

Figure 23 presents the ratio of measured force of plant in position 2 and 1 plotted for different flow velocities. The difference in measured drag force between positions 2 and 1 decreased with increasing flow velocities. This was result from plant reconfiguration, which describes the bending and streamlining of a plant under flow, and is known to decrease flow resistance caused by the plant (Västilä and Järvelä 2018). In position 2, most of the leaves are already aligned with the flow, whereas in position 1 in low velocities the leaves are more or less perpendicular to the flow. This led to lower ratio of drag forces between positions 2 and 1 at low velocities. At higher velocities, the plant in position 1 gets closer to having leaves in same position as the plant in position 2, causing the ratio to increase. These differences between plant positions implicate that it is important to properly align the plants when comparing some other parameters, for example different plant heights or leaf configurations, as the same plant can exert even 3-times higher forces depending on the alignment.

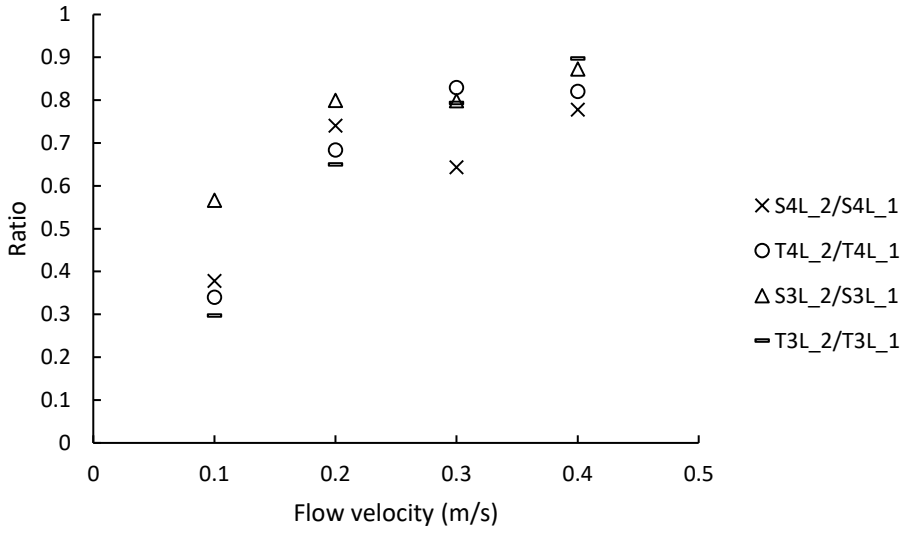

Figure 23: Ratio in measured drag forces between positions 2 and 1. The plant names represent the plant height (short or tall), number of leaves (4 or 3 clusters), and position (1 or 2) (see Section 3.1.4).

Development of drag force CVs for increasing measurement duration was studied (Figure 24) to assess suitable measurement duration. Generally, measured force varied very little in time, indicating that measurement duration can be short. With velocities larger than 0.1 m/s, most of the changes occurred during the first 10 seconds. With velocity of 0.1 m/s, the CV did not seem to fully stabilize even for measurement duration of 60 seconds, which indicated that the amount the force deviated from mean, changed in time. That being said, all of the plotted CVs were less than 3.5%, which means that the fluctuations in force were minor. With the relatively low frequency (5 Hz) of the measurements, studying minor temporal variations in the drag force is not recommended. With the very low CVs for short and longer measurement durations, the sensor is well suited for measuring mean drag forces exerted by plants.

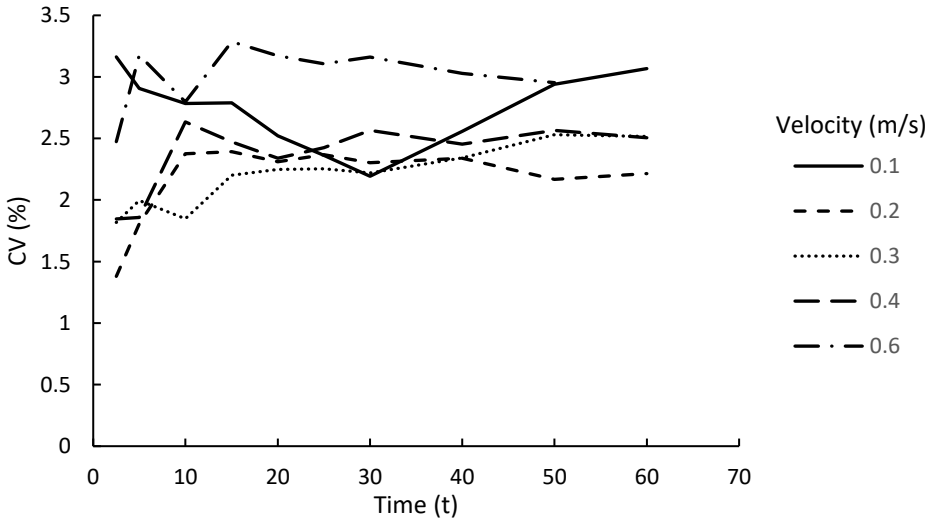

Figure 24: Drag force coefficients of variation (y-axis) for increasing measurement duration (x-axis) and different velocities. The data is from short plant in position 1, with 4 leaf clusters.

The results from removal and re-attachment of the plant are shown in Table 13. On average, relative difference between the repetitions was around 2%, indicating that the removal and re-attachment of plant has little impact on the mean drag force of the plant. This suggests that the measurement system is reliable, and that the attachment of the plant does not cause large errors. This allows reliable comparison for example of leafless stems and foliated plants, to derive parameter values used in advanced drag force equations with separate drag coefficients and reconfiguration parameters for foliage and stem (see Equation 4).

Table 13: Measured force of plant S4L_1 in 4 repetitive measurements after removal and re-attachment of the plant. Forces of each repetition are average from 1 minute of 5 HZ measurements.

Repetition	Flow velocity (m/s)	Force (N)
1	0.3	0.4
2	0.3	0.39
3	0.3	0.38
4	0.3	0.39
	avg.	0.39
	Stdev.	0.01
	CV (%)	2.09

4.3 Laboratory nutrient analysis of soil and sediment samples

4.3.1 Soil and sediment profiles, medium-term nutrient accumulation

The following results are from field samples analyzed for element concentrations as described in Section 3.2, to study changes in element concentrations in the core profiles. Point measurement data from years 2010 and 2019 was used to estimate amount of deposition since year 2010 channel excavation.

Cores C, D and E

Results from element analysis and bulk density calculations of three soil and sediment profiles from Ritobäcken are plotted in Figure 25, to compare if element ratios and bulk densities show similar patterns, possibly revealing the past ground level from year 2010. Point measurements could not be linked accurately to these cores, so the amount of deposition is not known. Core C (Figure 25a) shows decrease in bulk density above 5 cm, and Mg/Al and K/Al ratios also decrease more rapidly above 3 cm. While Mg/Al and K/Al ratios decrease throughout the profile when moving upwards in the vertical, decrease above 3 cm is more rapid compared to remaining of the profile. Core E (Figure 25b) is difficult to interpret, and especially element ratios do not show significant trends in comparison to bulk density. Core D (Figure 25c) shows spikes in bulk density and element ratios at same depths (1-2 cm, 10 cm), but conclusions regarding amount of deposition could not be made.

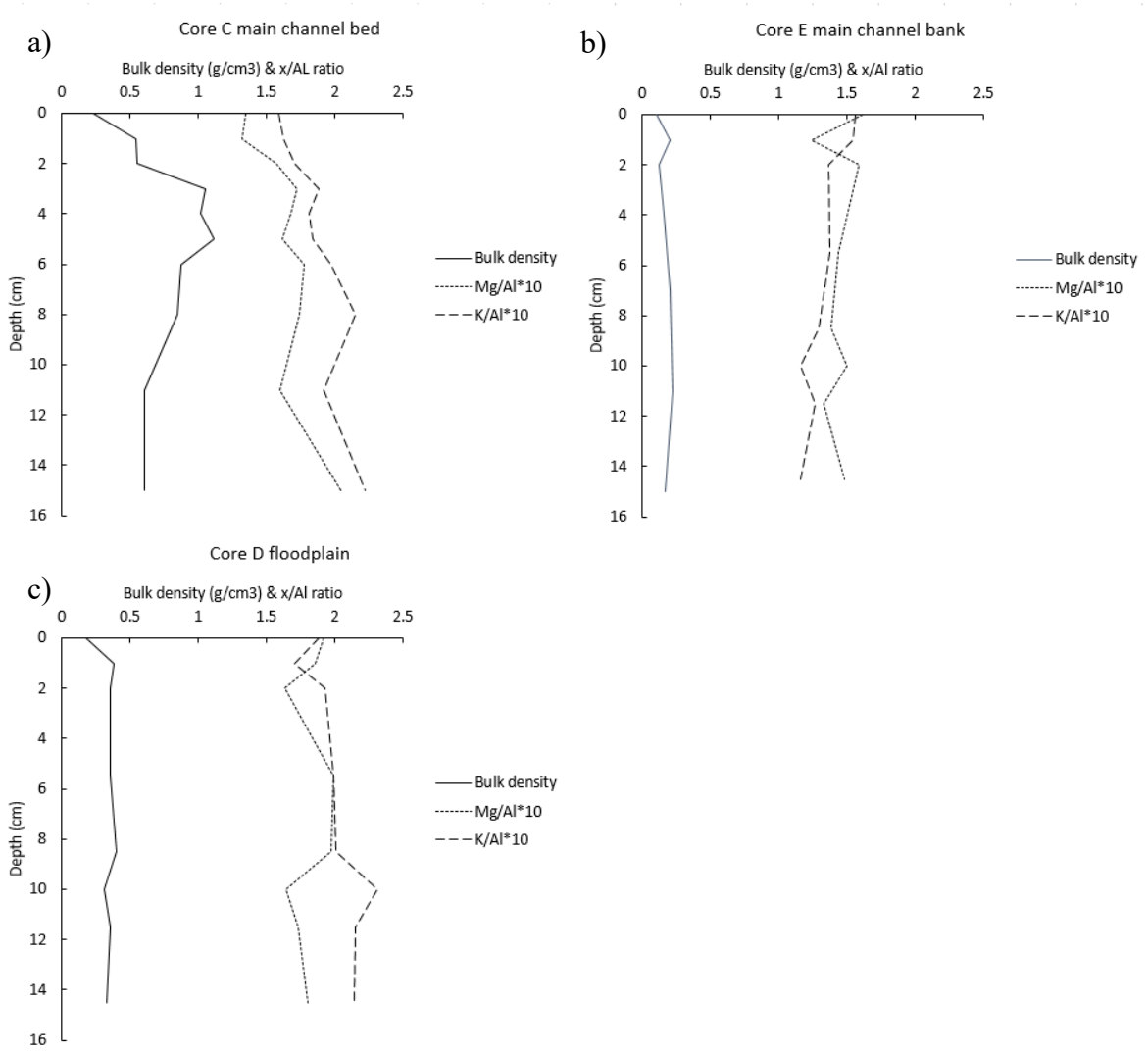

Figure 25: Bulk densities, Mg/Al and K/Al ratios of three soil and sediment cores. Mg/Al and K/Al ratios were multiplied by ten to improve visibility. Ratios are dimensionless.

Cores O and T, interface between main channel and floodplain

Comparison between bulk densities and element ratios of soil cores O and T (see Figures 14-15) characterized the variability at the interface between main channel and floodplain. Year 2010 ground level (excavation horizon) determined from point measurements is plotted as horizontal line (Figure 26). Both cores show similar pattern when depth increases: bulk density increases steadily until it starts to reach equilibrium at around 12-15 cm depth. Ground level after excavation in year 2010 locates close to this equilibrium for core O, but is very different for Core T. Regardless of the similar sampling location between these two cores (interface between main channel and floodplain), ground level in year 2010 is in different part of the soil profile. The ground level was chosen from point measurement nearest to the coring location, and the level plotted in Figure 26 equals to height difference between years 2010-2019. There is a spike in the bulk density plot of Core T at same depth as the year 2010 ground level (more visible when not using moving average), but its connection to excavation horizon is unclear. In studies reviewed in Section 2.3.1, bulk density was shown to decrease with time and especially in the top-most layers (Ballantine and Schneider 2009, Passoni et al. 2009). This may suggest that regardless of deposition, bulk density decreases

towards the topmost soil layers, meaning that even if the deposition can be associated with low bulk density, natural decrease in density towards the top layers might lead to this difference being less visible. That being said, there is still possibility that the change in density is larger close to the layer where deposition on top of excavated ground began.

Ratios of magnesium, potassium, manganese and sulfur to aluminum are also plotted in Figure 26 for cores O and T. Overall, the ratios appear to decrease with increasing depth, opposite of the bulk density. Also, the element ratios seem to be quite stable until certain depth, after which they start to decrease. This depth seems to match quite well with the year 2010 ground level on both cores.

Based on the point measurements, change in ground level between years 2010-2019 can differ tens of centimeters between points just 20 cm apart because of the high deposition at interface between floodplain and main channel. For this reason, using average ground level across several points is not very accurate for determining ground level in year 2010 for single core. Using just one point would be more accurate in case where the core is taken exactly at same point where co-ordinate measurement is available. The cores O and T shown in Figure 26 were taken very close to the point measurements, and hence single point measurement was used for the ground level. Nevertheless, there is a possibility that the coring location does not exactly match the point measurement, which could cause bias in the ground level shown in Figure 26.

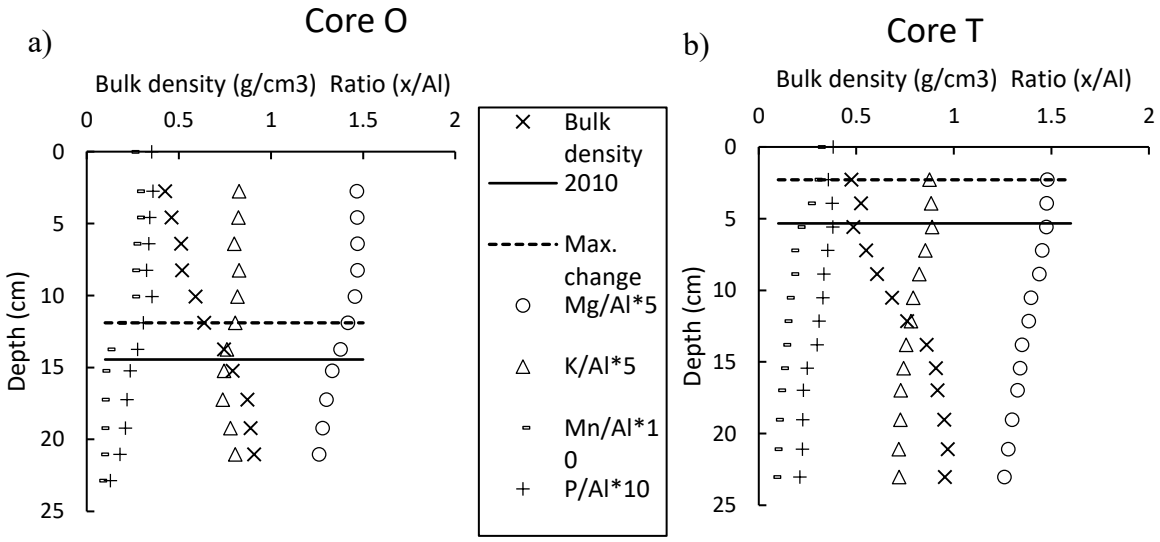

Figure 26: Bulk density and element ratio profiles a) from cross section 19 and b) from cross section 15. Core O was taken approximately 6.65 m from right side of the cross section, and Core T 7.065 m from the right side. Solid horizontal line indicates ground level in year 2010, when the channel was excavated to its current form, and dotted line indicates point of maximum change in bulk density. 3-Point moving average was used for the bulk density, Mg and K plots. Element ratios were multiplied by either 5 or 10 to improve visibility.

Cores K and G, Floodplain

Point measurements further from floodplain and main channel interface (see Figures 14-15) in Ritobäcken suggested that in the middle of the floodplain, only few centimeters of soil has been deposited between years 2010-2019. This is visible in Figure 27 as the ground level of year 2010 is almost at the surface. Bulk density profiles of floodplain cores K and G do not show visible cues regarding the year 2010 ground level being this close to the surface. Potassium profile is also different compared to cores O and T (Figure 26), as it increases with depth. The rest of the element ratios (Mg/Al, Mn/Al and P/Al) showed similar behavior with all of the cores O, T, K and G; decreasing below the excavation horizon.

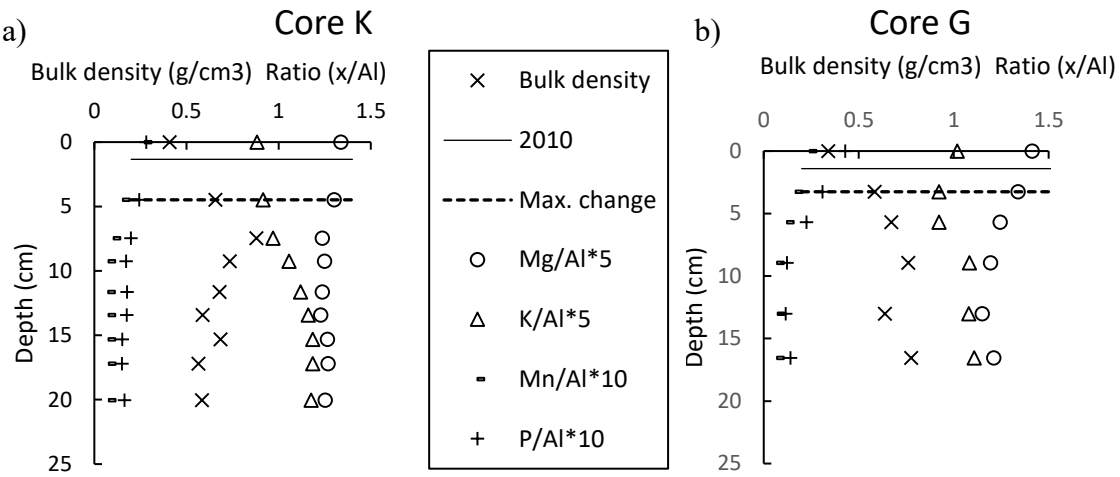

Figure 27: Bulk density and element profiles a) from cross section 15 and b) from cross section 7. Core K was collected approximately 5.06 m from right side of the cross section, and Core G 3.06 m from the right side.

To assess the detection accuracy of year 2010 ground level, maximum change in bulk density between two adjacent samples were plotted as dotted lines in Figures 26-27 (at depth between the two samples). In the four core plots, the dotted line locates on average 2.6 cm off from the excavation horizon determined as year 2010 ground level. Maximum and minimum differences were 3.1 and 1.8 cm, respectively. While the relative error in case of low amount of deposition is large, visual interpretation of bulk density patterns is more difficult. For example, bulk density of cores O and T (Figure 26) showed similar patterns, meaning that any visual interpretation could arrive at same conclusion in case of both cores. However, the year 2010 ground level determined from point measurements was different for these two cores. Scaling of the change in bulk density with sample thickness was attempted, but it led to worse result. Fortunately, the samples are quite uniform in thickness. The maximum change between two samples might not be as visible from the plots themselves, for they are smoothed with 3-point moving average.

Sulfur concentrations

Sulfur concentrations of cores from main channel, floodplain and interface at Ritobäcken are visualized in Figure 28. The sulfur profiles were studied to see if the concentration increases deeper in the profile, similar to Boman et al. (2010) discussed in Section 2.3.1. In the main channel cores J and C (see Figure 15), sulfur concentration increases dramatically after depth of 10 cm. In core N, sulfur concentrations are high throughout the profile, with largest peaks

at around 6-7 cm and 16 cm. The sulfur concentrations of floodplain and main channel-floodplain interface cores K, G, O and T remain fairly constant throughout the profile. The concentration is slightly increasing with depth, but there are no large peaks visible. In Section 2.3.1, behavior of sulfur in AS-soils was discussed. In Figure 6, a peak in sulfur concentration was observed at depth which had always been submerged. The peak concentration was approximately 1-1.5% of sample dry weight. In main channel cores (Figure 28a), peak sulfur concentrations were approximately between 8000-18000 ppm, which correspond to concentrations of 0.8-1.8% and have similar magnitude to the values by Boman et al. (2010). This can indicate that water level has not been lower than the observed peak concentration depths of sulfur in the main channel. The assumption is that the soil with lower sulfur contents has been subject to oxygen at some point in history, converting sulfur to more mobile forms (Section 2.3.1). The channel bed has not been lower than the sulfur peaks even when the channel was originally excavated. This is because at the time of excavation, oxygen might have reached the soil below the channel bed, meaning that soil still high in sulfur should have remained submerged at some distance away from the bed.

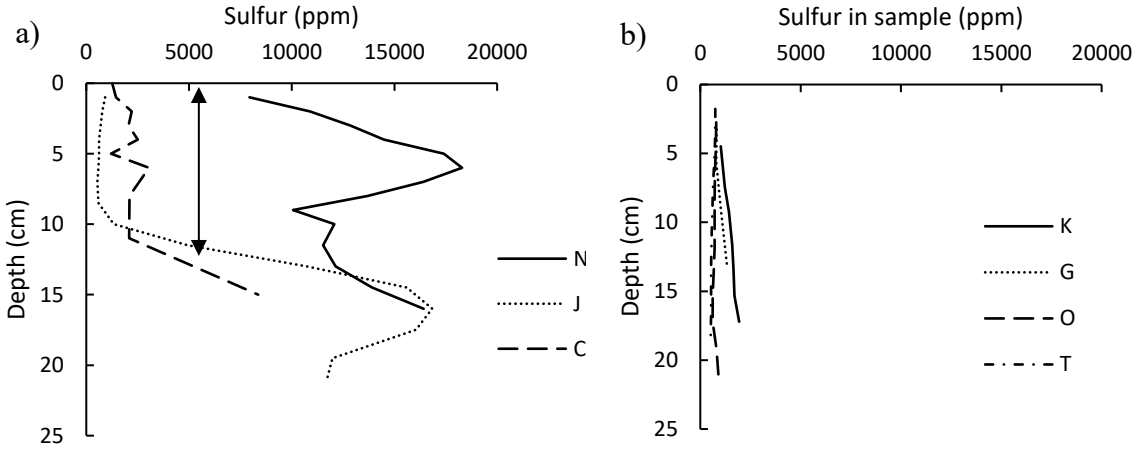

Figure 28: Sulfur concentrations of a) main channel cores and b) floodplain/interface cores. 3-point moving average was used for every core except C. Arrow in the left image indicates the maximum estimated change in ground level (amount of deposition since channel excavation).

Normalization for detecting excavation horizon

Mg/Al and Mn/Al ratios were chosen for further analysis, as they were visually the most promising in locating the year 2010 ground level (Figures 26-27). Mg might be more reliable based on its chemical characteristics. Magnesium is found often in clay minerals (Sposito 2008), and is geochemically immobile. Mineralogical difference between old soil and deposited material should hence be visible in the magnesium profiles. Manganese oxides on contrary are very reactive, and can form a geochemical barrier in oxic environments, leading to accumulation of certain elements near the barrier through sorption and redox reactions (Mayanna et al. 2015). For example, adsorption of phosphate to manganese oxides has been observed (Kawashima et al. 1986). Mn and P profiles were both elevated towards the surface (Figures 26-27), suggesting that this effect might be present in the field site if the water table is close to the surface. Because of this, the Mn dynamics seen in the soil profiles may not be

only result from difference in composition of deposited and original soil, and use of Mn/Al ratios alone is not recommended.

To study if the Mg/Al and Mn/Al ratios differ above and below the ground level of 2010, the results were normalized. In this normalization, sample which located at depth closest to the excavation horizon was chosen as reference, and element ratios and depths of other samples were divided by this reference sample. This was done for cores O, T, K and G, all of which are plotted in Figures 29a-30a along with plot where the depths of the samples are not normalized (Figures 29b-30b). Cores O and T are shown independently in Appendix B. For normalized Mg/Al ratios in the left image (Figure 29), it can be seen that almost every sample that locates higher than the reference depth (horizontal line) has scaled Mg/Al ratio higher than 1. This means that in each studied core, samples higher than the excavation horizon had almost always higher Mg/Al ratio than at the horizon. Similarly, samples below the horizon have almost always lower Mg/Al ratio than at the horizon. This same effect can be seen with normalized Mn/Al ratios (Figure 30a), but here the difference above and below the reference depth appears much larger. For the plots with non-normalized depths (Figures 29b-30b), it is visible that samples with scaled element ratio higher than 1 locate in quite broad range between depths ~0-15 cm. This means that the depth alone does not control the element ratios, suggesting that depth in relation to reference (year 2010 ground level, Figures 29a-30a) better explains the changes in Mg/Al and Mn/Al ratios. That being said, if the element ratio steadily decreases with increasing depth, no matter where the reference value is chosen, samples above and below the reference depth will have larger and smaller element ratios, respectively. Judging from the core plots in Figures 26-27, this happens to some extent, meaning that this information alone cannot be used to determine the amount of deposition after channel excavation in year 2010.

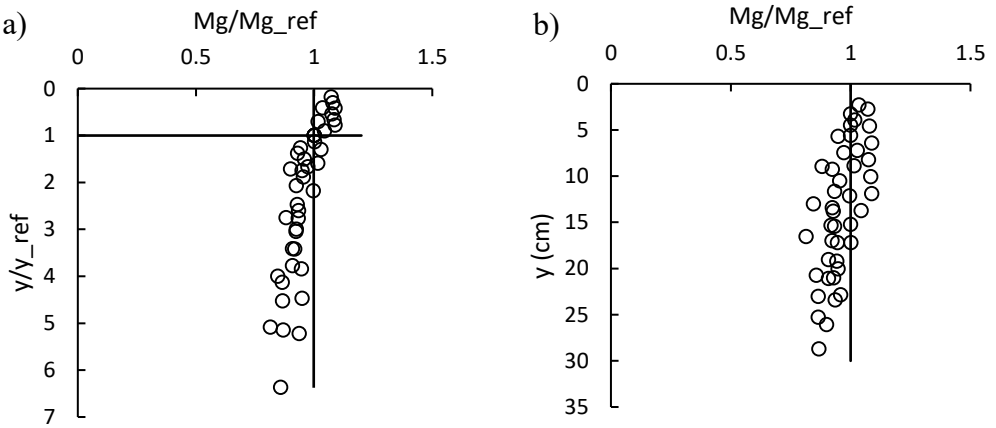

Figure 29: a) Normalized and b) un-scaled relations between depth (y) and sample Mg/Al ratios taken from cores O, T, K and G. In the left image, sample which located at depth closest to the year 2010 ground level was chosen as reference, and Mg/Al ratios and depths of other samples were divided by this reference. Values larger than 1 in the y-axis of left image corresponds to samples taken deeper than the 2010 ground level and vice versa, and similarly values larger than 1 in x-axis indicate Mg/Al ratio to be higher than the reference. Horizontal line indicates the reference depth, and vertical line indicates the reference Mg/Al ratio.

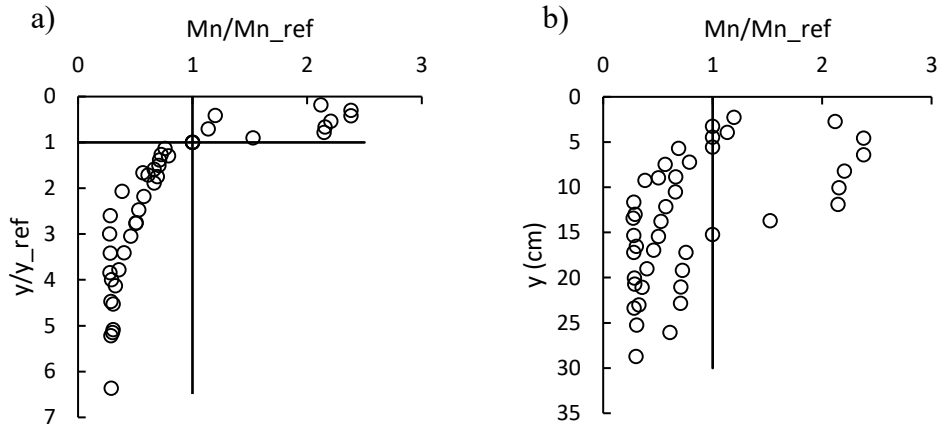

Figure 30: a) Normalized and b) un-scaled relations between depth (y) and sample Mn/Al ratios taken from cores O, T, K and G. In the left image, sample which located at depth closest to the excavation horizon was chosen as reference, and Mn/Al ratios and depths of other samples were divided by this reference. Values larger than 1 in the y-axis of left image corresponds to samples taken deeper than the excavation horizon and vice versa, and similarly values larger than 1 in x-axis indicate Mn/Al ratio to be higher than the reference. Horizontal line indicates the reference depth, the depth of sample located closest to the excavation horizon. Vertical line indicates the reference Mn/Al ratio.

The normalization with potassium (Figure 31) suggested that contrary to Mg and Mn, the reference depth does not appear to divide the K/Al ratios in similar way. Both higher and lower K/Al ratios are present above and below the reference depth.

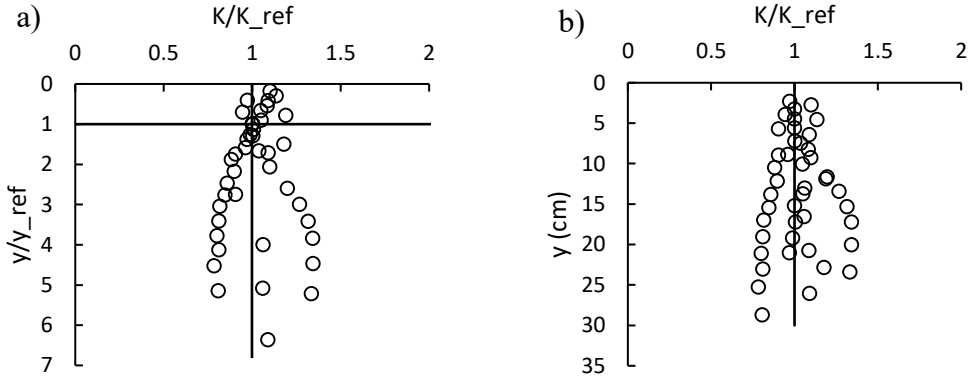

Figure 31: Normalized (a) and un-scaled (b) relations between depth (y) and sample K/Al ratios taken from cores O, T, K and G. Horizontal line indicates the reference depth, and vertical line indicates the reference K/Al ratio.

Since the Mn/Al ratios seemed to have large difference above and below the reference depth, maximum change in Mn/Al ratio between two adjacent samples was calculated, similar to maximum change in bulk density discussed earlier in this section. This time the difference was also scaled with distance between the samples (thickness of the upper sample), which did not affect the outcome. These resulting depths are shown in Table 14. On average, the maximum change in Mn/Al ratio locates 2 cm off from the year 2010 ground level, which is

slightly better than when using maximum change in bulk density. That being said, the maximum change in bulk density was at same depth with maximum change in Mn/Al ratio in all of the cores except T. This method could possibly locate the year 2010 ground level even better, but the difference can only be calculated between two samples, meaning that the accuracy is up to how thin the samples are. Due to core compaction during the sampling, the samples were estimated to represent larger thickness than the actual sample slice was, further increasing the distance between adjacent samples.

Table 14: Comparison of using maximum change in bulk density and Mn/Al ratio between to adjacent samples to estimate amount of deposition since channel excavation in year 2010. The depth of maximum change corresponds to the top of the lower sample.

	Depth of max. change (cm)			Abs. difference (cm)	
Core	**Bulk density**	**Mn/Al**	**Depth, 2010 ground level (cm)**	**Bulk density**	**Mn/Al**
K	4.48	4.48	1.34	3.14	3.14
G	3.18	3.18	1.41	1.78	1.78
O	11.9	11.9	14.45	2.55	2.55
T	2.29	5.58	5.33	3.04	0.25
			avg.	2.63	1.93

4.3.2 Effect of pre-processing steps on measured nutrient and element content

Repeatability of CN and ICP-OES analysis

Table 15 shows the CN-analysis results of three replicas taken from four different, unsieved, electro-mechanically ground samples (see Section 3.2.3). On average, CVs were 2 % and 2.6% for nitrogen and carbon content, respectively. How much of this variation was caused by the analysis itself and how much by the differences in replicate samples, is not considered. Nonetheless, the sample is presumably very homogeneous for replicate sub samples to provide results this uniform. In the light of these results, even just one CN analysis per sample could be sufficient. For ICP-OES repeatability, the results are in Table 16. Depending on the element, the CVs ranged in 3.1-22.24%. One should note that these results were from manually ground >63 µm fractions. Firstly, the element concentrations in >63 µm fractions were on average much lower than in non-sieved samples (average Al concentration is ~6 times higher in non-sieved sample), which likely caused higher relative variation. Secondly, the results from CN-analysis suggested that MEK grinding would likely produce more homogeneous samples and lead to better repeatability (lower CVs on MEK samples, Table 17). Even with the manual grinding, the repetitive ICP-OES analysis appeared to give reliable results.

Table 15: Analysis repetitions for Carbon and Nitrogen contents of four unsieved, electro-mechanically ground samples. Three repetitions were conducted for each sample.

Sample	**N avg. (%)**	**CV (%)**	**C avg. (%)**	**CV (%)**
68	0.3	1.91	5.58	0.73
74	0.2	1.12	3.29	4.24
92	0.39	3.8	5.79	3.83
100	0.19	1.13	3.23	1.55
avg.	0.27	1.99	4.47	2.59

Table 16: Coefficients of variation of element concentration (ppm), 2 replicate measurements taken from samples 250, 252 and 255. The repetitive measurements were done on manually ground >63 µm fractions. These samples are from other site not discussed in this work.

Sample	Al	Ba	Ca	Fe	K	Mg	Mn	P	S	Zn
250 CV (%)	4.02	5.81	2.86	3.59	3.56	4.27	7.73	5.24	8.03	17.09
252 CV (%)	0.16	3.48	-	2.46	1.21	0.07	0.3	1.46	1.44	46.08
255 CV (%)	5.13	12.71	4.41	6.66	1.08	5.62	10.41	8.17	9.35	3.54
avg.	**3.1**	**7.33**	**3.64**	**4.24**	**1.95**	**3.32**	**6.15**	**4.96**	**6.27**	**22.24**

MEK-MAN comparison, effect of wet-sieving

Results of CN-analysis are summarized in Table 17 for samples 26, 28, 32. The >63 µm fractions of these samples do not contain nitrogen, meaning that grinding type does not have effect on the measured nitrogen concentrations. Overall, the manually ground samples tend to have slightly higher carbon concentration (and nitrogen), and coefficients of variation are clearly larger for manually ground samples. Also, manually ground samples had higher maximum and lower minimum carbon concentration than mechanically ground sample in two out of the three samples. These results indicate that replicate analysis made from the same sample have higher variation if the sample was manually ground. This in turn might be result from the manual sample being less homogeneous. Coefficients of variation from these samples should not be used as estimate on variability of CN-analysis; the variability is relatively large due to element contents being close to zero.

Average arithmetic differences between MEK-MAN grinding was calculated for carbon concentration from samples 26, 28 and 32 (Table 17), and were compared with average C concentrations of mechanically ground unsieved samples 68, 74, 92 and 100 (Table 15). The arithmetic MEK-MAN difference is less than 4% of average C concentration of samples 68, 74, 92 and 100, which implies that the choice of grinding type has little effect on the final nutrient concentrations. On average, mechanically ground samples have ~0.15 percentage units lower carbon concentration. It should be noted that the average arithmetic difference between MEK-MAN grinding is of similar magnitude as standard deviations of the carbon content (of samples 26, 28 and 32). However, standard deviations of repetitions from samples 68, 74, 92 and 100 (not shown here) are lower than the MEK-MAN difference, meaning that grinding type has some effect on the nutrient contents.

Table 17: Statistics of CN-analysis for five replicates of samples 26, 28 and 32, consisting of sieved >63 µm fractions. Sample nitrogen concentrations were below detection limit, and are not shown here.

Sample	C concentration (%)	Max.	Min.	Stdev.	CV (%)
R26 MEK	0.39	0.49	0.31	0.08	21.2
R26 MAN	0.32	0.4	0.24	0.08	24.2
R28 MEK	0.8	0.91	0.65	0.12	15.3
R28 MAN	0.79	1.2	0.59	0.25	32.3
R32 MEK	0.81	0.94	0.71	0.1	11.7
R32 MAN	1.34	1.67	0.81	0.37	27.7
Avg. C concentration (%) (MEK)		0.66			
Avg. C concentration (%) (MAN)		0.82			
Difference MEK-MAN		-0.15			

MEK-MAN differences on ICP-OES analysis are shown in Table 18, and indicate that the two types of grinding provide results very close to each other in case of unsieved samples. The case is different for > 63 µm fractions of samples 26, 28 and 32, as the mechanically ground samples had on average 46% higher element concentration than manually ground samples, and the arithmetic difference is on average around 500 ppm. For the unsieved samples, the difference between the grinding types is very low, on average 0.5% higher element content in mechanically ground samples, with mean difference in concentration of around 260 ppm. The highest difference is on Mg concentration, mechanically ground sample having it 11% higher. Since the comparison was done only on 3 samples, the differences can occur also by chance (this was not tested statistically). The larger differences with the > 63 µm fractions are likely caused by overall smaller element concentrations. In any case, MEK-MAN difference on unsieved samples appears small in both CN and ICP-OES analysis. The differences are tested statistically for C and N contents in the end of this section.

Table 18: Average differences and ratios of element contents (PPM) between MEK and MAN grinding.

Samples	ICP-OES	Al	Ba	Ca	Fe	K	Mg	Mn	P	S	Zn	avg.
> 63 µm, 26, 28, 32	**Difference (PPM) MEK-MAN**	1112	5	460	2360	283	416	20	69	62	2	**479**
	Ratio MEK/MAN	1.3	2.4	1.33	1.37	1.39	1.3	1.5	1.47	1.29	1.21	**1.46**
Unsieved, 22, 25, 30	**Difference (PPM) MEK-MAN**	766	-4	19	1017	14	696	-21	-31	187	-5	**264**
	Ratio MEK/MAN	1.02	0.97	1	1.02	1	1.11	0.94	0.94	1.09	0.95	**1.005**

Effect of wet sieving (inclusion of >63 µm fractions) on measured element concentrations in both CN and ICP-OES analysis is low; wet sieving results on average 6% higher Carbon and Aluminum concentration, and 7% higher nitrogen concentration compared to not sieving the sample. Aluminum was chosen as an example element to avoid excess calculations when estimating effect of sieving on ICP-OES analysis. The higher concentration in sieved sample is explained by the removal of fractions with lower element contents. In the calculation,

average C or N concentrations of >63 µm fractions (Table 17) and non-sieved samples (Table 15) were used along with average ratio of <63 µm / >63 µm fractions (~14.6) across several sieved samples, to calculate the nutrient concentration in case if the > 63 µm fraction was excluded (Equation A1 in Appendix A). This same calculation was done with average aluminum concentrations from several non-sieved samples and >63 µm fractions, arriving close to the same result (~6% higher concentration in sieved sample). Effect of sieving is naturally larger if the sieved fractions are of similar mass.

Statistical tests

Statistical significance of the differences between MEK and MAN grinding was tested for and N concentrations of samples 26, 28 and 32, and only carbon content of sample 32 was observed to differ statistically between grinding types. T-test was used to test null-hypothesis that means of manually and mechanically ground samples would be equal with 95% confidence level. Before this, F-test was used to test null-hypothesis that variances of the populations are equal, to decide is T-test done assuming equal or unequal variances. Only sample 32 rejected null-hypothesis of F-test with carbon content (meaning that MEK and MAN samples had unequal variances), and same sample was only one to reject null-hypothesis of T-test with carbon content. In other words, only carbon concentration of sample 32 has statistically significant difference between mechanical and manual grinding. These same tests were conducted for nitrogen and carbon concentrations normalized for total sample mass (because there seemed to be trend between sample mass and nutrient concentration), and results of T-tests were identical. As the sample size is low with only 5 replicate samples, observing normal distribution, which is and assumption for T-test, is difficult. Six replicate samples were available for sample 23, and normality of this distribution was tested with Q-Q plot (not shown here), suggesting that the element concentrations of sub-samples are normally distributed.

Discussion of pre-processing effects on element concentrations

The differences in CN and ICP-OES results depending on type of grinding are very low. For CN-analysis, the difference is on average less than 4% compared to total carbon concentrations. For ICP-OES, the difference is between 0-11% for other elements. The small differences agree with literature; according Gregorich and Carter (2007), aggressive grinding is acceptable for soil samples subject to total and strong-acid extractable element analysis.

The difference in ICP-OES results was not proven statistically, but based on the data it may differ with each element, with most having difference very close to zero. MEK-MAN difference is very large in sieved >63 µm fractions, but this is believed to be caused by overall low element content in these fractions. For CN-analysis, the difference was proven statistically significant only for carbon content of sample 32, but the data overall suggests that there still is a difference.

Repeatability of the CN and ICP-OES analysis is good. Mechanically ground non-sieved samples used for CN-analysis had concentration CV of around 2% for nitrogen and 2.6% for carbon. In ICP-OES analysis, CVs of other element concentrations were between 3-22% for manually ground samples of >63 µm fractions. The ICP-OES analysis is believed to be much more accurate in case of non-sieved mechanically ground samples, but no repetitions were done to study this.

Effect of wet sieving on measured element concentrations is low, causing on average 6% higher carbon and other element concentrations by removing large particles generally having lower concentrations. Nitrogen was not present in the >63 µm fractions, but sieving these fractions out increased the overall concentration by around 7%. Originally the concern was that inclusion and grinding of the >63 µm fractions would increase the element concentrations and thus affect the results. While the MEK grinding increased the concentrations of >63 µm fractions (Table 18, top) the effect on the whole sample was low (Table 18, bottom). In case of large amount of >63 µm particles, it might be best to manually ground the sample. Wet-sieving does not seem necessary based on these results, but as mentioned in Section 2.3.2, the form of the elements may differ among the fractions. This means that for some purposes, the sieving is necessary. For example, according to Leong and Tanner (1999), the coarse particles contained more inorganic carbon, which was to be removed before analysis for organic carbon.

5 Conclusions

The goal of this work was to develop experimental methods for investigating flow resistance, sediment and nutrient transport in vegetated flows. The three specific objectives were to develop bed load and drag force measurement systems for flume conditions, and to develop methodology for studying decadal-scale nutrient accumulation in environmental channels. Downscaled Helley-Smith sampler (DHS) appears to have been used only on few occasions for flume bed load measurements, and regarding nutrient accumulation in vegetated channels, the soil- and sediment data of this work is used in relatively novel ways in estimating amount of sediment deposition in a human modified river-floodplain setting. Direct in-flume vegetative flow resistance measurements have been conducted before in other studies, but at Aalto EHL, drag forces have previously been measured in towing tank. Direct in-flume measurements allow for quicker adjustments to studied plants, and for longer duration of measurements.

The conducted experiments suggested that the downscaled Helley-Smith (DHS) sampler is suitable for in-flume measurements of bed load. The measurement variability was relatively low in tested conditions and were partly caused by natural fluctuations in suspended sediment and bed load transport. Comparison with optical backscatter technique (OBS) indicated that the DHS sampler measures approximately 34% higher SSC. While objective sampling efficiency was not determined in this work, the sampler is believed to measure in the correct order of magnitude. Errors caused by sampling time and sediment removal were low in comparison to amount of measured sediment. Common sampling time of 1 minute used with full-sized samplers functions also with the downscaled sampler in conditions of high bed load. With lower fluxes within vegetation, sampling time of 3 minutes or longer is recommended to capture higher weight to reduce effect of errors from sediment removal and weighing. The variability of measurements was relatively low, meaning that low number of samples may be enough to get indicative values of the bed load fluxes. Further tests to calibrate the sampler are recommended to find out relation between flow speed and sampling efficiency. This information is especially important when comparing bed load transport in parts of flume with highly different flow velocities such as within and outside of vegetation.

In-flume drag force measurements provided results that agreed with other studies, indicating that the sensor was properly measuring the drag forces induced on plant by the flow. Coefficients of variation of the measured forces were minor, and their development in relation to time suggested that most of the temporal variations are captured in the span of 10 seconds. The relative variation was largest with low flow velocities, possibly caused by combination of static noise from the sensor and from the plants being on the verge of reconfiguration. Alignment of the plant had larger impact on the measured force the lower flow velocity was. Removal and re-attachment of the plant caused only minor difference in the measured forces. Adjustments to the measurement system are recommended to reduce effect of sediment preventing movement of the sensor, which caused difficulties when measuring in high flow velocities.

There is potential in using bulk density, magnesium (Mg), manganese (Mn) and sulfur (S) concentrations of soil and sediment samples as tools for determining the amount of deposited soil in cases where the site has been modified by excavation but lack monitoring of the ground level changes. While most of the element ratios decreased with increasing depth, the ratios started to decrease more rapidly below the depth of the ground level at the time, when

the channel was excavated to its current form. The maximum change in bulk density between two adjacent samples was proposed as a method to estimate amount of deposition, by indicating the depth above which soil has been deposited. Additionally, visual interpretation of Mg/Al and Mn/Al ratios in soil profiles could be used for the same purpose. Finally, sulfur concentration can serve to detect the lower limit of past ground level in samples taken from the main channel, in areas characterized with AS-soils. Estimates of the soil and sediment deposition can be used along with element concentrations in the profiles to calculate deposition rates for different nutrients. This supports studying of nutrient deposition in different parts of the two-stage channel design. The linkage of elements and amount of deposition are recommended to be studied further on positions where point measurements are available, to study if the observed element ratios behave in the same way also with other cores and field sites.

Experiments with soil- and sediment samples indicated that the samples can be mechanically ground with only small differences caused by the coarse fractions. Mechanical grinding resulted in lower variation between replicate samples, and manual grinding is recommended only when the sample has large amount of coarse particles, because ICP-OES results indicated that mechanical grinding of >63 µm fractions increases the element concentrations. This is mostly not concern, as the samples often had low amount of coarse fractions, and they generally had lower element concentration than the finer fractions. This resulted on average 6% lower element concentration when the sample was not sieved. Overall, with the taken sampling and pre-processing practices, the repeatability of the CN and ICP-OES analysis was good, indicating that single measurement per sample can provide accurate representation of the element concentrations.

References

Admiraal, D.M. and Garcia, M.H., 2000. Laboratory measurement of suspended sediment concentration using an Acoustic Concentration Profiler (ACP). *Experiments in Fluids,* 28(2), pp. 116-127.

Alomary, A.A. and Belhadj, S., 2007. Determination of heavy metals (Cd, Cr, Cu, Fe, Ni, Pb, Zn) by ICP-OES and their speciation in Algerian Mediterranean Sea sediments after a five-stage sequential extraction procedure. *Environmental monitoring and assessment,* 135(1-3), pp. 265-280.

Ballantine, K. and Schneider, R., 2009. Fifty-five years of soil development in restored freshwater depressional wetlands. *Ecological Applications,* 19(6), pp. 1467-1480.

Barton, J.R. and Lin, P., 1955. Study of the sediment transport in alluvial channels, Report No. 55JRB2, Colorado State University, Fort Collins, Colorado.

Bettinelli, M., Beone, G.M., Spezia, S. and Baffi, C., 2000. Determination of heavy metals in soils and sediments by microwave-assisted digestion and inductively coupled plasma optical emission spectrometry analysis. *Analytica Chimica Acta,* 424(2), pp. 289-296.

Bing, H., Wu, Y., Nahm, W. and Liu, E., 2013. Accumulation of heavy metals in the lacustrine sediment of Longgan Lake, middle reaches of Yangtze River, China. *Environmental earth sciences,* 69(8), pp. 2679-2689.

Boman, A., Fröjdö, S., Backlund, K. and Åström, M.E., 2010. Impact of isostatic land uplift and artificial drainage on oxidation of brackish-water sediments rich in metastable iron sulfide. *Geochimica et Cosmochimica Acta,* 74(4), pp. 1268-1281.

Boman, A., Åström, M. and Fröjdö, S., 2008. Sulfur dynamics in boreal acid sulfate soils rich in metastable iron sulfide—the role of artificial drainage. *Chemical Geology,* 255(1-2), pp. 68-77.

Box, W., Västilä, K. and Järvelä, J., 2018Transport and deposition of fine sediment in a channel partly covered by flexible vegetation, *E3S Web of Conferences* 2018, EDP Sciences, pp. 02016.

Brownlie, W.R., 1981. *Compilation of alluvial channel data: laboratory and field.* California Institute of Technology, WM Keck Laboratory of Hydraulics.

Bunte, K., Abt, S.R., Potyondy, J.P. and Swingle, K.W., 2008. A comparison of coarse bedload transport measured with bedload traps and Helley-Smith samplers. *Geodinamica Acta,* 21(1-2), pp. 53-66.

Burton, E.D., Bush, R.T., Johnston, S.G., Sullivan, L.A. and Keene, A.F., 2011. Sulfur biogeochemical cycling and novel Fe–S mineralization pathways in a tidally re-flooded wetland. *Geochimica et Cosmochimica Acta,* 75(12), pp. 3434-3451.

Callaghan, F.M., Cooper, G.G., Nikora, V.I., Lamouroux, N., Statzner, B., Sagnes, P., Radford, J., Malet, E. and Biggs, B.J.F., 2007. A submersible device for measuring drag forces on aquatic plants and other organisms. *New Zealand Journal of Marine and Freshwater Research,* 41(1), pp. 119-127.

Chand, V. and Prasad, S., 2013. ICP-OES assessment of heavy metal contamination in tropical marine sediments: a comparative study of two digestion techniques. *Microchemical Journal,* 111, pp. 53-61.

Charles, B. and Fredeen, K.J., 1997. Concepts, instrumentation and techniques in inductively coupled plasma optical emission spectrometry. *Perkin Elmer Corporation, USA*.

Childers, D., 1999. *Field comparisons of six pressure-difference bedload samplers in high-energy flow.* Vancouver, Wash.; Denver, CO: U.S. Dept. of the Interior, U.S. Geological Survey; Branch of Distribution distributor.

Claff, S.R., Burton, E.D., Sullivan, L.A. and Bush, R.T., 2010. Effect of sample pretreatment on the fractionation of Fe, Cr, Ni, Cu, Mn, and Zn in acid sulfate soil materials. *Geoderma,* 159(1-2), pp. 156-164.

Conklin, A.R.J., 2014. *Introduction to soil chemistry : analysis and instrumentation.* Second edition edn. Hoboken, New Jersey: John Wiley & Sons.

Curran, J.C. and Hession, W.C., 2013. Vegetative impacts on hydraulics and sediment processes across the fluvial system. *Journal of Hydrology,* 505, pp. 364-376.

Davis, B.E., 2005. A guide to the proper selection and use of federally approved sediment and water-quality samplers. (No. 2005-1087). US Geological Society.

Dosskey, M.G., Vidon, P., Gurwick, N.P., Allan, C.J., Duval, T.P. and Lowrance, R., 2010. The role of riparian vegetation in protecting and improving chemical water quality in streams1. *JAWRA Journal of the American Water Resources Association,* 46(2), pp. 261-277.

Downing, J., 2006. Twenty-five years with OBS sensors: The good, the bad, and the ugly. *Continental Shelf Research,* 26(17-18), pp. 2299-2318.

Druffel, L., Emmett, W.W., Schneider, V.R. and Skinner, J.V., 1976. *Laboratory hydraulic calibration of the Helley-Smith bedload sediment sampler*. (No. 76-752). US Geological Survey.

Edwards, T.K., Glysson, G.D., Guy, H.P. and Norman, V.W., 1999. *Field methods for measurement of fluvial sediment.* US Geological Survey Denver, CO.

Einstein, H.A., 1950. *The bed-load function for sediment transportation in open channel flows.* Washington: U.S. Dept. of Agriculture.

Emmett, W.W., 1980. *A Field Calibration of the Sediment-Trapping Characteristics of the Helley-Smith Bedload Sampler.* Washington: U.S. Govt. Print. Off.

EPA, 1996. *Acid Digestion of Sediments, Sludges, and Soils.* Washington, DC: U.S Environmental Protection Agency.

Gaudet, J.M., Roy André, G. and Best, J.L., 1994. Effect of Orientation and Size of Helley-Smith Sampler on Its Efficiency. *Journal of Hydraulic Engineering,* 120(6), pp. 758-766.

Gaweesh, M.T. and van Rijn, L.C., 1994. Bed-Load Sampling in Sand-Bed Rivers. *Journal of Hydraulic Engineering,* 120(12), pp. 1364-1384.

Gregorich, E.G. and Carter, M.R., 2007. *Soil sampling and methods of analysis.* CRC press. Lewis, Boca Raton, Florida, USA.

Guillén, J., Palanques, A., Puig, P., De Madron, X.D. and Nyffeler, F., 2000. Field calibration of optical sensors for measuring suspended sediment concentration in the western Mediterranean. *Scientia Marina,* 64(4), pp. 427-435.

Guy, H.P., Simons, D.B. and Richardson, E.V., 1966. *Summary of alluvial channel data from flume experiments, 1956-61.* US Government Printing Office.

Helley, E.J. and Smith, W., 1971. *Development and calibration of a pressure-difference bedload sampler.* (No. 73-108), Menlo Park, California, USGS.

Hubbell, D.W., Stevens, H.H., Skinner, J.V. and Beverage, J.P., 1985. New Approach to Calibrating Bed Load Samplers. *Journal of Hydraulic Engineering,* 111(4), pp. 677-694.

Hubbell, D.W., 1964. *Apparatus and techniques for measuring bedload.* Washington: U.S. Govt. Print. Off.

ISO, 2006. *Soil quality — Pretreatment of samples for physico-chemical analysis.*

Jalonen, J., Järvelä, J. and Aberle, J., 2012. Leaf area index as vegetation density measure for hydraulic analyses. *Journal of Hydraulic Engineering,* 139(5), pp. 461-469.

Järvelä, J., Dec 11, 2018-last update, Environmental Hydraulics Lab. Available: https://www.aalto.fi/services/environmental-hydraulics-lab [4.4.2019].

Järvelä, J., 2004. Determination of flow resistance caused by non-submerged woody vegetation. *International Journal of River Basin Management,* 2(1), pp. 61-70.

Järvelä, 2002. *Flow resistance of flexible and stiff vegetation: a flume study with natural plants. Journal of hydrology*, *269*(1-2), pp.44-54.

Julien, P.Y., 2010. *Erosion and sedimentation.* 2nd ed edn. Cambridge ; New York: Cambridge University Press.

Kennedy, J.F. and Brooks, N.H., 1965Laboratory study of an alluvial stream at constant discharge, *Proceedings* 1965, US Govt. Print. Off., pp. 320.

Kim, Y.H. and Voulgaris, G., 2003Estimation of suspended sediment concentration in estuarine environments using acoustic backscatter from an ADCP, *Proceedings of Coastal Sediments* 2003.

Lee, K., Isenhart, T.M. and Schultz, R.C., 2003. Sediment and nutrient removal in an established multi-species riparian buffer. *Journal of Soil and Water Conservation,* 58(1), pp. 1-8.

Leong, L.S. and Tanner, P.A., 1999. Comparison of methods for determination of organic carbon in marine sediment. *Marine pollution bulletin,* 38(10), pp. 875-879.

Luhar, M. and Nepf, H.M., 2013. From the blade scale to the reach scale: A characterization of aquatic vegetative drag. *Advances in Water Resources,* 51, pp. 305-316.

Mackereth, F., 1965. Chemical investigation of lake sediments and their interpretation. *Proceedings of the Royal Society of London.Series B.Biological Sciences,* 161(984), pp. 295-309.

Marr, J.D.G., Gray, J.R., Davis, B.E., Ellis, C. and Johnson, S., 2010. Large-scale laboratory testing of bedload-monitoring technologies: overview of the StreamLab06 Experiments. In: JOHN R. GRAY, JONATHAN B. LARONNE and JEFFREY D.G. MARR, eds, *Bedload-surrogate monitoring technologies.* U.S. Geological Survey, pp. 266-282.

Merten, G.H., Capel, P.D. and Minella, J.P., 2014. Effects of suspended sediment concentration and grain size on three optical turbidity sensors. *Journal of soils and sediments,* 14(7), pp. 1235-1241.

Muste, M., Lyn, D., A, Admiraal, D., M, Ettema, R., Nikora, V. and Garcia, M.H., 2017. *Experimental Hydraulics: Methods, Instrumentation, Data processing and Management.* Leiden, The Netherlands: CRC Press.

Naozuka, J., Vieira, E.C., Nascimento, A.N. and Oliveira, P.V., 2011. Elemental analysis of nuts and seeds by axially viewed ICP OES. *Food Chemistry,* 124(4), pp. 1667-1672.

National Research Council, Division on Earth and Life Studies and Water Science and Technology Board, 2002. *Riparian areas: functions and strategies for management.* National Academies Press.

Nepf, H.M., 2012. Hydrodynamics of vegetated channels. *Journal of Hydraulic Research,* 50(3), pp. 262-279.

Nyberg, M.E., Österholm, P. and Nystrand, M.I., 2012. Impact of acid sulfate soils on the geochemistry of rivers in south-western Finland. *Environmental earth sciences,* 66(1), pp. 157-168.

Olesik, J.W., 1991. Elemental analysis using ICP-OES and ICP/MS. *Analytical Chemistry,* 63(1), pp. 12-21A.

Owens, P.N., Batalla, R.J., Collins, A.J., Gomez, B., Hicks, D.M., Horowitz, A.J., Kondolf, G.M., Marden, M., Page, M.J. and Peacock, D.H., 2005. Fine-grained sediment in river systems: environmental significance and management issues. *River research and applications,* 21(7), pp. 693-717.

Owens, P.N. and Collins, A.J., 2006. *Soil erosion and sediment redistribution in river catchments: measurement, modelling and management.* CABI.

Passoni, M., Morari, F., Salvato, M. and Borin, M., 2009. Medium-term evolution of soil properties in a constructed surface flow wetland with fluctuating hydroperiod in North Eastern Italy. *Desalination,* 246(1-3), pp. 215-225.

Pimentel, D., 2006. Soil erosion: a food and environmental threat. *Environment, Development and Sustainability,* 8(1), pp. 119-137.

Recking, A., 2010. A comparison between flume and field bed load transport data and consequences for surface-based bed load transport prediction. *Water Resources Research,* 46(3).

Rowiński, P.M. and Kubrak, J., 2002. A mixing-length model for predicting vertical velocity distribution in flows through emergent vegetation. *Hydrological sciences journal,* 47(6), pp. 893-904.

Ryan and Porth, 1999. *A field comparison of three pressure-difference bedload samplers. Geomorphology*, *30*(4), pp.307-322.

Schillereff, D.N., 2015. 3.7. 1. A review of in situ measurement techniques for investigating suspended sediment dynamics in lakes. Geomorphological Techniques, Chap. 3, Sec. 7.1

Schoellhamer, D.H. and Wright, S.A., 2003. Continuous measurement of suspended-sediment discharge in rivers by use of optical backscatterance sensors. *IAHS PUBLICATION,* , pp. 28-36.

Simpson, S., Batley, G., Maher, B., Kumar, A., Taylor, A., Chariton, A., Pettigrove, V., Baird, D., Adams, M., Spadaro, D. and Hook, S., 2016. *Sediment Quality Assessment, A Practical Guide.* 2 edn. Clayton South, Australia: CSIRO Publishing.

Skordas, K., Kelepertzis, E., Kosmidis, D., Panagiotaki, P. and Vafidis, D., 2015. Assessment of nutrients and heavy metals in the surface sediments of the artificially lake water reservoir Karla, Thessaly, Greece. *Environmental Earth Sciences,* 73(8), pp. 4483-4493.

Smith, T.B. and Owens, P.N., 2014. Flume-and field-based evaluation of a time-integrated suspended sediment sampler for the analysis of sediment properties. *Earth Surface Processes and Landforms,* 39(9), pp. 1197-1207.

Stålnacke, P., Grimvall, A., Libiseller, C., Laznik, M. and Kokorite, I., 2003. Trends in nutrient concentrations in Latvian rivers and the response to the dramatic change in agriculture. *Journal of Hydrology,* 283(1-4), pp. 184-205.

Statzner, B., Lamouroux, N., Nikora, V. and Sagnes, P., 2006. The debate about drag and reconfiguration of freshwater macrophytes: comparing results obtained by three recently discussed approaches. *Freshwater Biology,* 51(11), pp. 2173-2183.

Thomas, R.B. and Lewis, J., 1993. A new model for bed load sampler calibration to replace the probability-matching method. *Water Resources Research,* 29(3), pp. 583-597.

Vanoni, V.A., 2006. *Sedimentation engineering.* 2nd ed. Reston, VA: American Society of Civil Engineers.

Vargas-Luna, A., Crosato, A. and Uijttewaal, W.S.J., 2015. Effects of vegetation on flow and sediment transport: comparative analyses and validation of predicting models. *Earth Surface Processes and Landforms,* 40(2), pp. 157-176.

Västilä, K., Järvelä, J. and Koivusalo, H., 2015. Flow–vegetation–sediment interaction in a cohesive compound channel. *Journal of Hydraulic Engineering,* 142(1), pp. 04015034.

Västilä, K. and Järvelä, J., 2018. Characterizing natural riparian vegetation for modeling of flow and suspended sediment transport. *Journal of Soils and Sediments,* 18(10), pp. 3114-3130.

Västilä, K., 2015. *Flow–plant–sediment interactions : vegetative resistance modeling and cohesive sediment processes*, DSc thesis, Aalto University, Espoo.

Västilä, K., Järvelä, J. and Aberle, J., 2013. Characteristic reference areas for estimating flow resistance of natural foliated vegetation. *Journal of hydrology,* 492, pp. 49-60.

Västilä, K. and Järvelä, J., 2011. Environmentally preferable two-stage drainage channels: considerations for cohesive sediments and conveyance. *International journal of river basin management,* 9(3-4), pp. 171-180.

Vericat, D., Church, M. and Batalla, R.J., 2006. Bed load bias: Comparison of measurements obtained using two (76 and 152 mm) Helley-Smith samplers in a gravel bed river. *Water Resources Research,* 42.

Vousdoukas, M.I., Aleksiadis, S., Grenz, C. and Verney, R., 2011. Comparisons of acoustic and optical sensors for suspended sediment concentration measurements under non-homogeneous solutions. *Journal of Coastal Research,* , pp. 160-164.

Wilson, C.A., Hoyt, J. and Schnauder, I., 2008. Impact of Foliage on the Drag Force of Vegetation in Aquatic Flows. *Journal of Hydraulic Engineering,* 134(7), pp. 885-891.

Wunder, S., Lehmann, B. and Nestmann, F., 2009Measuring drag force of flexible vegetation directly: Development of an experimental methodology, *Conference proceedings, 33rd IAHR Congress* 2009, pp. 1483-1489.

Yamamuro, M. and Kayanne, H., 1995. Rapid direct determination of organic carbon and nitrogen in carbonate-bearing sediments with a Yanaco MT-5 CHN analyzer. *Limnology and Oceanography,* 40(5), pp. 1001-1005.

Yen, B.C., 2002. Open Channel Flow Resistance. *Journal of Hydraulic Engineering,* 128(1), pp. 20-39.

Yuvanatemiya, V. and Boyd, C.E., 2006. Physical and chemical changes in aquaculture pond bottom soil resulting from sediment removal. *Aquacultural Engineering,* 35(2), pp. 199-205.

Appendix A.

Calculation of element concentration in sieved sample containing only <63 µm fraction. The equation was used in cases where average m_1/m_2 ratio and element concentration in non-sieved sample was known, to estimate how the element concentration would differ had the > 63 µm fraction been removed from the sample.

$$C_1 = \frac{C_3(m_1+m_2)-m_2C_2}{m_1} \qquad \text{(A1)}$$

Where
C_1 is the element concentration in <63 µm fraction
C_2 is the element concentration in >63 µm fraction
C_3 is the element concentration in non-sieved sample
m_1 is the mass of <63 µm fraction
m_2 is the mass of >63 µm fraction

The equation was solved from:

$$\frac{m_1C_1+m_2C_2}{m_1+m_1} = C_3 \qquad \text{(A2)}$$

Appendix B.

Mg/Al, Mn/Al and P/Al ratios and depths of cores O and T, normalized by reference values, chosen as the sample locating closest to the ground level after channel excavation in year 2010.